



**KUNGL
TEKNISKA
HÖGSKOLAN**

**Royal Institute of Technology
Department of Naval Architecture
S-100 44 Stockholm, Sweden**

Combined Wave Induced Stresses in a Lo/Lo Container Ship

**Application of a Rationally Based
Direct Calculation Method**

Part 1

**by
Mikael Huss
1987**

Report TRITA-SKP 1059

ISSN 0349-0025

**COMBINED WAVE INDUCED STRESSES IN A LO/LO CONTAINER SHIP;
APPLICATION OF A RATIONALLY BASED DIRECT CALCULATION METHOD**

PART 1

by
Mikael Huss
1987

Report TRITA-SKP 1059

Royal Institute of Technology
Department of Naval Architecture
S-100 44 Stockholm, Sweden

ABSTRACT

Stress response in regular and irregular waves have been calculated for different structural members at the midship hold of a lo/lo container ship. A direct rationally based method was developed incorporating all major low-frequency wave load components. Structural response was calculated using ordinary hull beam idealization for global loads and FE-analysis for local hydrodynamic pressure loads and for inertia loads from ship cargo. Results from structural analysis were coupled with strip calculations using influence coefficients. Non-linear stress response close to the still water line was evaluated using a time step procedure. Results show clearly the relative importance of various load components and their correlation. A complete set of transfer functions and response operators for a side stringer, a transverse web, the bottom center girder and the hatch side coaming is presented in appendices.

CODEN: TRITA/SKP-87/1059

ISSN 0349-0025

CONTENTS

	Page
1 INTRODUCTION	1
1.1 <i>Structural design procedure</i>	1
1.2 <i>Loads</i>	1
1.3 <i>Design criteria</i>	2
1.4 <i>References</i>	3
2 WAVE INDUCED LOW-FREQUENCY STRESS VARIATION	5
2.1 <i>Linear load response in regular waves</i>	5
2.2 <i>Non-linear load response in regular waves</i>	10
2.3 <i>Structural response</i>	13
2.4 <i>References</i>	15
3 STRUCTURAL MODEL	35
3.1 <i>Finite element model for local loads</i>	36
3.2 <i>Global loads</i>	39
4 RESULTS	41
4.1 <i>Ship motions and loads characteristics</i>	43
4.2 <i>Stress components</i>	48
4.3 <i>Non-linear stress response</i>	54
4.4 <i>Correlation of normal and shear stress in irregular sea</i>	58
4.5 <i>Comments on calculation procedure and results</i>	60
5 CONCLUSIONS AND FURTHER WORK	62
ACKNOWLEDGEMENT	63
REFERENCES	64
NOTATION	68
APPENDIX 1: STRESS RESPONSE IN REGULAR WAVES	A1.1
APPENDIX 2: STRESS RESPONSE IN IRREGULAR LONGCRESTED SEA	A2.1

1 INTRODUCTION

In this report is presented results from a rationally based method of calculating wave induced low-frequency stresses in ship structures. The method is rational in the sense that it is not based on any empirical data. It takes into account the ship performance in a seaway governed by the main hull dimensions as well as the structural response governed by the local structural design.

1.1 Structural design procedure

A fully rational design procedure should be direct and probabilistic. Many of the various components in a direct design system which links the predicted lifetime environmental conditions direct to the structural strength is today in practical use. However, the whole procedure is seldom performed due to the time-consuming calculations which rarely can be commercially justified.

A probabilistic approach demands knowledge of the uncertainties in the design procedure. Estimates of probability distributions must be made for environmental conditions, responses, materials, fabrication and other factors that might influence the probability of structural failure. Lack of statistical data and reliability criteria still makes the probabilistic approach far from practical use. Common is for instance to treat the wave loads and the fatigue strength of structural details as stochastic variables, while the uncertainties in structural response and yield stress of the material are neglected.

A direct design method became necessary in the development of new types of ships such as ULCC and large open containerships for which the previous design methods were not applicable. It was developed and verified in accordance with results from large full scale measurement programs onboard ships and with results from model tests. One of the major contribution at this time was that the L/20 equivalent wave height for calculation of design loads was abandoned. It was surely not a rational approach to assume design wave heights according to the ship length. Better understanding of the wave induced loads has influenced the classification rules and has made the semi-direct procedure for practical design more rational.

1.2 Loads

The various loads acting on the ship structure can be distinguished by the frequency of their appearance.

* Still water loads from cargo and displacement distribution are important for global hull girder properties such as sectional area and moment of inertia as well as for local scantlings of secondary and tertiary structural members. The frequency is of the order 10 to 100 times per year.

* Wave induced first order loads occur with a frequency of about 10 times per minute. The maximum values are of the same magnitude as the permissible still water loads.

* Vibrations can be induced by waves or by machinery/propeller and occur globally in the hull as a whole or in local members at frequencies of 1 to 50 times per second. Stress amplitudes induced by vibrations are generally small.

* Transient loads from slamming, wave impact and sloshing can result in very high local stresses. These loads are usually avoided by speed reductions and weather routing. The frequency of appearance might therefore be low although the duration in time of the load peaks are very short.

Wave induced loads are in general coupled so that for instance the maximum bending moments probably occur in the same weather condition as the maximum transient loads. The phase between maximum values of the different components should therefore be taken into account when calculating the maximum combined stress response. However, due to the difference in frequency, the four load groups here mentioned can usually be treated separately.

1.3 Design criteria

There are two types of design criteria:

* Ultimate strength concerning failure modes such as yielding, brittle fracture and plastic buckling.

* Fatigue strength.

The ultimate strength of the structure should to an acceptable level of probability withstand the maximum combined load during ship service time. The collapse can be catastrophic when the load exceeds the ultimate strength, and the safety margins to global collapse for this design criterion is large. Detailed fatigue strength calculations are not yet in common use in ship structural design, although fatigue is by far the most common mode of structural failure. The Classification Societies' scantling rules consider fatigue by having low acceptable nominal stress levels. However, cracks initiate and grow according to the local stress distribution, the type of weld and the skill of the welder.

Fatigue cracks in ships are usually detected and arrested before they reach critical lengths, but the costs of repairing badly designed cracked structural details can be very high. In offshore structures where hard weather can not be avoided and where inspection is difficult, much more attention is paid to the fatigue strength in the design process.

Palmgren-Miner's law of accumulated linear damage is the usual design tool for estimating fatigue life. The stress history is in this approach sufficiently represented by the statistical distribution of stress levels, without knowledge of the actual stress sequence.

A direct procedure for calculating stress amplitude distribution for fatigue design at a certain detail can be described by the following steps:

- * Calculation of structural response to external unit loads, i.e. deterministic stresses from global hull forces, inertia forces and hydrodynamic pressure distribution.

- * Calculation of ship responses in regular waves. Transfer functions for global hull forces, motions and hydrodynamic pressures multiplied by the structural response are combined in accordance to their phases to give transfer functions for stresses.

- * Calculation of stress responses in irregular sea.

- * Calculation of life time stress distribution under expected environmental conditions

The procedure is valid for wave induced low-frequency stresses which are the most important ones for fatigue design. Although the steps might seem straight-forward, many simplifications and assumptions have to be made and the significance of these in the final results can be difficult to supervise.

In this report the procedure is performed with simplifications according to normal design practice but an attempt is also made to examine the non-linearity of stress response due to pressure variations near the still water line.

1.4 References

Design procedures in general have been discussed by ISSC since 1964 and a direct design approach was first described at the 1967 Congress, [1] although it was titled "deterministic", contrary to the previous "evolutionary" approach. Surveys of rationally design concepts are also presented within SSC, [2], 1973, in [3] edited by Evans 1975 and in [4] by Hughes 1983. Probabilistic approaches in general are presented for instance by Faulkner and Sadden 1978, [5] by Stiansen et al 1979, [6] and by Mansour et al 1984, [7]. Soares have developed probabilistic models for still water loads and examined the uncertainty of standard methods for predicting wave induced global loads in [8] 1984. A survey of methods for predicting hull longitudinal loads are also presented by Lewis and Zubaly 1984, [9]. Geometrical uncertainties of the ship hull cross section are analysed by Ivanov 1986, [10]. Fatigue design can be performed with two different methods. The standard method relates the local cumulative stress history to the fatigue capacity of different classes of weld joints. This method is used by for instance DnV, [11], and is based on analysis of fatigue tests at the British Welding Institute, [12]. The other method can be represented by Munse et al, [13], 1983, and by Tomita and Fujimoto, [14], 1982. They use nominal cumulative stress history and fatigue data from actual ship structures or notched specimens to evaluate fatigue life.

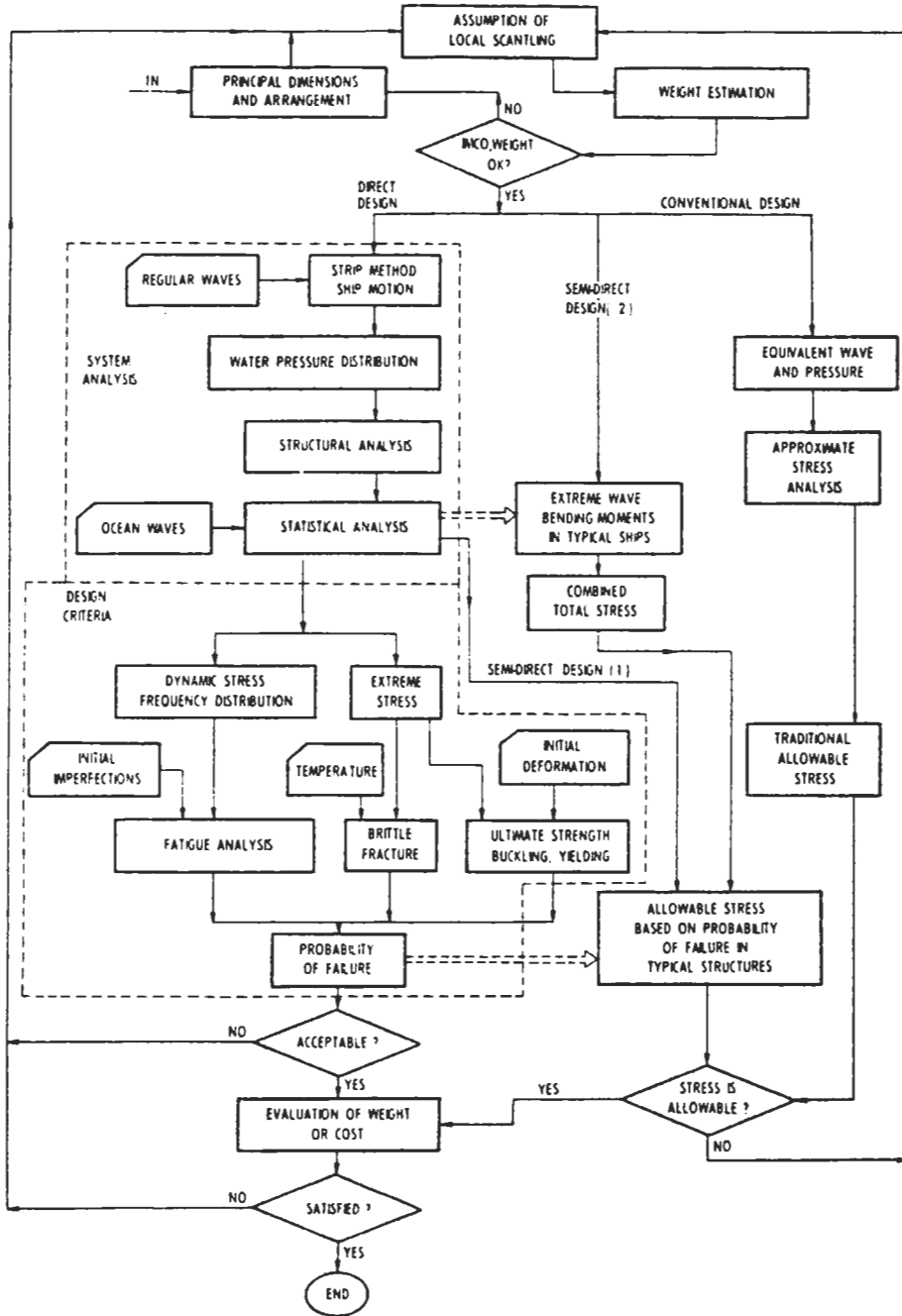


Fig. 1.1 Design procedures as presented by ISSC Committee V.1 1976, [15].

2 WAVE INDUCED LOW-FREQUENCY STRESS VARIATION

Still water loads are in general deterministic. Even though the history of still water loads is uncertain, the level can be limited by appropriate loading manuals in a way that is not possible with the wave induced loads. The unlimited stochastic character of the first order wave induced loads makes it necessary to couple every design criteria to an acceptable probability of occurrence.

The structural wave induced loads can be separated into:

- * Global bending moments, shear forces and torsional moment in the ship hull girder.
- * Local external hydrodynamic forces
- * Local internal inertia forces from cargo.

The combined stress response depends on both the amplitude and the relative phase of the load components. The phase varies with the frequency of the waves and with the position of the structural member. The only strict way of obtaining local stress response is to calculate the stress components simultaneously for each separate member of interest. This is a very extensive work that can not be used in an ordinary design procedure. The design rules and guidelines from Classification Societies are therefore based on assumptions such as fixed correlation between load components and estimate of local loads from quasi-static analysis. However, for principle studies of the wave induced stress history there is still need for a direct approach. Such a direct procedure based on a chain of well known, practical calculation methods is realized in the computer program WAIST, [16],. The main properties of the procedure are summarized here.

2.1 Linear load response in regular waves

Load response in regular waves is calculated with strip theory. The ship hull is divided into a number of prismatic strips for which the hydrodynamic properties are calculated under assumption of two-dimensional flow. By longitudinal integration of the forces on each strip, the general equation of motion in five degrees of freedom can be solved.

$$[N + A]\{\ddot{\eta}\} + [B]\{\dot{\eta}\} + [C]\{\eta\} = \{F_w\} \quad (2.1)$$

With assumption of linear, harmonic wave forces, $\{F_w\}$, and constant coefficients in the matrices of mass and hydrodynamic added mass, $[N+A]$, of damping, $[B]$, and of restoring forces, $[C]$, also the motion responses, $\{\eta\}$, become linear and harmonic.

$$\{\eta\} = \begin{cases} z = z_0 \sin(\omega_e t + \epsilon_z) & \text{heave} \\ \theta = \theta_0 \sin(\omega_e t + \epsilon_\theta) & \text{pitch} \\ y = y_0 \sin(\omega_e t + \epsilon_y) & \text{sway} \\ \psi = \psi_0 \sin(\omega_e t + \epsilon_\psi) & \text{yaw} \\ \phi = \phi_0 \sin(\omega_e t + \epsilon_\phi) & \text{roll} \end{cases} \quad (2.2)$$

Global loads

Wave induced hull girder sectional moments and shear forces at stress position i are calculated from the sum of inertia forces, hydrostatic and hydrodynamic forces from ship motions, and wave forces at each strip, integrated along the length of the ship.

$$BM_{y_i} = \int_{x_i}^{x_b} (x-x_i) \frac{dF}{dx} dz \quad \text{vertical moment} \quad (2.3)$$

$$BM_{z_i} = \int_{x_i}^{x_b} (x-x_i) \frac{dF}{dx} dy \quad \text{lateral moment} \quad (2.4)$$

$$TM_{x_i} = \int_{x_i}^{x_b} \frac{dM}{dx} dx \quad \text{torsional moment} \quad (2.5)$$

$$T_{z_i} = \int_{x_i}^{x_b} \frac{dF}{dx} dz \quad \text{vertical shear force} \quad (2.6)$$

$$T_{y_i} = \int_{x_i}^{x_b} \frac{dF}{dx} dy \quad \text{lateral shear force} \quad (2.7)$$

Strip forces, (F_z, F_y, M_x) , as well as global moments and shear forces varies linearly with the wave height and harmonically in time with encountering frequency, ω_e , as the motions in (2.2).

The motions and loads above refer to a room-fixed system of coordinates moving uniformly with the ship speed V and with origo at ship centre of gravity, see fig.2.1. The sectional moments and shear forces are in WAIST defined positive according to fig.2.2.

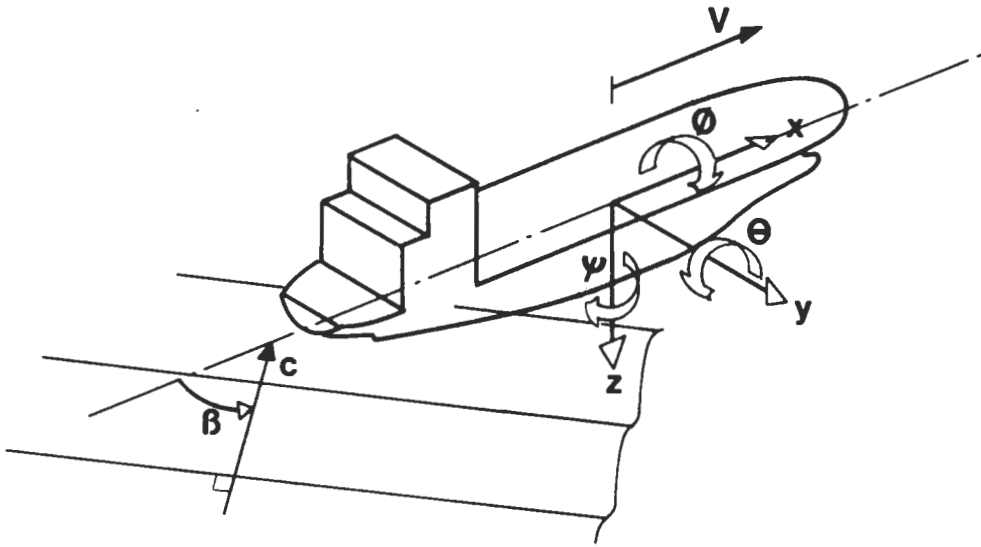


Fig.2.1 Definition of system of coordinates and of ship oscillations in waves

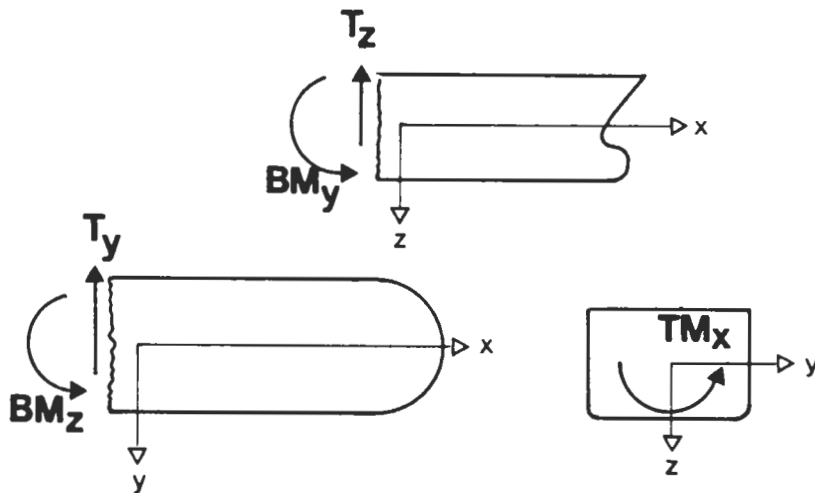


Fig.2.2 Definition of positive directions for sectional moments and shear forces in program WAIST.

Local hydrodynamic pressure

The hydrodynamic pressure distribution around each strip section is assumed to be composed of the following components:

* Incident Froude-Kriloff pressure calculated from wave potential without influence from ship hull, p_{FK} .

* Diffracted wave pressure on the hull surface when the ship is being maintained fixed, p_D .

* Wave pressure from radiation when the ship oscillates in five degrees of freedom in calm water, p_R .

* Variation in hydrostatic pressure when the ship oscillates in three degrees of freedom (vertical motion) in calm water, p_{VM} .

Each of the pressure components varies harmonically with the wave frequency but with different phases. The total pressure variation at a certain position j is formed by the sum of the momentary pressure components:

$$P_j = P_{FK_j} + P_{D_j} + P_{R_j} + P_{VM_j} = P_{0_j} \sin(\omega t + \epsilon_{P_j}) \quad (2.8)$$

The pressure response calculated from strip theory is true only for small wave amplitudes and long wavelength, but shows sufficient agreements with measurements below the still water line within wide ranges. Some comparisons are presented below under 2.4 References.

Local mass forces

Local inertia forces on the hull structure at position k with coordinates (x_k, y_k, z_k) is for small amplitudes described by:

$$F_{Ix_k} = m_{x_k} (-z_k \ddot{\theta} + y_k \ddot{y}) \quad (2.9)$$

$$F_{Iy_k} = m_{y_k} (z_k \ddot{\theta} - x_k \ddot{y} - \ddot{y}) \quad (2.10)$$

$$F_{Iz_k} = m_{z_k} (-y_k \ddot{\theta} + x_k \ddot{\theta} - \ddot{z}) \quad (2.11)$$

Here $(m_{x_k}, m_{y_k}, m_{z_k})$ is the "active" mass in the ship's longitudinal, transverse and vertical direction working at the specific position k .

Centrifugal forces are not included since they occur with the double frequency of the motions.

Including also the first order gravity components for small amplitudes of roll and pitch, the total mass forces in a ship-fixed system of coordinates become:

$$F_{mx_k} = m_{x_k} (-g\theta - z_k\ddot{\theta} + y_k\ddot{y}) \quad (2.12)$$

$$F_{my_k} = m_{y_k} (g\phi + z_k\ddot{\phi} - x_k\ddot{y} - \ddot{y}) \quad (2.13)$$

$$F_{mz_k} = m_{z_k} (-y_k\ddot{\phi} + x_k\ddot{\theta} - \ddot{z}) \quad (2.14)$$

Equations (2.12-14) are valid for solid cargo but can be used for liquid cargo in full tanks assuming the relative velocity of the liquid is small. The variation of "hydrostatic" mass force then becomes the sum of the three force components, see fig.2.3. Linear pressure variation from liquid cargo in tanks is also discussed by Westin in [17] and by Nagamoto et al in [18].

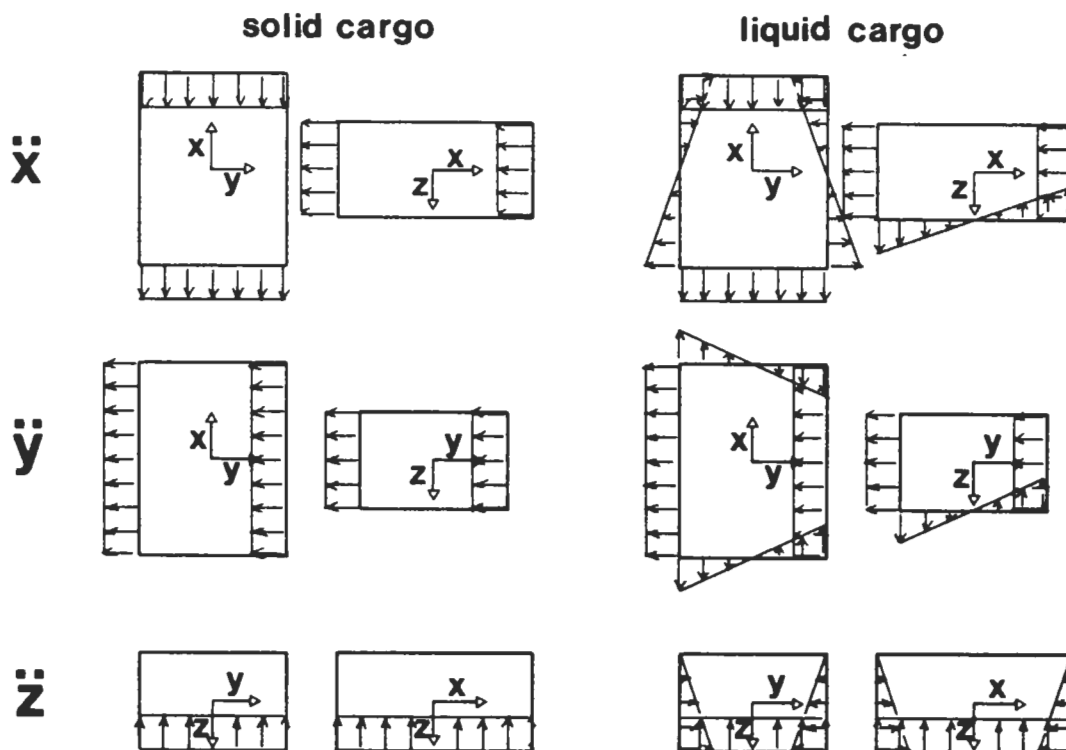


Fig.2.3 Distribution of internal dynamic pressure due to ship motions.

2.2 Non-linear load response in regular waves

Strip theory is usually used for linear response calculations which form the base of frequency-domain analysis of response in irregular sea. Although the coefficients for restoring forces, damping as well as exciting forces, are known to be amplitude dependent in the equation of motion, the linear approach has shown to give reasonable results especially for calculation of vertical motions and global forces for ordinary shaped ship hulls.

The time variation of the local hydrodynamic loads in the area near the still water line (SWL) is however basically non-harmonic and the amplitudes non-linear. With linear strip theory the hydrodynamic pressure variations are calculated up to SWL. In the area within the relative motion between ship and wave these pressures must be corrected or extrapolated to fulfil the boundary conditions of zero pressure above the wave surface and generally non-zero pressure below.

The correction of hydrodynamic pressures is performed in a time step procedure based on ship motions calculated from linear theory. In comparison with a complete time domain simulation, this approach is very efficient for calculation of local effects. It is based on the assumption that the local non-linearity does not influence the overall response of the rigid hull.

Pressure components at ship side are in program WAIST modified as follows:

* Pressure variation from wave potential, p_{FK} , and from ship vertical motions, p_{VM} , is assumed to be linearly distributed from the value at the wave surface to zero at SWL when the surface is below SWL, and from the value at SWL to zero at the wave surface when it is above.

* Pressure variation from diffraction, p_D , and radiation, p_R , is cut at the wave surface when it is below SWL and kept konstant from SWL up to the surface when it is above.

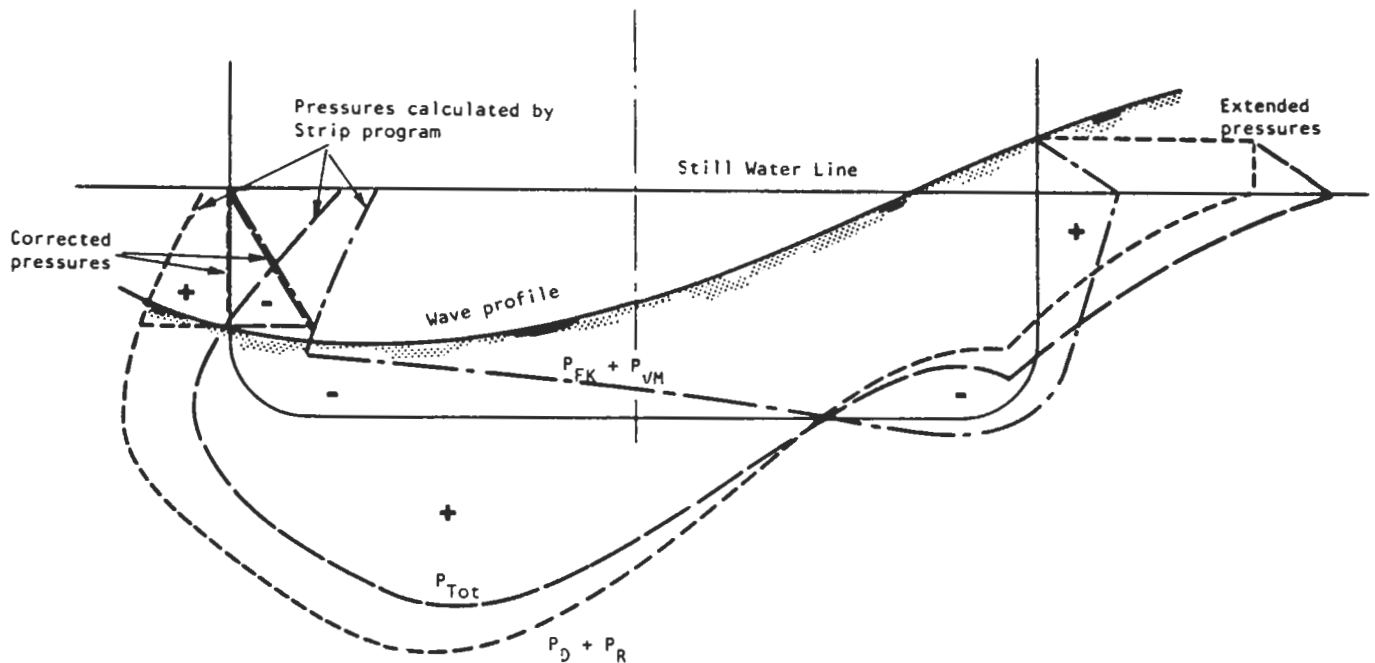


Fig.2.4 Modifications of hydrodynamic pressure components around the still water line, as used in the present method.

The modification of diffraction and radiation pressure components is not trivial. Finnigan et al, [19], 1984 have discussed two alternative modifications of wave theory for the surge response calculation of Tension Leg Platforms in extreme sea states. The "stretched linear wave theory", (SLWT), applies the kinematics from linear Airy wave theory at SWL to the actual wave surface, while in the "extended linear wave theory", (ELWT), the kinematics at SWL are extended exponentially. The present modification should give results in between SWLT and ELWT, see fig.2.5.

The approach of keeping both extended pressure p_D and p_R constant above SWL has been chosen since it introduces no problem in low frequency waves where the relative velocities between ship and fluid is close to zero. In such waves the amplitudes of p_D and p_R are large while the combined amplitude, $p_D + p_R$, is very low. Different modifications of the two pressure components could therefore result in large non-linearities that are not existing in reality.

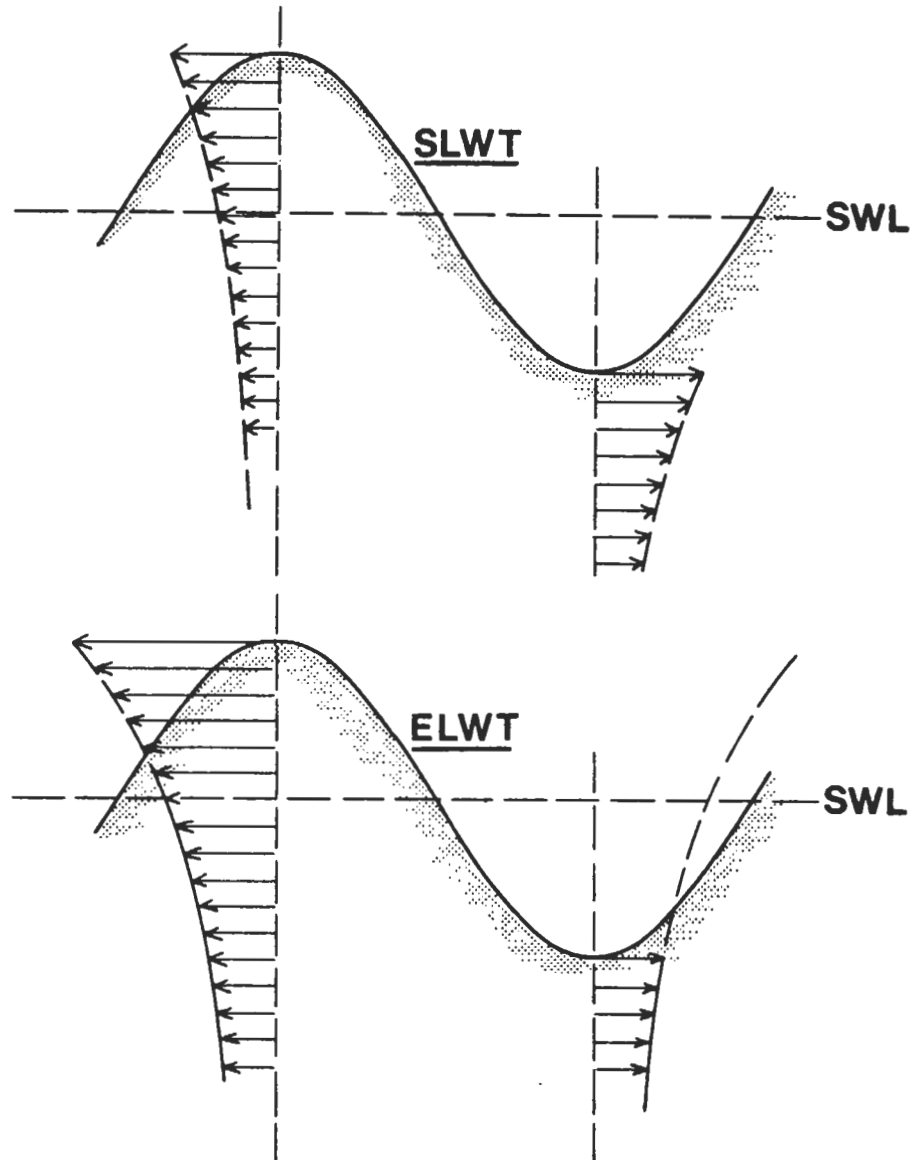


Fig 2.5 Principal figure of distribution of horizontal fluid velocities around the still water line in Stretched Linear Wave Theory (SLWT) and in Extended Linear Wave Theory (ELWT).

Other non-linearities or second order effects could be taken into account in the time step procedure of load calculation. There is however, in the present approach, little use in including effects beyond the validity of the linear strip theory, and the pressure fluctuation close to SWL is considered to be the most important within these limits.

2.3 Structural response

The structural response to wave induced loads can be evaluated either as local hot-spot stress or as nominal normal and shear stress in the structural member. The latter representation is usually of more general interest since hot-spot stresses for different local geometries can be calculated from nominal stresses with use of stress concentration factors (SCF).

With ideal elastic material properties the stress response varies linearly with the amplitudes of the loads.

Stress response to global loads

The local stress response at position i can be coupled to the global loads with use of stress coefficients.

$$\sigma_{hs_i} = C_{My_i} BM_{y_i} + C_{Mz_i} BM_{z_i} + C_{TM_i} TM_{x_i} + C_{Tz_i} T_{z_i} + C_{Ty_i} T_{y_i} \quad (2.15)$$

When using nominal stress representation, the response in longitudinal members can be expressed in a more traditional way.

$$\sigma_B = \frac{(-z_i + z_{NA})}{I_{y_i}} BM_{y_i} + \frac{-y_i}{I_{z_i}} BM_{z_i} + C_{TM_i} TM_{x_i} \quad (2.16)$$

$$\tau_{B_i} = \frac{\mu_{z_i}}{A_i} T_{z_i} + \frac{\mu_{y_i}}{A_i} T_{y_i} \quad (2.17)$$

I_y and I_z are sectional moment of inertia around the y- and z-axis and z_{NA} is the vertical coordinate of the neutral axis at the section. C_{TM} is a coefficient relating the warping stress to the global torsional moment. This coefficient must be calculated for a presumed moment distribution since the warping stress in Vlassov beam theory is dependent on the boundary conditions and the load distribution as well as the total sectional value of the torsional moment. Söding, [20], 1971, has described a method for calculating torsional stress response by superposition of stress components calculated from unit moments at different positions along the ship length. This method incorporates a large amount of calculations and seems appropriate only for structures such as the deck structure of open ships where the warping stresses can be of great significance.

Shear stress is related to the global shear forces with local coefficients μ/A , where A is the sectional area of the structure. Shear stress from torsional moment is not taken into account.

Both C_{TM} and μ are conveniently calculated by finite element (FE) analysis.

Stress response to local loads

Local stress responses from hydrodynamic pressures are calculated by simultaneously superposition of discrete responses from pressures at a large number of hull area segments j around the stress position i .

$$\sigma_{P_i} = \sum_j (C_{\sigma P_{ij}} p_j) \quad (2.18)$$

$$\tau_{P_i} = \sum_j (C_{\tau P_{ij}} p_j) \quad (2.19)$$

$C_{\sigma P_{ij}}$ and $C_{\tau P_{ij}}$ are influence coefficients equal to stress at position i per unit pressure at area segment j , and p_j is the combined hydrodynamic pressure at j according to eq. (2.8). Due to the non-linear pressure variation around SWL, the pressure induced stresses will also be non-linear. This is significant especially for structural members close to SWL.

Local stress responses σ_m and τ_m from cargo mass forces (inclination and inertia) are treated in a similar manner as the pressure induced stresses.

$$\sigma_{M_i} = \sum_k (C_{\sigma My_{ik}} F_{My_k} + C_{\sigma MZ_{ik}} F_{Mz_k}) \quad (2.20)$$

$$\tau_{M_i} = \sum_k (C_{\tau My_{ik}} F_{My_k} + C_{\tau MZ_{ik}} F_{Mz_k}) \quad (2.21)$$

$C_{\sigma My_{ik}}$, $C_{\sigma MZ_{ik}}$, $C_{\tau My_{ik}}$, $C_{\tau MZ_{ik}}$ are influence coefficients equal to stress at position i per unit force at position k . F_{My_k} and F_{Mz_k} are forces at k according to eq. (2.13-14). Hull stresses from longitudinal mass forces are usually small and here not included in the equations. Stress response from mass forces is linear.

The influence coefficients are easily evaluated from FE analysis of the structure around the stress position, each coefficient represented by one separate load case.

2.4 References

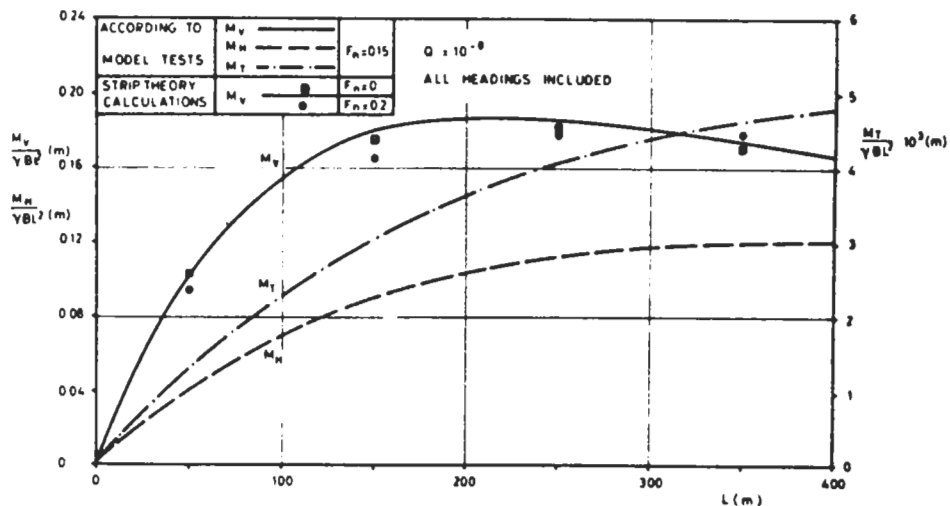
A large number of full scale measurements, model tests and calculations have been carried out concerning the wave induced low-frequency loads. Most of this work is concentrated upon the global loads for determining longitudinal strength of the hull girder. A short review of references will show the development of today's knowledge.

Abrahamsen described in [21], 1969, the state of the art in ship loads and strength calculation. Results from long time calculations of global moments and shear forces based on model tests and on calculations with the strip method were presented, see fig 2.6. Stresses from local pressure distribution were also discussed and it was stated that:

"the total (static + dynamic) external water pressures on a cross section on a given probability level vary linearly from zero at the distance RN above the water level to $d + h$ at the bottom. Here RN is the relative motion and h the dynamic bottom pressure on the same probability level."

The studied ship was a 95 000 tdw tanker, and h was calculated to approximately $0.5 \cdot RN$ amidships and $0.9 \cdot RN$ at the forward perpendicular.

The correlation between relative motions and stresses at the forward perpendicular was measured in full scale and shown to be good, see fig.2.7.



Vertical and horizontal bending moments as well as torsional moments amidships as functions of ship length

Fig.2.6 Long term extreme values of global moments ,[21]

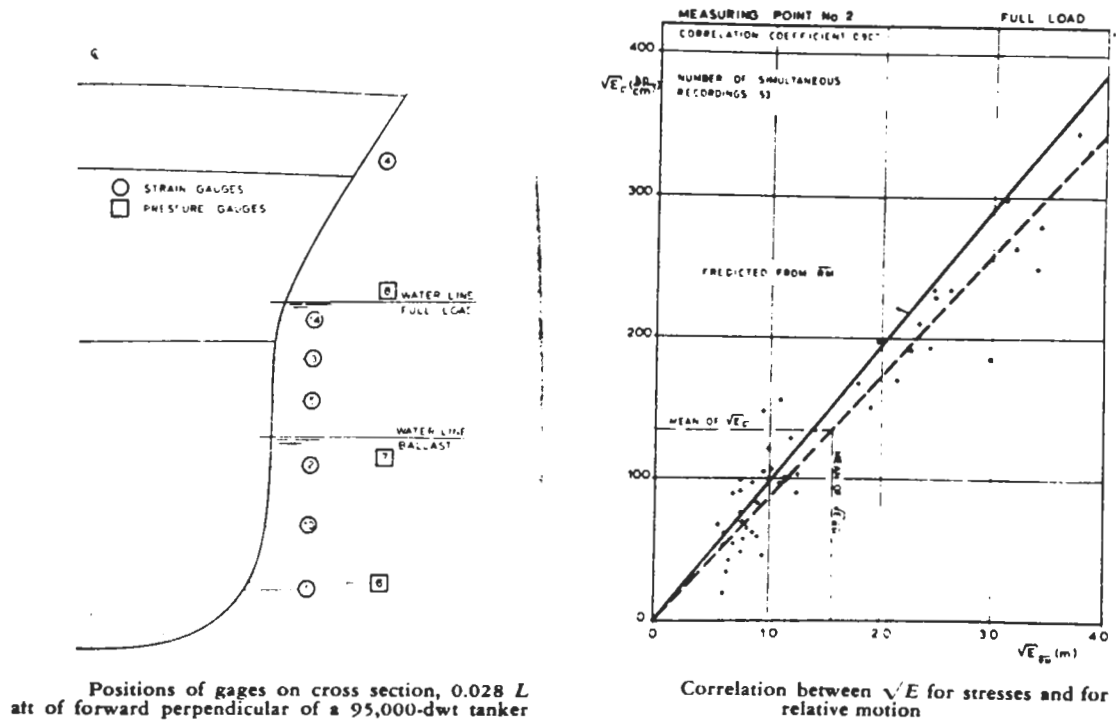


Fig.2.7 Correlation between stress response and relative motion at forward perpendicular of 95 000 tdw tanker, [21].

Little and Lewis reported in [22], 1971, results from ABS full scale measurement program for wave induced vertical bending moments in large tankers. Stresses were measured at the deck and automatically recorded 30 minutes every 4 hour. The total number of records for all five ships was over 13 000. The records were filtered so that low-frequency stresses and springing stresses were separated. The results were extrapolated to long-term distributions, fig.2.8, and the most probable maximum moment of $n = 10^6$, expressed as equivalent design wave height h_e , was evaluated, fig 2.9. The results confirmed that the $L/20$ design wave height was not adequate for large ships.

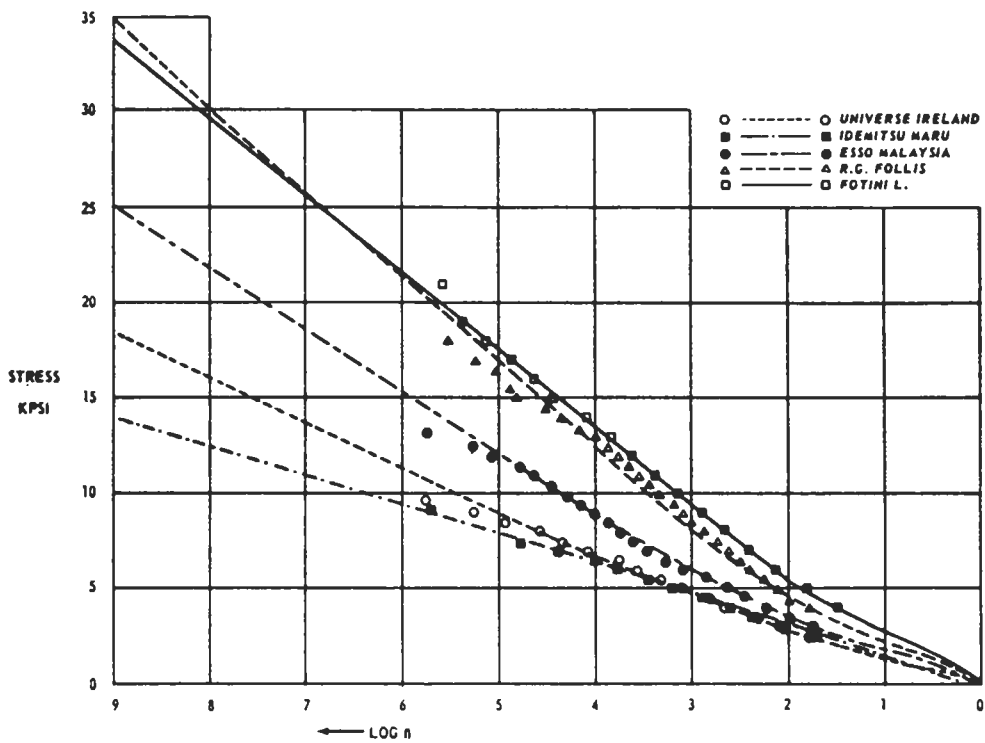


Fig.2.8 Long-term distribution of stresses for large tankers in actual all weather service, [22], 1971.

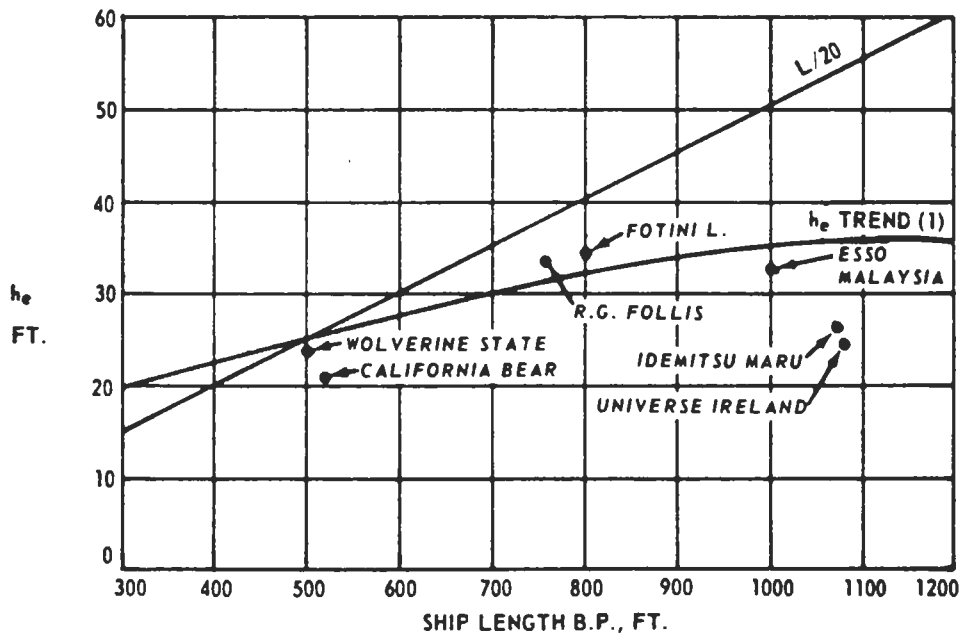


Fig.2.9 Extreme value corresponding to $n = 10^8$ of vertical bending moment for different large tankers, [22].

Within the Ship Structure Committee (SSC) project "Ship Statistics Analysis" were compared full scale measurements and predictions of long term wave induced bending moments on dry cargo ships. From the conclusions in the final report, [23], 1972, is quoted:

"The first step toward developing a design tool is described in this report. It is shown that long-term trends of wave bending moment can be predicted from model tests and ocean wave data, using the results of full-scale statistical analysis and extrapolation as a check of predicted trends."

"Another step in design application will be the determination of a probability level to adopt for design wave bending moment"

"The final step in the practical application of new techniques to ship design will be the rational combining of wave bending moments with other design loads,"

"a long-term distribution curve of bending moment or stress can also be utilized as a partial definition of anticipated loads for fatigue considerations. However, this interesting possibility does not lie within the scope of this project or this report."

Fig.2.10 shows long-term distribution of vertical bending moment for four different ships.

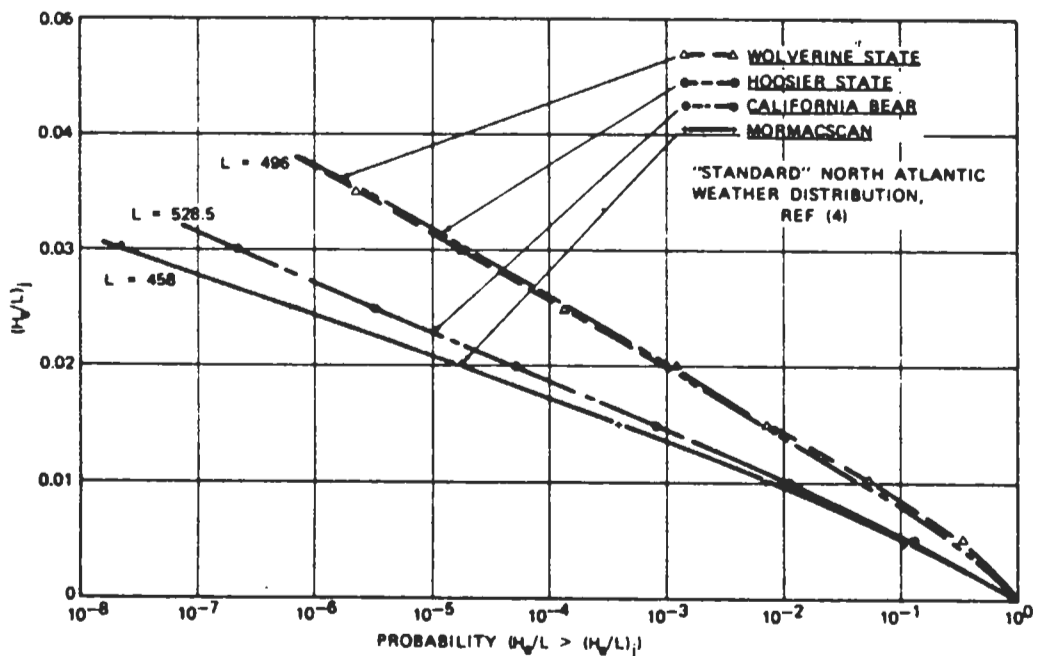


Fig.2.10 Long-term distributions of vertical bending moment for different dry cargo ships in standard North Atlantic weather, [24], 1972.

The SSC project did only study the vertical bending moment, but as noted by Abrahamsen in [21] for larger ships the horizontal bending moment becomes relatively more important. A study of the correlation in long-term responses of vertical and horizontal forces and moments was performed at DnV 1973 by Kikuiri and Mathisen, [25]. They used strip theory for the calculations and presented correlation coefficients as functions of ship length, speed and C_B at different positions along the hull. For vertical and horizontal moments the correlation coefficient was found to lie between 0.2 and 0.5, slightly increasing with ship length and speed. Example is given in fig.2.11.

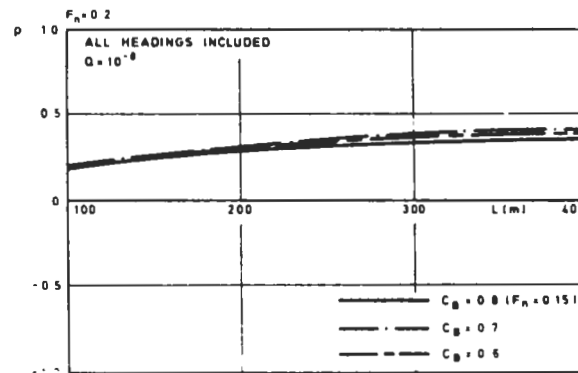


Fig.2.11 Correlation coefficient between vertical and horizontal bending moment amidships, [25], 1973.

The development of specialized lo/lo container ships with large deck openings made the torsional moment an important part of the combined design loads. A number of full scale measurements were performed on container ships of different sizes. Westin, [26], 1977, analysed and compiled results from calculations, measurements and model tests on 11 different ship types covering a length range from 151 m to 274 m. Among the conclusions is quoted:

"The assumption that the peak-to-trough values of the responses are Rayleigh-distributed seems to be adequate."

This implicates that the reported respons spectra are narrow banded and that the responses are linear.

"Strip theory generally predicts responses in fair agreement with those measured."

"Vertical bending is the dominant load over the major part of the hull. Calculated and measured peak values of horizontal bending moment and torsional moment are between 40-80% and 10-40% respectively of the peak value of the vertical bending moment."

"However, torsional moments can give rise to very high warping stresses because of the small rigidity against torsion. These higher warping stresses will occur at the fore end and after end of the open part of the hull."

In the mid seventies the strip method had been proven efficient for calculation of motions and loads. Methods for predicting long-term wave and response statistics had been verified, and the use of advanced structural analysis methods such as FEM had come common. Many papers were published in which direct system analysis of various kinds were outlined for the determination of stresses. However, those methods were considered to be too time consuming and were in most cases only discussed in principle or used for comparison with full scale measurements.

As an example is here quoted Nitta from the PRADS Symposium 1977, [27].

"In order to perform the reliability analysis on the strength of ship structures, a relevant system analysis must be made on either external loads, resultant forces and moments, or stress components in the structural members of ships in service. This is usually called the direct calculation procedure, in which the theoretical analysis is made on ships motion among irregular waves, induced wave loads and structural responses as well as the statistical distributions and the characteristic extreme values of the responses on the basis of observed data of ocean waves."

"further study should be made to develop an approximate method of rationally evaluating the statistical values of the stresses" ... "by taking into consideration the correlation between each component of the load vectors with phase lag."

A direct rationally based system analysis was not adopted at this time because of uncertainty of the transverse wave loads, uncertainty of how to combine different stress components and concentration on the extreme values instead of the stress history because the design criteria did not include explicit the fatigue strength.

The reports from 1976 ISSC committees for design loads and design procedure summarize the attitudes to and expectation of the direct method.

About low frequency dynamic response is quoted from [15]:

"The computational effort required to carry out the above type of calculation rises rapidly if a similar technique is applied to transverse strength analysis, especially if a fine mesh model is introduced. This associated with the present limited knowledge of low frequency pressure prediction, is to be regarded as the biggest obstacle preventing dynamic low frequency stress prediction as a common tool in the ship structural design process. Various methods have been applied to overcome this problems" ... "but at this point in time no reliable method is available. It is important to realise the need for a good method of load prediction incorporating non-linear effects before such methods can be employed in a practical way."

And about combination of loads is quoted from [28]:

"The prediction of the combination of loads causing maximum local stresses is much more difficult. There are no means of reconstructing the condition, in which the maximum value will occur. Every value may of course occur in every spectrum, but with different probabilities. The final probability as reads off the long-term curve is a sum of all these short-term probabilities, and not to be interpreted as valid for

any special condition. For combined loading it is therefore possible that the concept of an effective - most severe condition - has to be revived."

"An effective wave spectrum derived along these principles may be a useful tool in a semi-direct method. For a truly direct design the prediction of loads and stresses will depend on the development of theories for combining all loads."

A research program for combined loads was 1977 outlined by Ulfvarsson within the Swedish Ship Research Foundation (SSF). It included projects for both low and high frequency wave loads and for fatigue design, [29]. The program was however only partially fulfilled and the present work can be seen as a continuation of this work.

Results from direct analysis methods for wave induced stresses in transverse frameworks of tankers were presented by Nagamoto et al, [18], 1976 and by Westin, [17], 1977. In [18] was presented a complete three phase system analysis, fig.2.12. The external pressure distribution was divided into a number of unit distributions to which the stress response was calculated. The total response was obtained with the use of influence coefficients. Pressure distribution was calculated up to the actual water level so that non-linear effects could be taken into account (although diffraction and radiation pressure components seem not to be included). Stress response results in regular waves are presented in fig.2.13, and long-term distribution in fig.2.14. It is not clear if the non linear effect is included in the long-term prediction

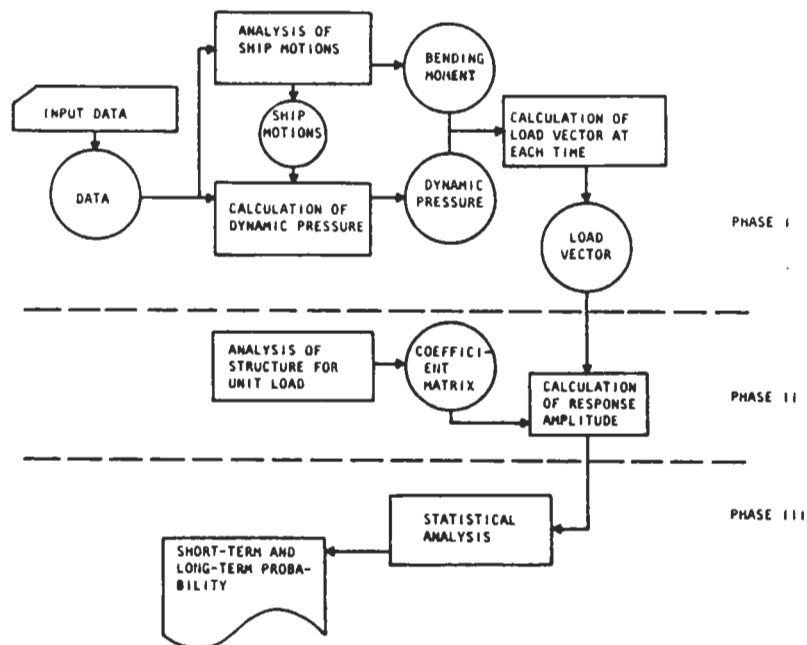


Fig.2.12 Flow chart of total analysis system as presented in [18]. The analysis system is in principal equal to the system used in the present studie.

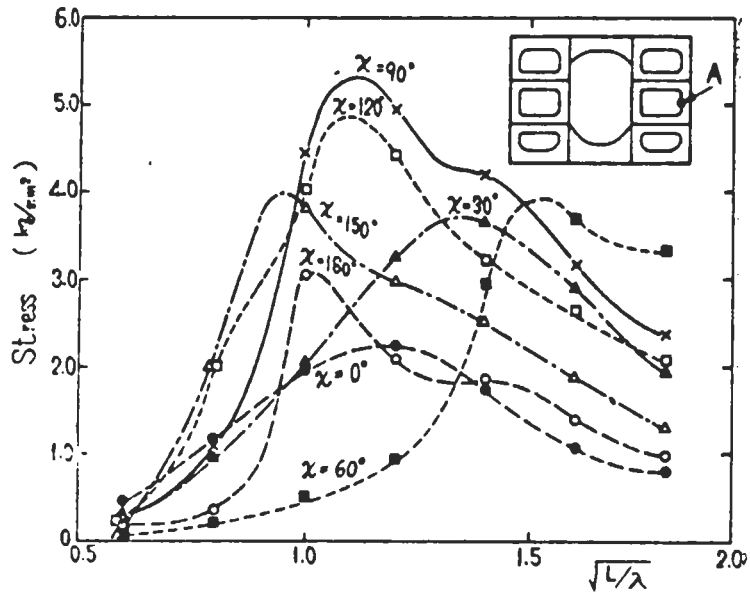


Fig.2.13 Stress response in regular waves, [18]

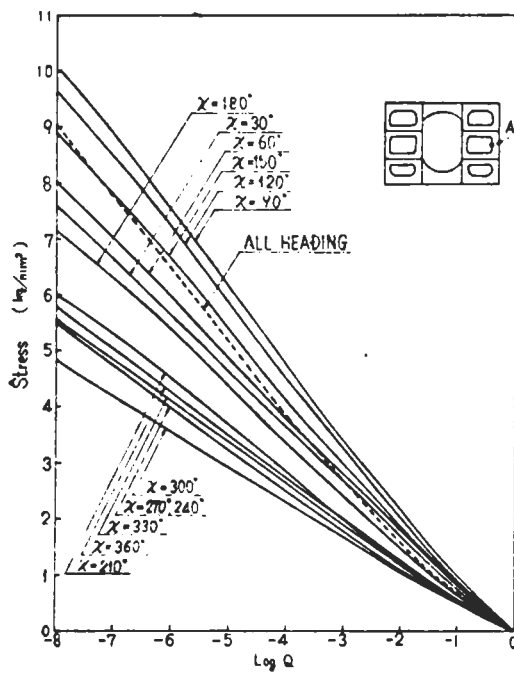


Fig.2.14 Long-term distribution of stresses, [18]

Westin studied the long-term maximum stress distribution in a tanker framework with a different approach. Instead of separate structural and load response calculation, a plane framework analysis program was incorporated into a strip program for "simultaneous" calculation. Results were presented according to fig.2.15. The loads included hydrodynamic pressures from ship motions and waves as well as from liquid cargo. Non-linear effects of pressures above SWL were not accounted for in a realistic way since the pressure value at the SWL was linearly extrapolated to zero at the deck. The advantage of incorporating structural analysis into a strip calculation is that stress response can be evaluated anywhere in the modelled structure while a system of influence coefficients only refer to stresses at a specific position. However, for larger structures the computational costs and the amount of output will be enormous and the method can not be generally applied.

Fig.2.15 shows long-term stress levels in the bottom of the framework under load condition with full draft and empty tanks at the section.

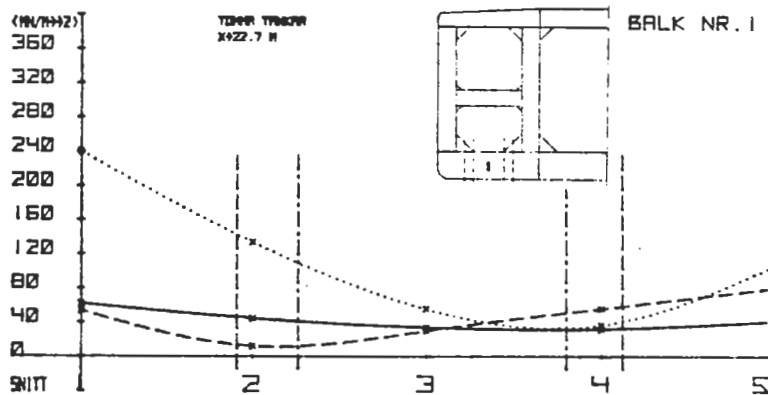


Fig.2.15 Distribution of long-term stress levels in tanker framework, [17]

During the last ten years methods for wave induced loads as well as for structural response have been improved and established. Caretti, [30], 1980, and Kim, [31], 1982, have presented comparisons between strip theory calculated local hydrodynamic pressure distributions and results from model tests, fig.2.16. Different strip theories seem to give near to equal results, and generally in satisfactory agreement with model tests. However, in some conditions such as beam sea, short waves or leeward side the calculations overestimate pressures. Non-linearities in the diffracted pressure component or in the radiated potential of the roll motion as well as overestimated resonance in heave, have been mentioned as an explanation for this. There are only few results available from model tests, and it seems necessary to verify these before any general conclusions can be drawn.

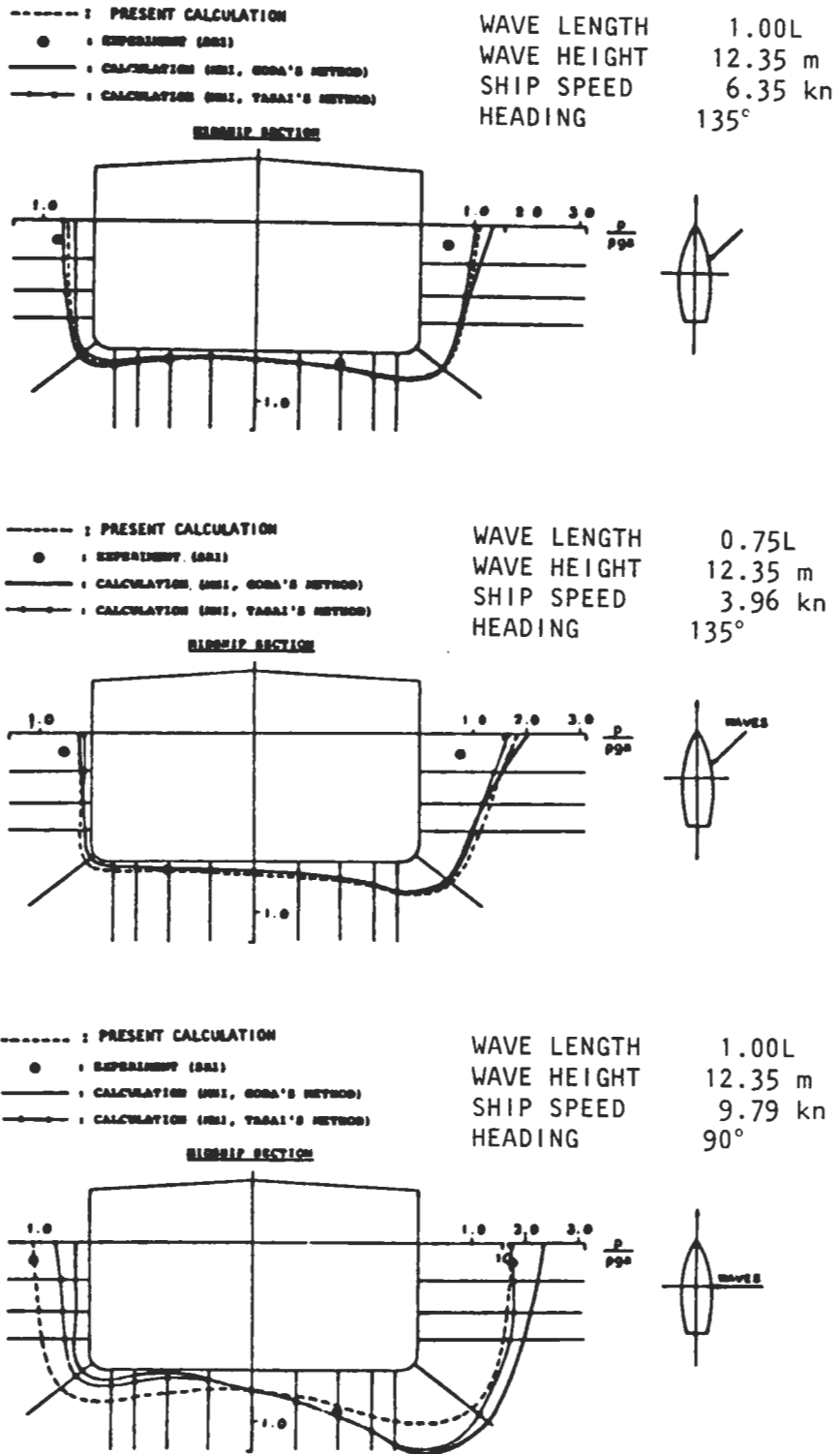


Fig.2.16 Comparison between calculated and measured hydrodynamic pressure amplitudes, [31]. (Tasai's method is used in program WAIST, with which the stress responses presented in this report have been calculated).

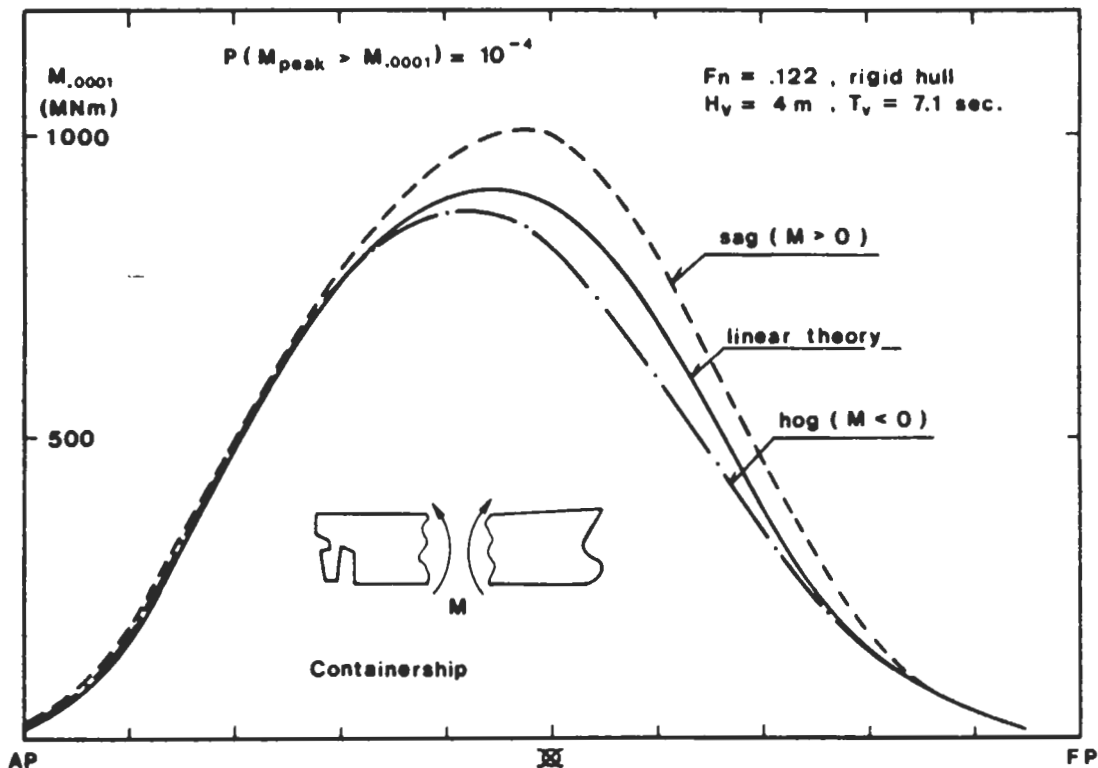
The reliability of different linear strip theories has been studied by Soares, [8], 1984. He used a constant bias model, independent of the wave frequency, for comparison. Measurements from various model tests were compared with calculations and the bias a was evaluated according to $a = \Gamma(X_1 H_1) / \Gamma(H_1^2)$ where X_1 is measured and H_1 calculated transfer functions at different frequencies. For vertical bending moment the ordinary strip theory according to Korvin Kroukowsky and Jacobs, and theory according to Kaplan and Raff in SCORES, underestimates the model test results by in average about 20 %, while improved strip theory according to Salvensen, Tuck and Faltinsen underestimates test results by in average 10%. However, since the bias are taken from the whole range of frequencies the scatter between tests and theory might not represent realistic conditions. It would have been of greater value to compare calculated response in an "ordinary" irregular sea for "ordinary" large ships. Fig.2.17 shows average constant bias for different strip theories.

CB	FN	FOLLOW SEAS				BEAM SEAS				AVERAGES	
		10	30	50	70	90	110	130	150		170
.5	.25	1.14	1.27	1.40	1.53	1.48	1.18	1.07	.97	.86	1.21
.6	.25	1.16	1.29	1.42	1.55	1.52	1.24	1.13	1.03	0.92	1.25
.7	.20	1.05	1.18	1.31	1.44	1.49	1.30	1.19	1.09	0.98	1.23
.8	.15	0.94	1.07	1.19	1.32	1.46	1.35	1.25	1.14	1.03	1.17
GLOBAL AVERAGE FOR O.S.T. = 1.22											
.5	.25	1.06	1.14	1.04	1.30	1.26	1.08	1.04	.99	.95	1.10
.6	.25	1.24	1.32	1.22	1.48	1.40	1.19	1.15	1.10	1.06	1.24
.7	.20	1.17	1.25	1.33	1.41	1.40	1.26	1.21	1.16	1.12	1.26
.8	.15	1.11	1.19	1.27	1.35	1.40	1.32	1.27	1.23	1.18	1.26
GLOBAL AVERAGE FOR SCORES = 1.22											
.5	.25	1.06	1.13	1.20	1.28	1.35	1.28	1.20	1.12	1.04	1.18
.6	.25	1.10	1.17	1.24	1.32	1.38	1.30	1.22	1.14	1.06	1.21
.7	.20	1.06	1.13	1.20	1.27	1.35	1.28	1.20	1.12	1.04	1.18
.8	.15	1.02	1.09	1.16	1.23	1.32	1.25	1.17	1.09	1.01	1.15
GLOBAL AVERAGE FOR SCORES BASED THEORIES = 1.12											
.5	.25	0.76	0.88	1.01	1.13	1.28	1.19	1.09	0.99	.89	1.02
.6	.25	0.83	0.95	1.08	1.20	1.35	1.26	1.16	1.06	0.96	1.09
.7	.20	0.83	0.96	1.08	1.21	1.38	1.31	1.21	1.11	1.01	1.12
.8	.15	0.84	0.96	1.09	1.21	1.40	1.36	1.26	1.16	1.06	1.15
GLOBAL AVERAGE FOR S.T.F. = 1.10											

Predictions of the Regression Equations Of the Bias in the Ordinary Strip Theory (O.S.T.), in the Scores Program, in the Various Modifications of Scores and in the Theory of Salvensen, Tuck and Faltinsen (S.T.F.).

Fig.2.17 From [8]

Jensen and Pedersen, [32], 1978 have presented a second-order strip theory that includes non-linear wave forces, non-vertical ship sides and non-linear variation of hydrodynamic forces due to vertical motion. Their theory also includes flexibility of the hull described by Timoshenko beam theory. In a comparative study, [33], 1981, they showed that there is a significant difference in the response of vertical bending moment calculated by second-order theory and by linear theory for a container ship, fig.2.18, while the difference is small for a VLCC. When springing was taken into account the variance of the wave induced vertical bending moment increased by about one third for both types of ships. The comparison was made for moderate irregular long-crested head sea.



Longitudinal distribution of the most probable largest bending moment amplitudes during 10 000 maxima. $F_n = 0.122$; $H_v = 4 \text{ m}$; $T_v = 7.1 \text{ s}$. The effects of springing are neglected (rigid hull)

Fig.2.18 Distribution of maximum non-linear vertical bending moment in a short-term wave condition, at probability level 10^{-4} . From [33].

Another way of incorporating non-linear effects in the strip theory is to calculate the sectional hydrodynamic forces according to the actual submerged part of the section in a time step procedure. Such a method was presented by Fujino and Yoon, [34], [35], 1985. They compared two different kinds of non-linear calculations with linear calculation and model tests. Both non-linear methods included the time variation of sectional draft and one of them also included the hydrodynamic coupling effect due to the asymmetry of the submerged portion of a heeled ship section. The results indicated that ship motions are well predicted with linear as well as non-linear theory, see fig.2.19. Calculations with both non-linear approaches gave accurate results for global vertical moment and shear force as well as for horizontal shear force. Horizontal bending moment was overestimated with all calculations at higher frequencies while good agreement was found between the more complete non-linear method and experiments for torsional moment. Some comparative results for a heading angle of 120 deg and zero forward speed are shown in figs.2.20-21.

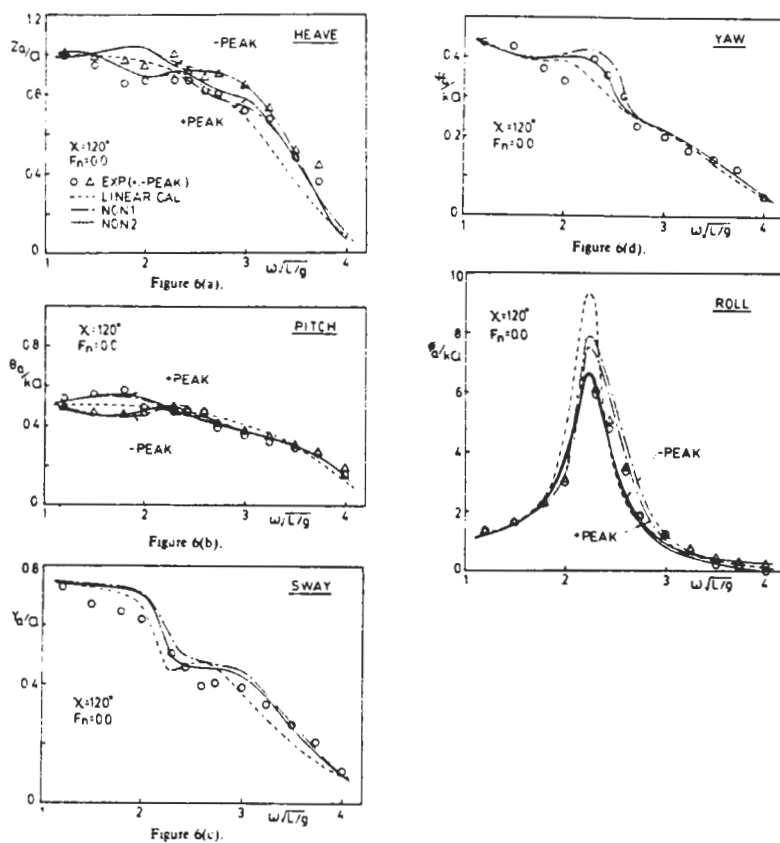


Fig.2.19 Results from model tests and calculations of ship motions, [35]

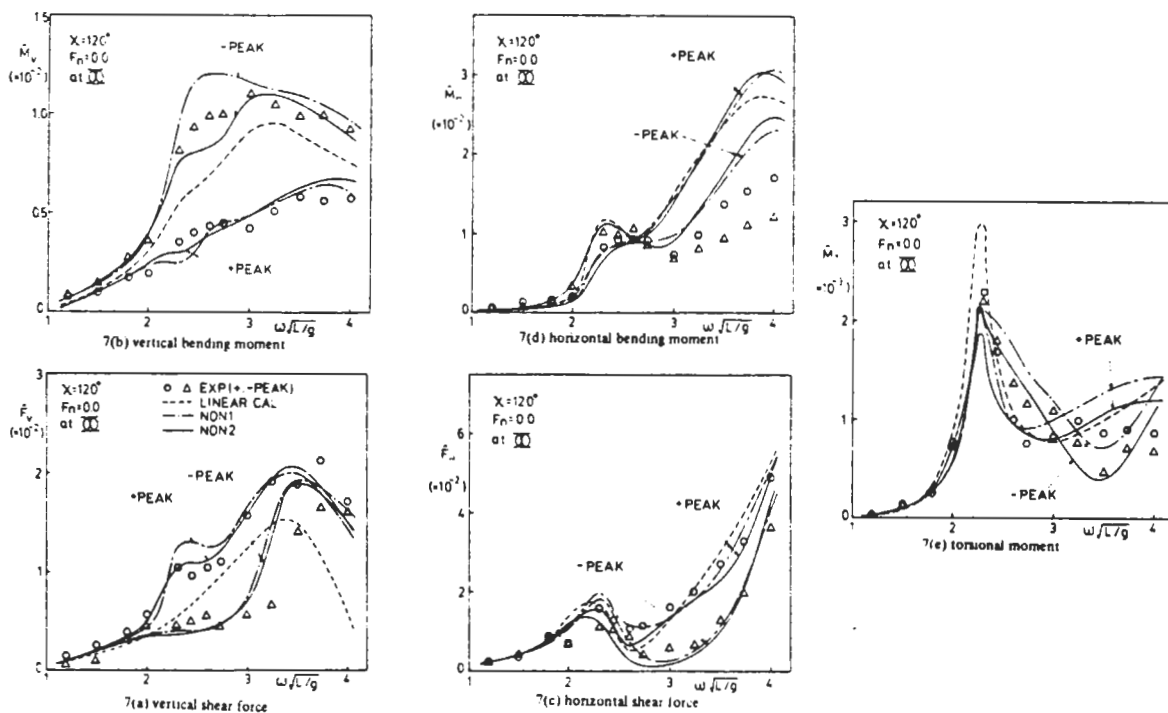


Fig.2.20 Results from model tests and calculations of wave induced global forces and moments, [35]

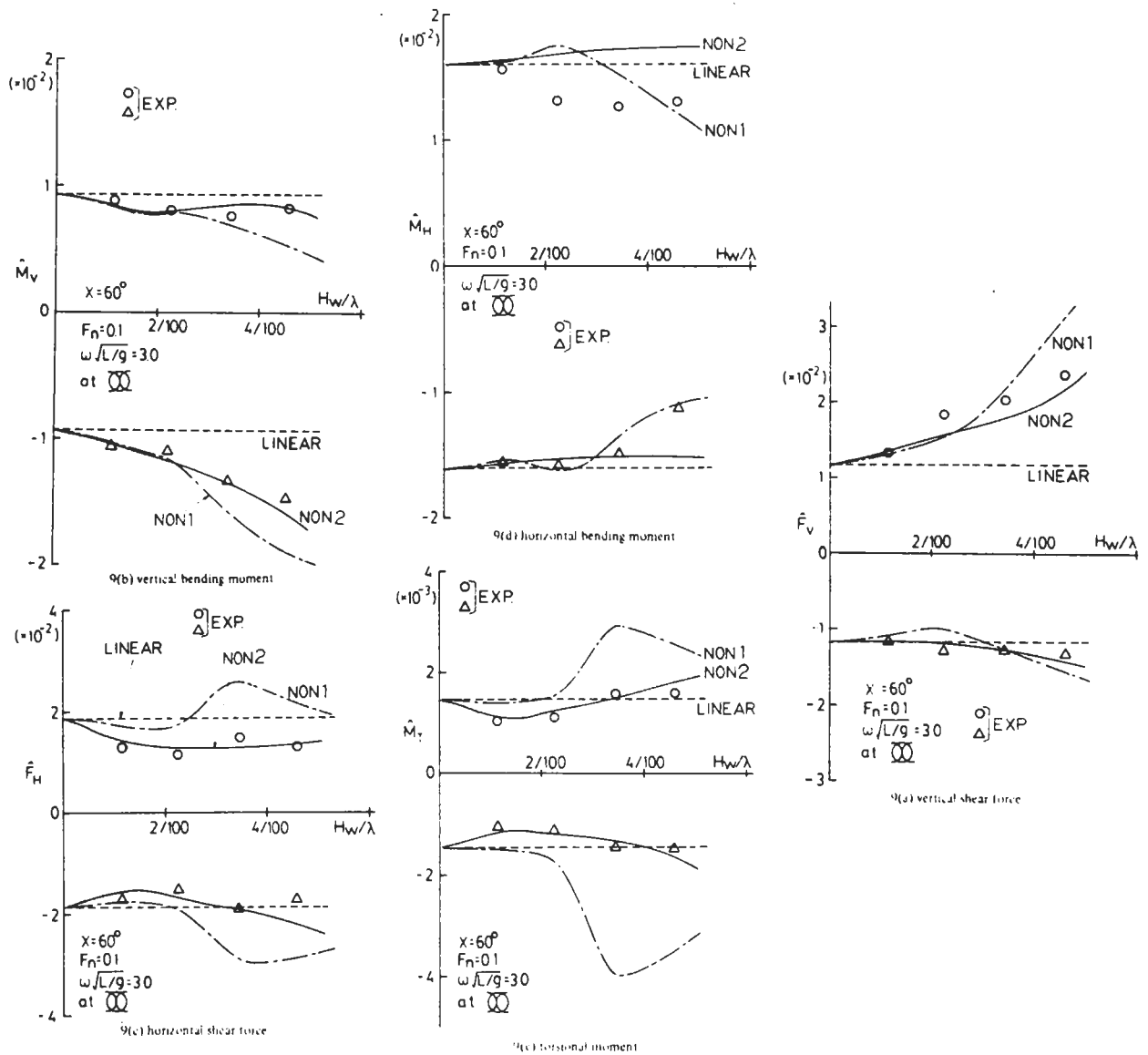


Fig.2.21 Wave height dependence of global forces and moments, [35]

The correlations between different wave induced stress components have been further investigated by Fukuda and Shinkai, [36], 1982, by Hattori et al, [37], 1985, and by Kawamura et al, [38], 1986. In [36] was presented statistical methods for predicting extreme values for von Mises equivalent stresses induced on longitudinal members of the ship hull in irregular waves. Two different assumptions for the correlation between normal stress and shear stress were investigated; full dependence and full independence respectively. The methods were based on linear, Gaussian normal and shear stress response. Short-term and long-term correlation coefficients between wave normal stress and wave shear stress in longitudinal members in a large tanker were

derived with time simulation, fig.2.22. Based on these calculations the following conclusions were drawn:

"1) From a practical viewpoint, the approximate methods dependent on the assumptions of $\rho = \pm 1$ and $\rho = 0$ might be employed for evaluating the extreme values of equivalent stress.

2) The prediction method dependent on the assumption of $\rho = 0$ may be adequately utilized for evaluation the extreme values of equivalent stress.

3) The prediction method dependent on the assumption of $\rho = 1$ or $\rho = -1$ may be utilized to evaluate the upper limit of the extreme values of equivalent stress."

It could however, be questioned if these conclusions have any general validity.

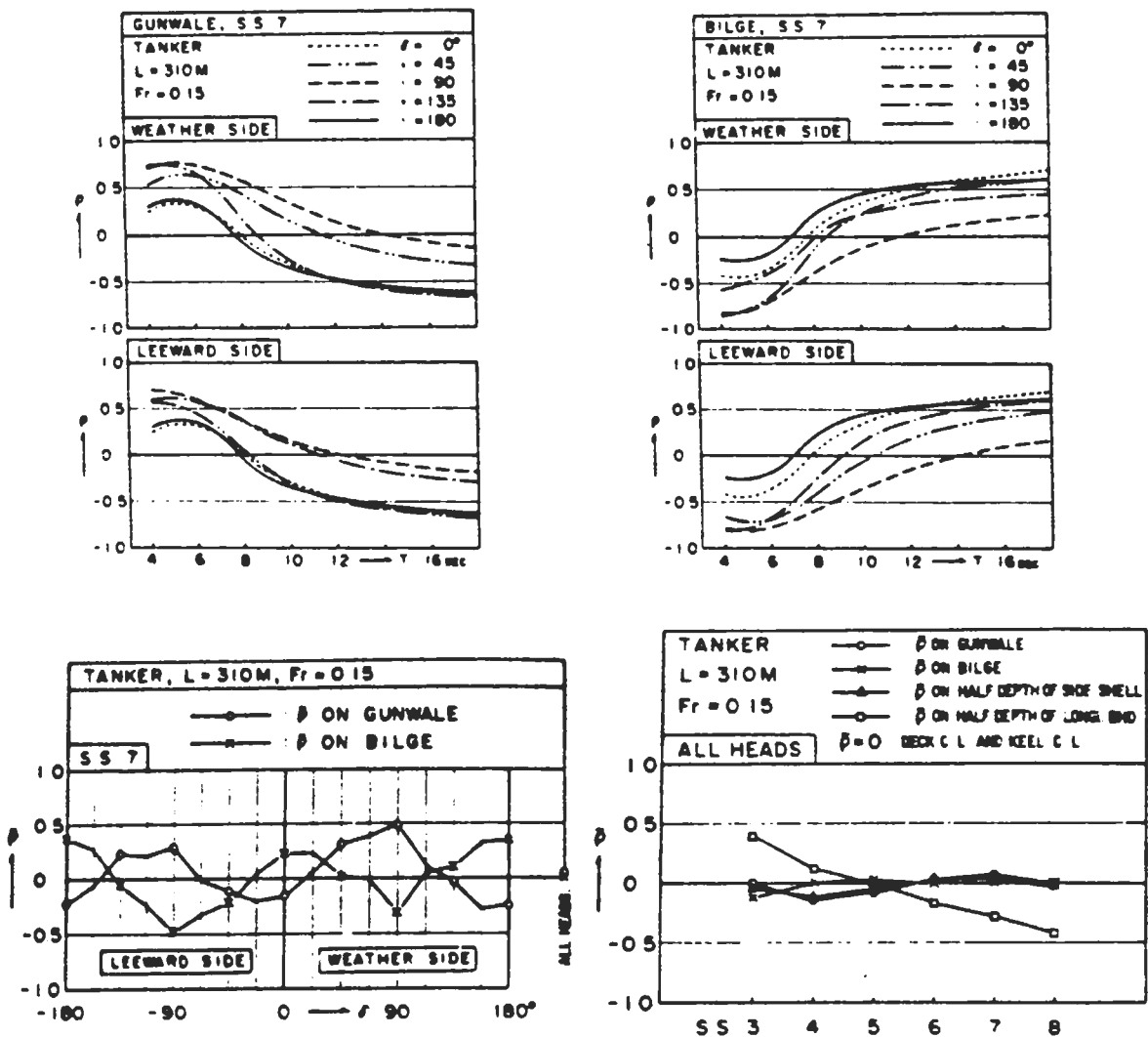


Fig.2.22 Short-term and long-term correlation coefficients between wave induced normal and shear stresses in longitudinal members of a large tanker, [36].

In [37] Hattori et al presented studies on the combined stresses in the bottom shell plating of a bulk carrier. Correlation coefficients between dynamic wave pressure and cargo inertia force, as well as between local double bottom bending stress and hull girder bending stress, were evaluated using strip method for ship motion analysis and quasi-static analysis for the structural response. The local bending stresses were obtained from FE-analysis of the entire cargo hold part of the ship. Some results are presented in figs.2.23-24. It was stated that correlation coefficients between local bending at double bottom and hull girder bending are approximately 0 for empty holds and larger then 0.5 for loaded holds. Long-term stresses in North Atlantic sea at the probability level 10^{-6} were also calculated, see fig.2.25. It was found that an equivalent short-term condition with 10 significant wave height and mean wave length $\lambda = 0.83L$ resulted in equal amplitudes at probability level 10^{-3} along the ship length, while no deterministic equivalent regular wave could describe the longitudinal stress distribution accurately.

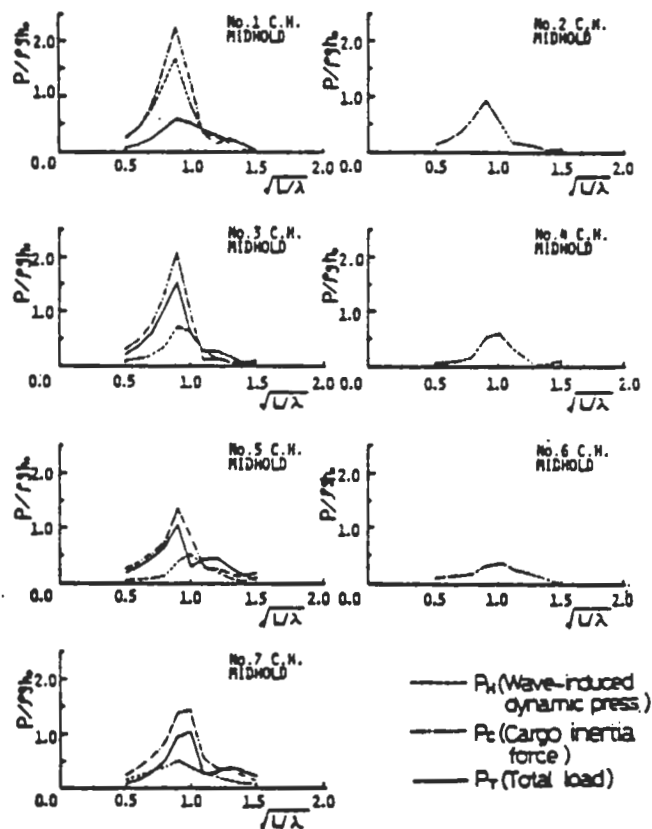


Fig. 6 Frequency response amplitude of wave load acting on double bottom at C. L. in regular wave

Fig.2.23 Wave load response from hydrodynamic pressure and from cargo inertia forces in regular waves, [37]

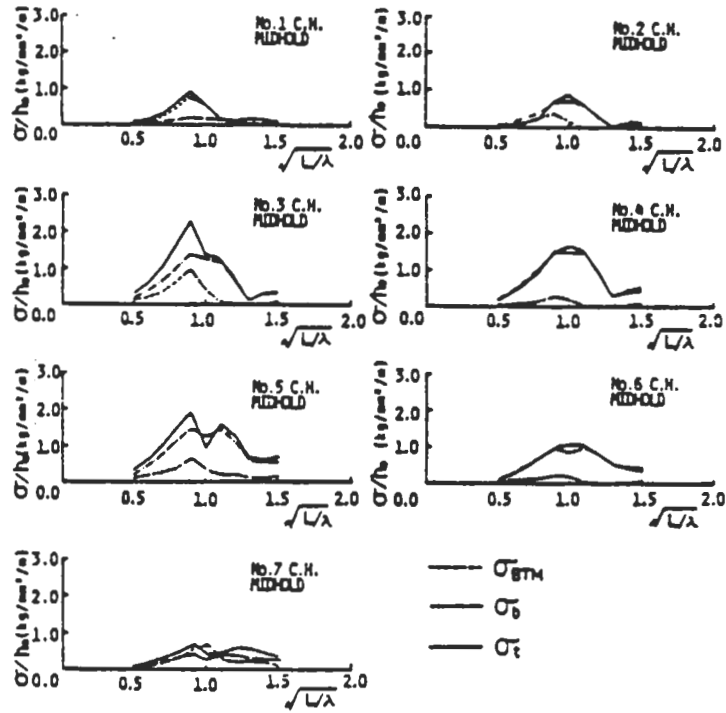
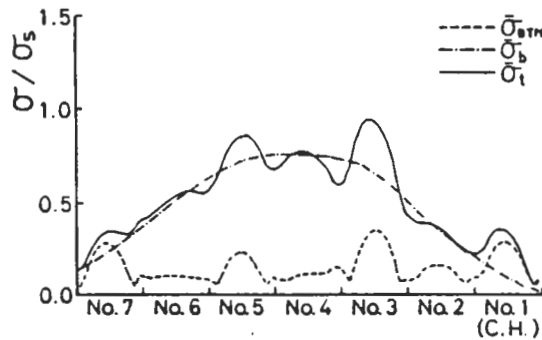


Fig. 10 Frequency response amplitude of longitudinal stress in bottom plate at C.L. in regular head waves

Fig.2.24 Longitudinal wave induced stress response from local double bottom bending and from vertical hull girder bending in regular waves, [37]



Longitudinal distribution of longitudinal stress in bottom plate at C.L. ($Q=10^{-3}$)

Fig.2.25 Long-term longitudinal stress distribution, [37]

In [38], Kawamura et al studied the phase differences between different load components in a 63000 DWT bulk carrier. The combined wave induced stresses in the double bottom were evaluated along the length of the ship. The load calculations were verified with model tests, and comparison was made between stress response calculations with detailed time history FE-analysis and calculations with discrete analysis using superposition of load/stress influence coefficients. The results were summarized as follows:

"(1) Stress components on double bottom induced by inner and outer pressure mostly cancel each other. (2) Resultant stress on double bottom due to combination of hull girder bending and local bending is lower than the stress value obtained by simple summation of the stress components owing to the effect of phase difference."

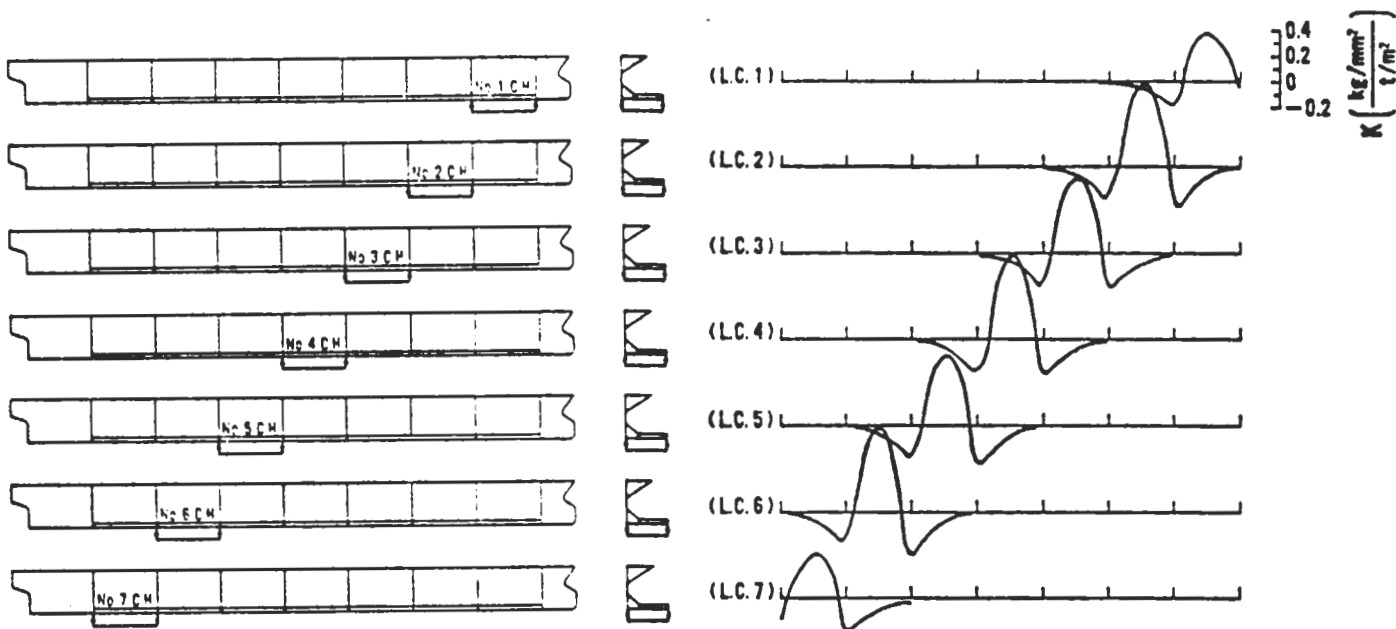
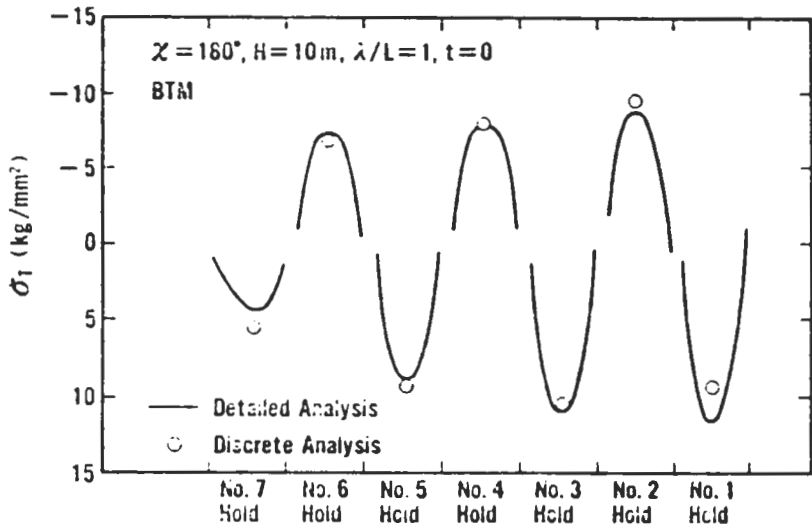
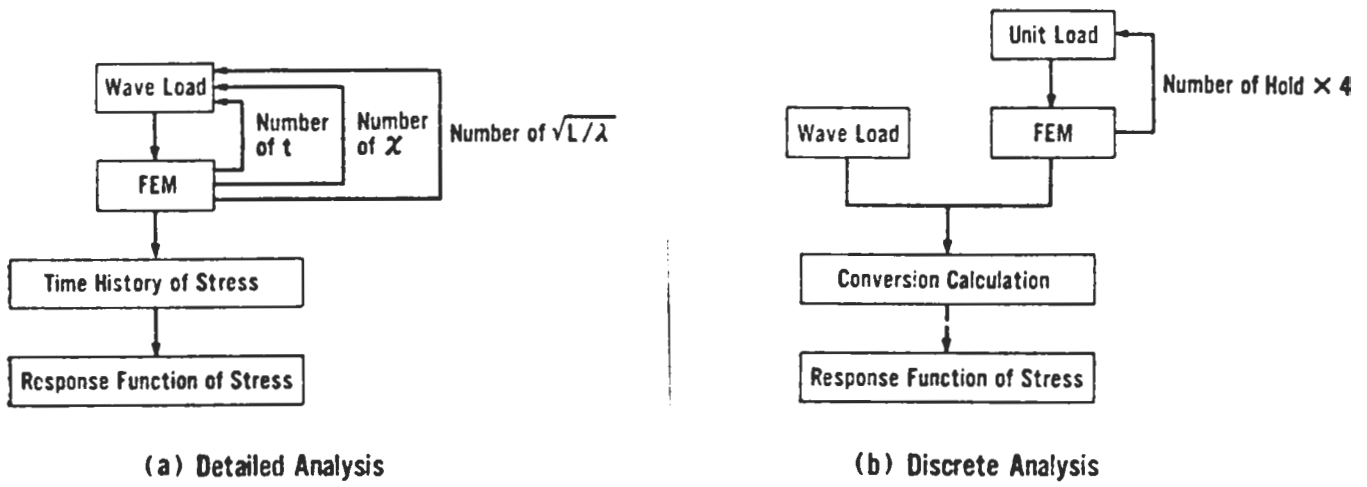


Fig. 2.26 Example of discrete load conversion coefficients. Stresses in double bottom induced by inner and outer bottom pressure, [38].



(a) Bottom

Fig.2.27 Stress response in regular waves, comparison between detailed analysis and discrete analysis, [38].

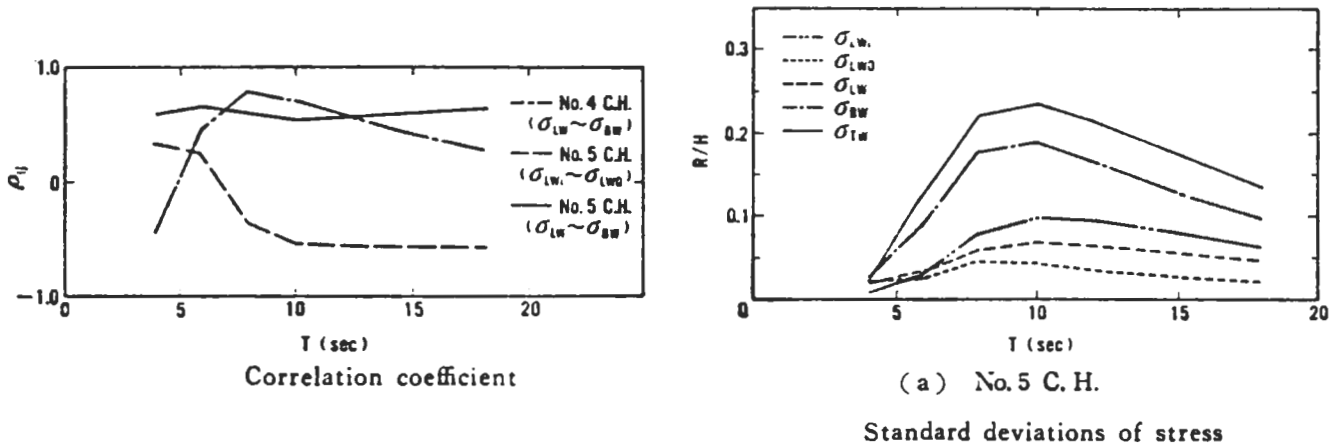


Fig.2.28 Stress response in double bottom in irregular waves. Correlation between local (LW) and global (BW) components, [38].

The use of equivalent regular waves, or some times equivalent short-term wave conditions, is in many case a useful tool for evaluating maximum long-term, non-linear responses of complex structures. The method gives however little information about the curvature of the long-term distribution which is of large importance for the fatigue life time of the structure. Fatigue design methods such as in [11] and in [13] are in fact based upon assumptions of the shape of the long-term stress history, and the only data available for these assumptions are the recorded global load histories from full scale measurements such as those mentioned in this survey of references. It is not verified that the shape of these long-term distributions sufficiently represent the real local stress history which is formed by superposition of various irregular load components.

Direct system analysis seems to be the only realistic method for studying local stress response history. Unfortunately very few results from such studies have been published and there is today no base for general conclusions that could be used in an ordinary design process. In recent years Prowatke, [39], 1984, has shown results from a direct calculation of local stress history and failure modes of a transverse girder. Further such studies, together with in-service measurements and failure analyses, could, if they were presented systematically, make it possible to develop more rational designs and optimized structures.

3 STRUCTURAL MODEL

The stress responses presented in this report refer to the midship structure of lo/lo container ship BO JOHNSON, fig.3.1. The hull has a typical double shell structure with secondary strength members stringers, girders, webs and floors of approximately the same stiffness in both longitudinal and transverse direction. The shell-plates are stiffened with longitudinals at bottom and between upper and 2nd deck, and with transverse frames at sides. The midship section is shown in fig.3.2.

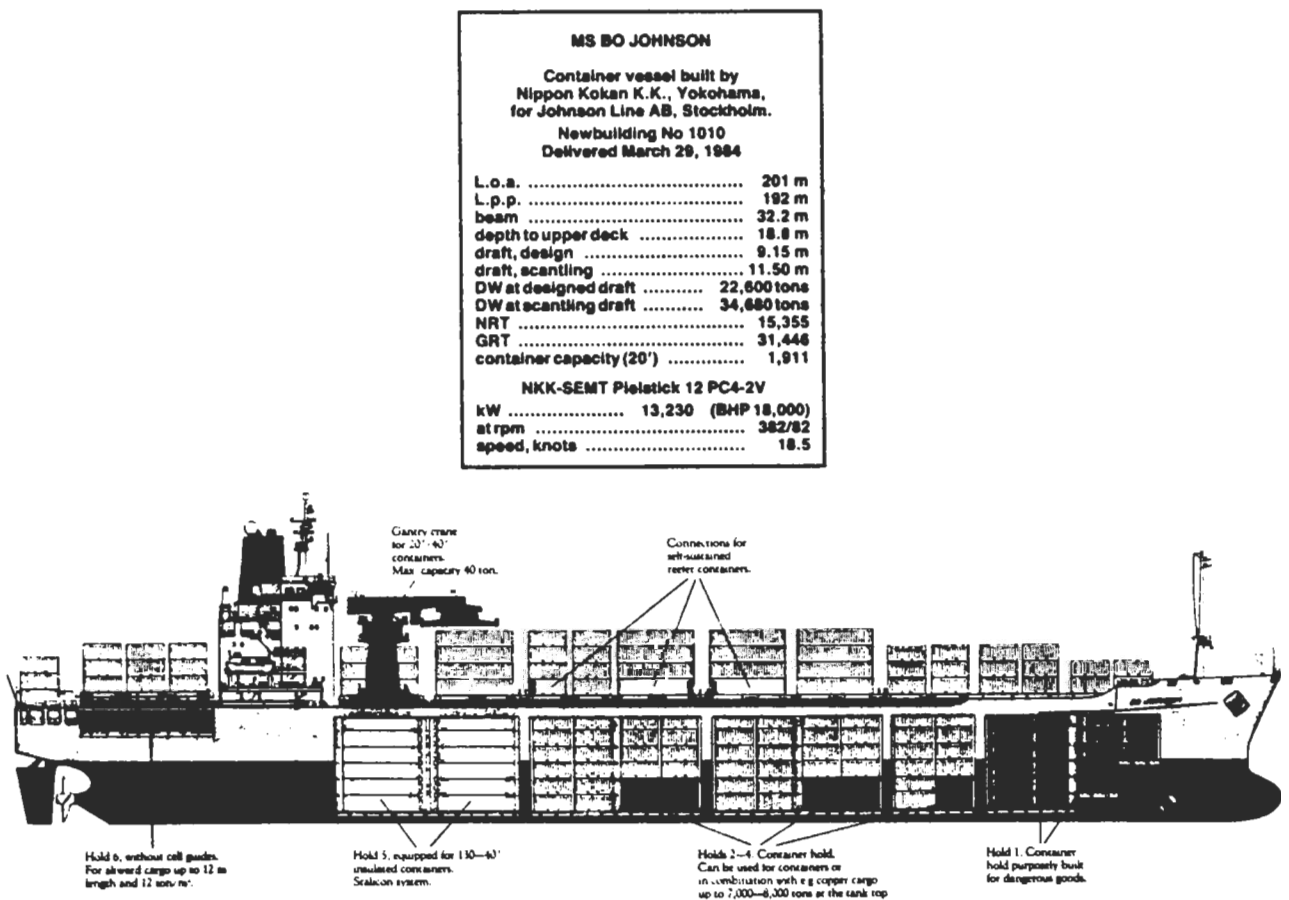


Fig.3.1 Lo/lo container ship BO JOHNSON, main particulars

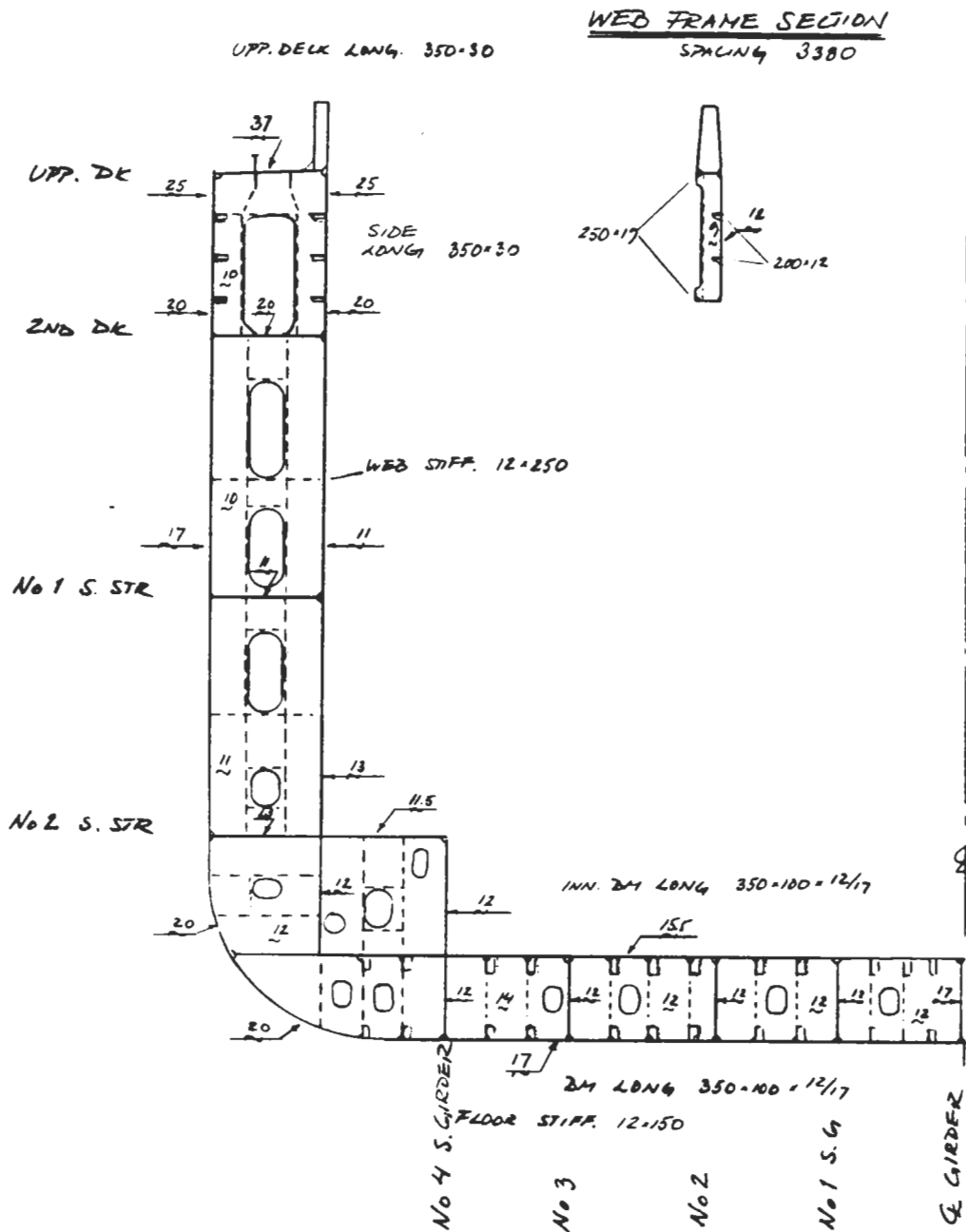


Fig.3.2 Midship section

3.1 Finite element model for local loads

The influence coefficients for external hydrodynamic pressure and for internal mass forces were calculated with FEM. The model consisted of the entire steel structure forming cargo hold 4. It included inner and outer shell plating, bottom girders and floors, side stringers and webs, and deck strips (with pillars). See fig.3.3. Ordinary transverse frames and longitudinals were included in the model with their sectional area added to the plate thickness, without taking into account the direction of the stiffeners. This simplification caused a slight relative overestimation of the bending stiffness of side stringers and bottom floors.

The element used in the FE-model were 4-noded hybrid membran elements with linear distribution of stresses $\sigma_x(y)$ and $\sigma_y(x)$ and with constant τ_{xy} . The entire FE-model consisted of about 900 elements and was not fine enough in the shell plating to simulate the effect of shear lag. For the purpose of the present studie, this is however of no major importance, and the model is considered to be accurate enough to give a good view of the nominal stress distribution along the webs of the secondary strength members.

The boundary conditions of the model were fixed zero displacements at the fore and aft bulkhead sections (web 0 and web 8), corresponding to longitudinal symmetry of the loads.

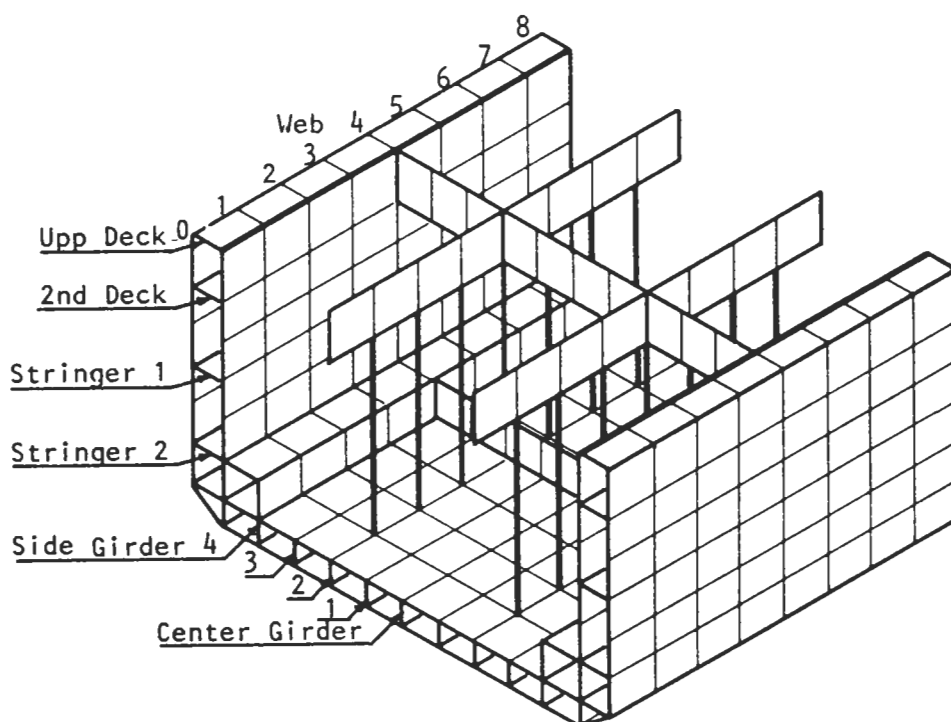


Fig.3.3 FE-model of midship hold (№ 4)

Stress response to external hydrodynamic loads was obtained through a large number of loading cases each representing unit pressure on a small discrete area of the hull. From the loading cases, influence coefficients $C_{\sigma 1,1}$ and $C_{\sigma 1,2}$ according to eqs. (2.18-19) were calculated for nominal stresses at certain positions. Each stress position and stress type was represented by a total of 120 coefficients at 4 sections in the hold.

Influence coefficients for internal massforces according to eqs. (2.20-21) were calculated from the FE-model in a similar way including also deck loads from containers. The subdivision of massload distribution was less fine than the one of pressure distribution, giving a total of 46 load positions with coefficients for both vertical and transverse forces. Longitudinal massforces were not included in the calculations.

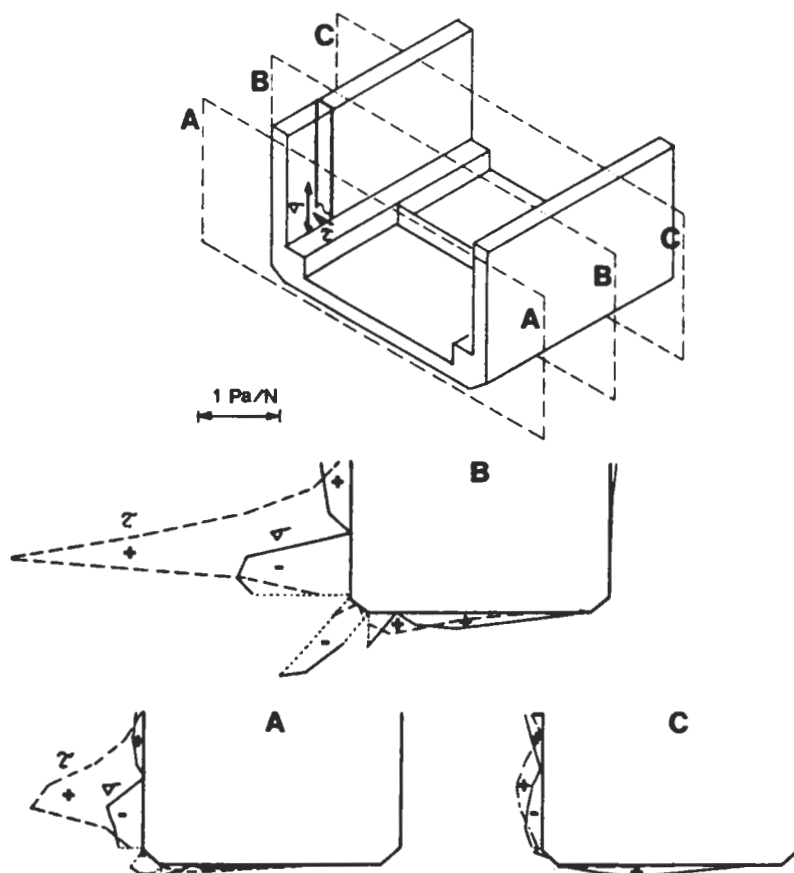


Fig. 3.4 Example of distribution of pressure influence coefficients for normal stress in web 2 at stringer 2. The curves represent stress per pressure acting on a unit area along three sections, (A, B, C) around the stress position

3.2 Global loads

Stress responses to global vertical- and horizontal bending moments were calculated from ordinary beam theory according to eq. (2.16).

Local shear stress responses to global shear forces were calculated with use of the FE-model by applying fixed shear deformation at the end section of the hold. The shear coefficients μ_x/A and μ_y/A in eq. (2.17) were obtained by dividing the stress response with the total reaction force at the displaced section.

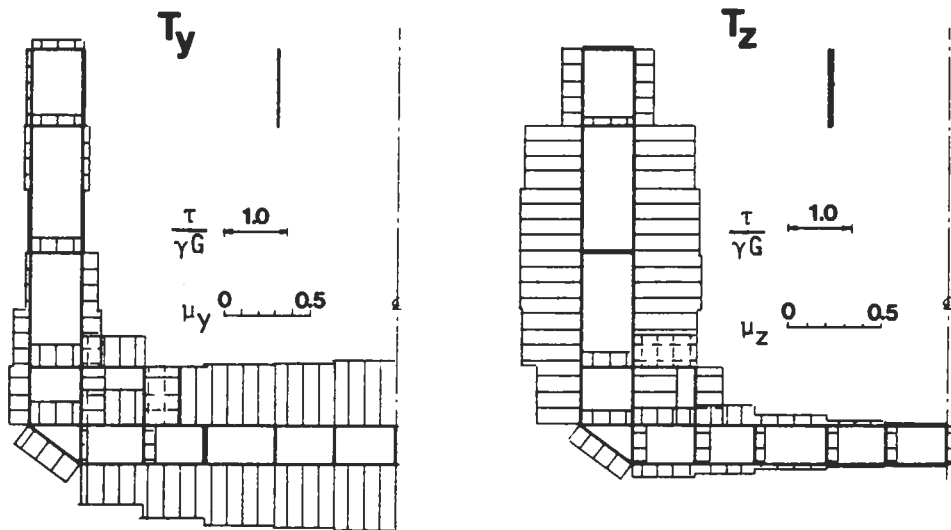


Fig.3.5 Distribution of sectional shear stress from vertical and horizontal shear forces. Non-dimensional coefficient $\mu = \tau A/T$ obtained from the FE-model.

Torsional stress response was calculated according to Vlassov theory with the open part of the hull modelled as a prismatic beam with sectional properties as in the midship section. Time variation of torsional moment distribution, $T_{\Omega}(x)$, was neglected and the bimoment, $N_{\Omega}(x)$, was obtained from the fixed distribution shown in fig.3.6. Coefficient C_{TM} in eq. (2.16) was calculated according to:

$$C_{TM} = \frac{N_{\Omega}(x)}{T_{\Omega} I_{\Omega\Omega}} \Omega(s) \quad (3.1)$$

Sectional distribution of $\Omega(s)$ is shown in fig.3.7.

Results from this very simplified calculation of torsional response showed good agreement with the shipyard/shipowners calculations for design purpose. There is however reason to believe that the warping restraint of the foreship is overestimated by this model. A weaker foreship model would result in larger bimoment levels at hold 4 and 5.

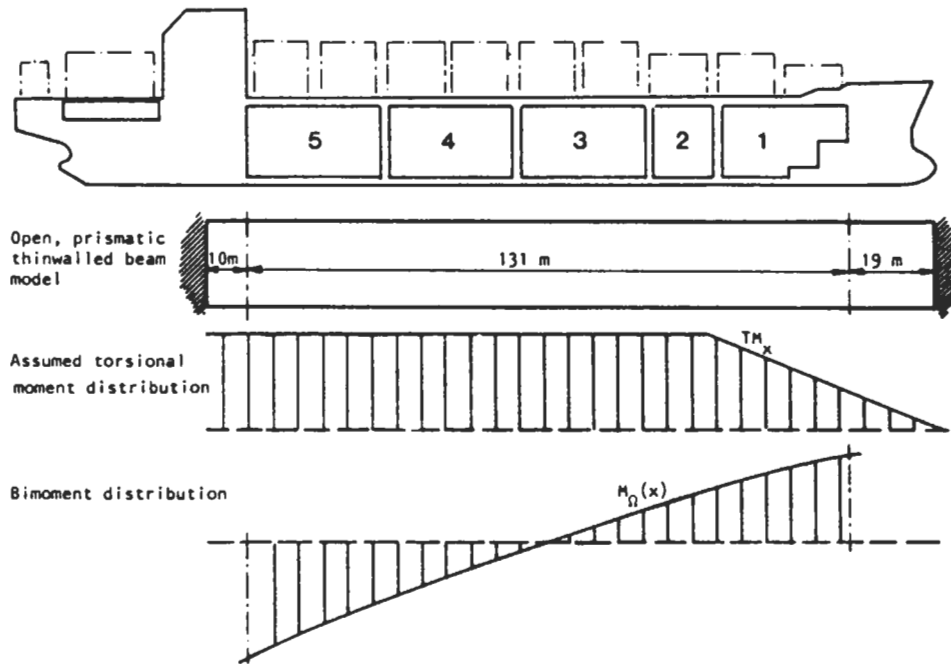


Fig.3.6 Beam model for calculation of torsional response

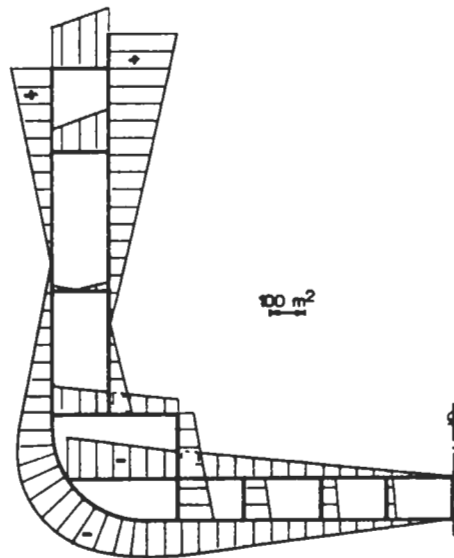


Fig.3.7 Distribution of normalized sectorial coordinate Ω

4 RESULTS

In two appendices is presented a complete set of response functions in both regular waves, (App.1), and irregular long-crested sea, (App.2). The extensive presentation has been chosen since there are very few results from systematic stress response studies previously published. Though the calculation procedure presented in this report includes several simplifications, as discussed in Chapter 2 and 3, the calculated response functions contain information that could be of general interest. Some of the results will be discussed briefly in this chapter, others will be further processed and discussed in coming reports concerning long-time stress histories for fatigue design.

It should be noticed that all the results refer to a full load design condition at a speed of 18.5 knots. The influence of different conditions is discussed in Section 4.5.

Nominal stress response have been evaluated for four different members:

- * Stringer 1 at portside inner shell, (STR1).
- * Center girder at bottom, (CGIR).
- * Web 2 at portside outer shell and bottom, (WEB2).
- * Top of hatch side coaming at portside, (HSID).

Locations of the studied members are shown in fig.4.1.

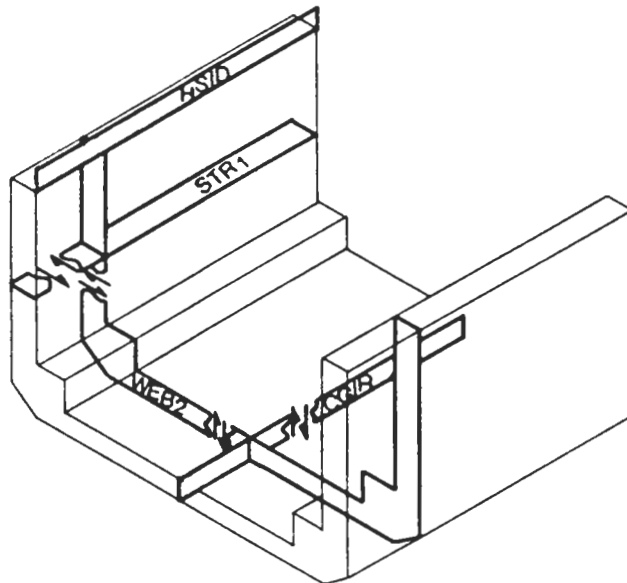


Fig.4.1 Structural members for which wave induced stresses have been calculated. Used definition of positive shear stresses is indicated.

Response spectrum for stresses in an irregular sea, S_σ , is calculated in usual way by multiplying the square of the linear response function $T_\sigma = \sigma/h$ by a stationary stochastic wave spectrum S_w over the range of frequencies:

$$S_\sigma(\omega) = S_w(\omega) T_\sigma(\omega)^2 \quad (4.1)$$

The variance of the stress response is equal to the area under the response spectrum, and under assumption of narrow banded spectra, the stress maxima follows a Rayleigh probability distribution. The "significant" stress response amplitude $\bar{\sigma}_{1/3}$, i.e the mean value of the largest one third of the stress maxima is calculated according to:

$$\bar{\sigma}_{1/3} = 1.416 * \text{SQRT} \left[2 \int_0^\infty S_\sigma(\omega) d\omega \right] \quad (4.2)$$

Non-linear response in irregular sea can not be calculated in the usual way by superposition of responses at different frequencies. Instead it must be evaluated from time simulation series. No such calculations have yet been performed, and therefore only non-linearities in regular waves are discussed in this report.

Stress response functions in irregular seas are in this report calculated for two-parameter wave spectra of the Pierson-Moskowitz type according to:

$$S_w(\omega) = \frac{\bar{H}_{1/3}^2}{8\pi^2} \frac{2}{\omega \bar{T}} \left(\frac{2\pi}{\omega \bar{T}} \right)^5 \text{EXP} \left[-\frac{1}{\pi} \left(\frac{2\pi}{\omega \bar{T}} \right)^4 \right] \quad (4.3)$$

Wave spectra for ten mean periods, ranging from 4 s to 13 s, as shown in fig.4.2, have been used in the calculations.

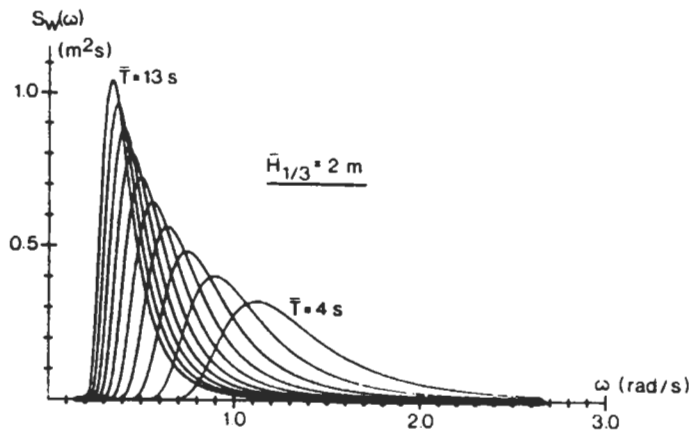


Fig.4.2 Pierson-Moskowitz two-parameter wave spectra

4.1 Ship motion and load characteristics

Responses of pitch, heave and roll motions, and of global hull girder sectional moments, are presented in figs.4.3-6. They have been calculated with the SCORES strip program by Kaplan and Raff, [40], used in program WAIST. Calculated motions in fig.4.3 also compared with results from a strip program based on the theory of Salvesen, Tuck and Faltinsen, [41].

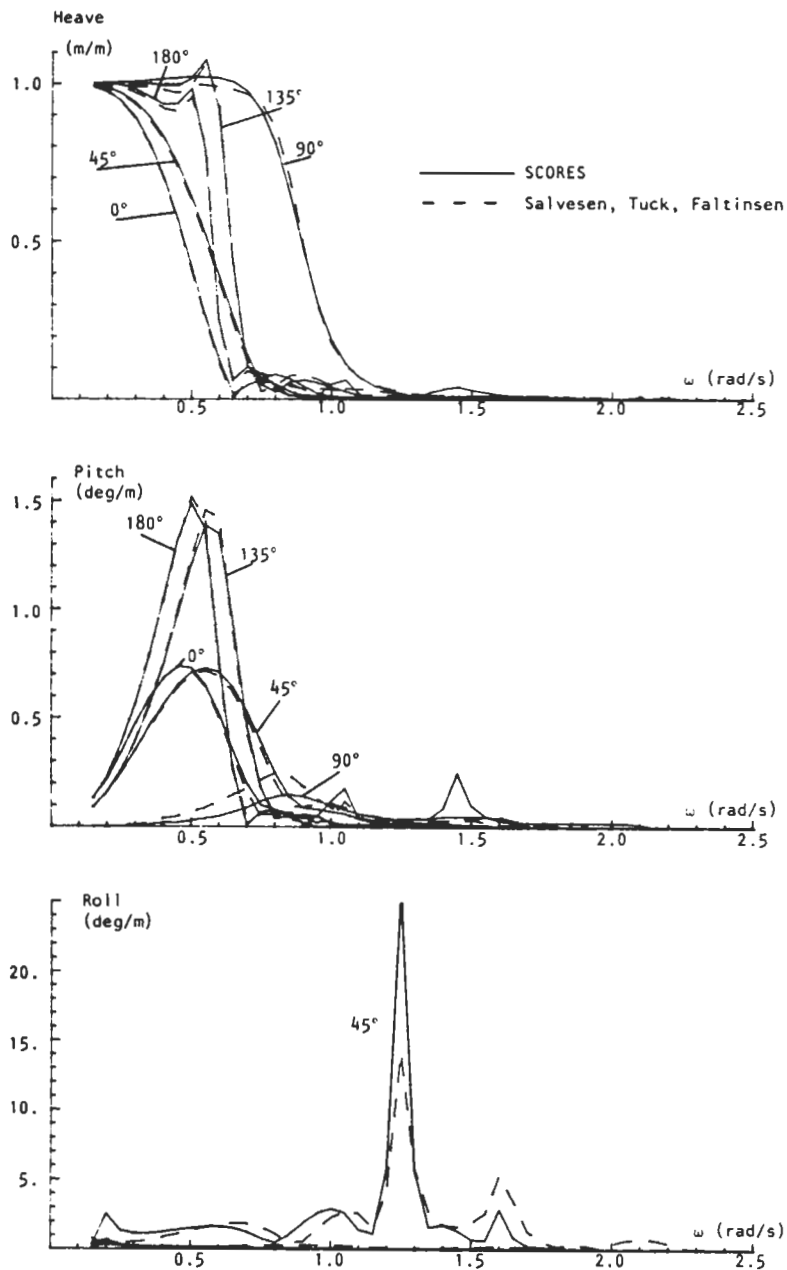


Fig.4.3 Ship motion response amplitude per wave amplitude in regular waves

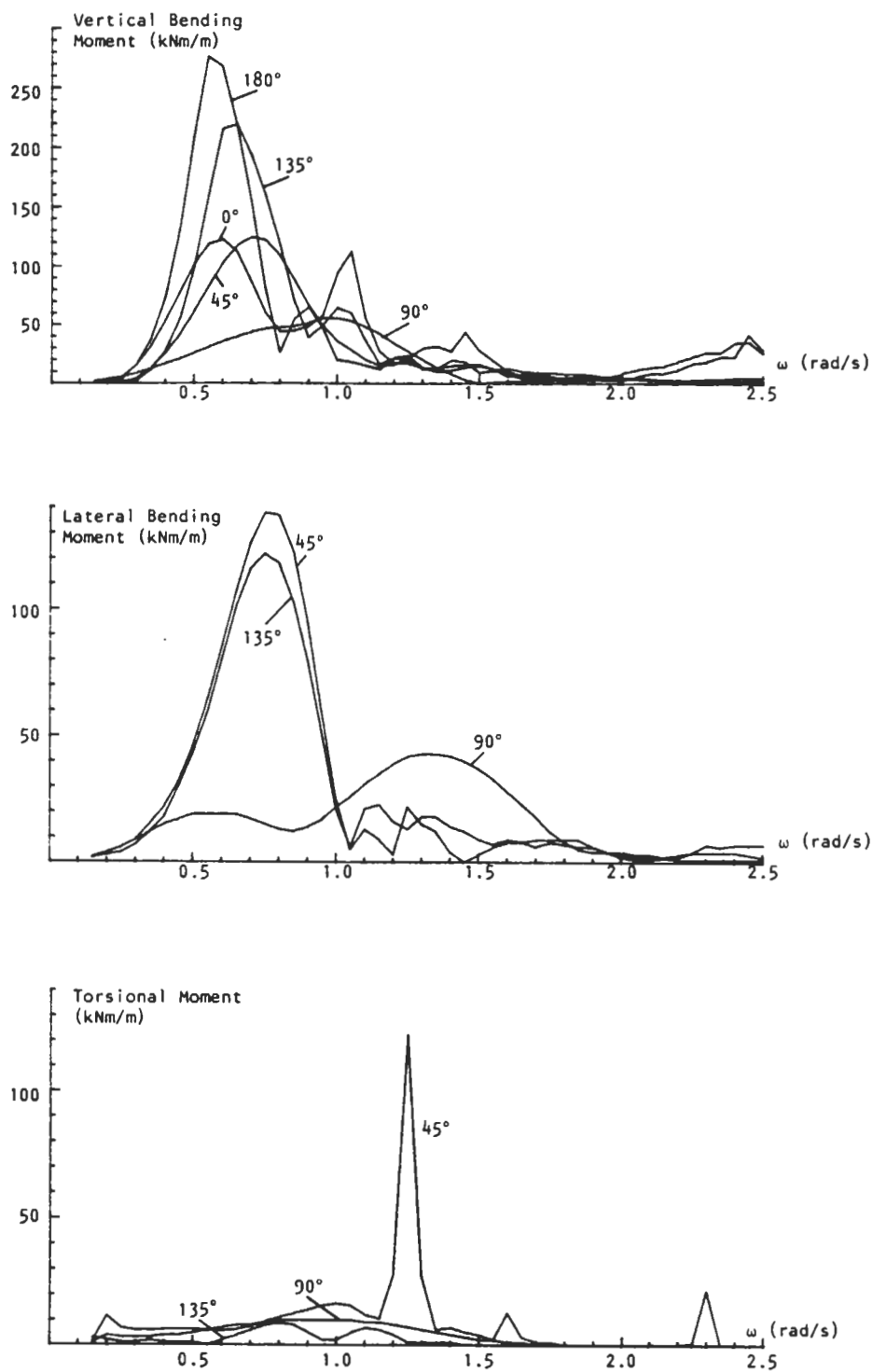


Fig.4.4 Ship hull girder bending and torsional moments response amplitude per wave amplitude at midship section in regular waves

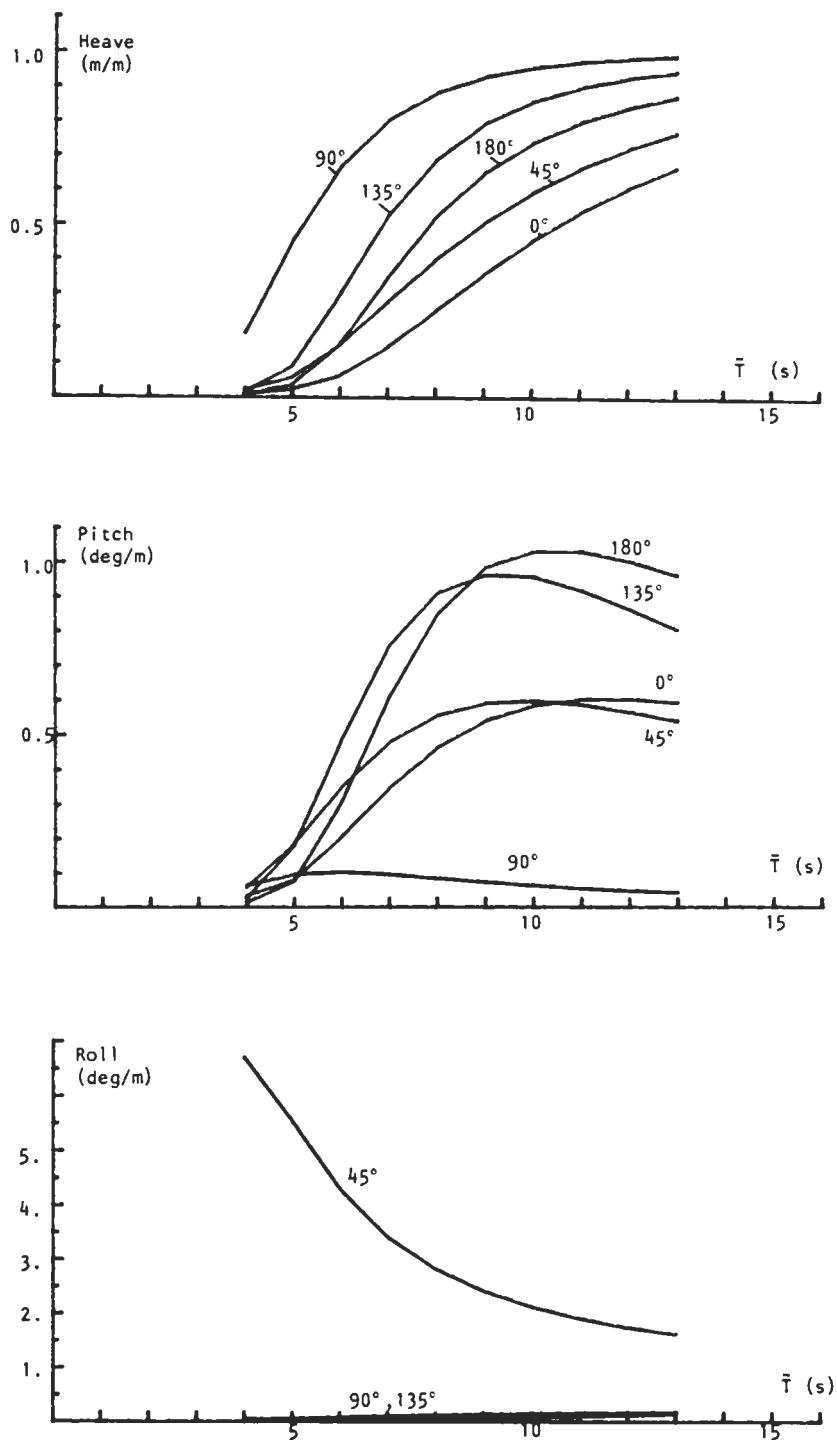


Fig.4.5 Ship motion response in irregular long-crested sea, significant response amplitude per significant wave amplitude

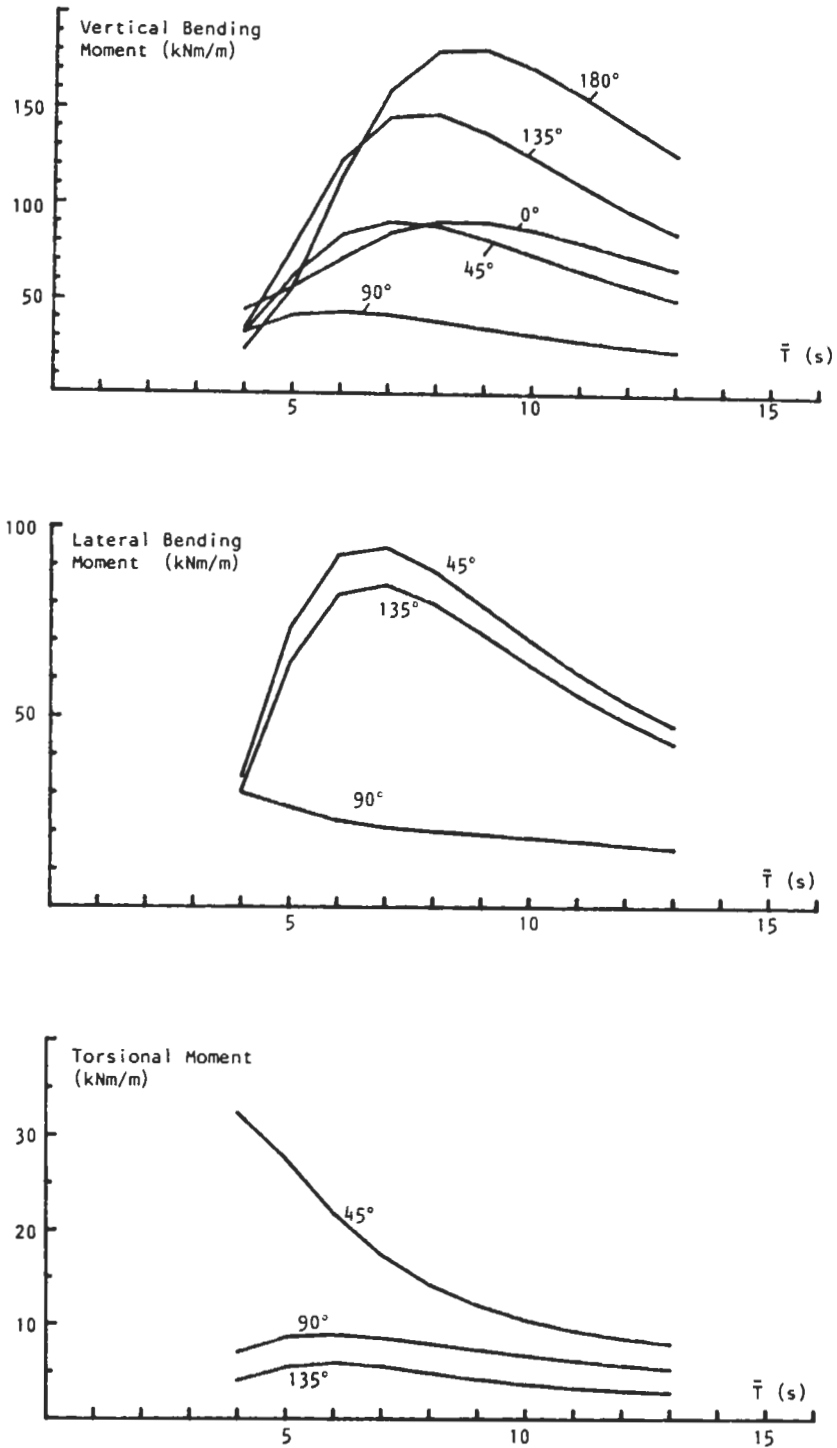


Fig.4.6 Ship hull girder bending and torsional moments response at midship section in irregular long-crested sea, significant response amplitude per significant wave amplitude

The hydrodynamic pressure is calculated with a method developed by Tasai, [42], [43], at 20 positions along each section. Figs.4.7-8 show distributions of components and combined pressure amplitudes at midship section for two different wave headings.

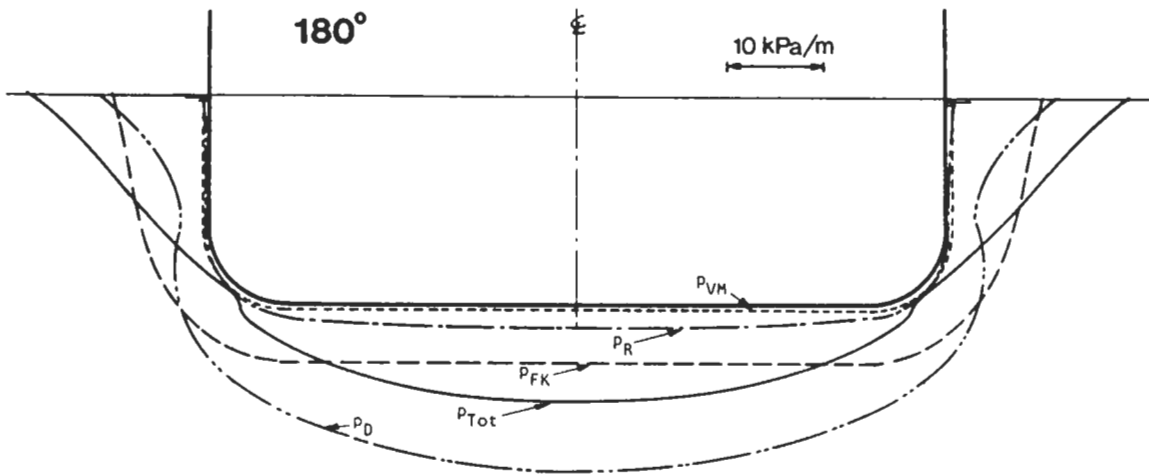


Fig.4.7 Distribution of hydrodynamic pressure amplitudes per wave amplitude at midship section in regular waves. Wave heading 180 deg, wave frequency 0.75 rad/s

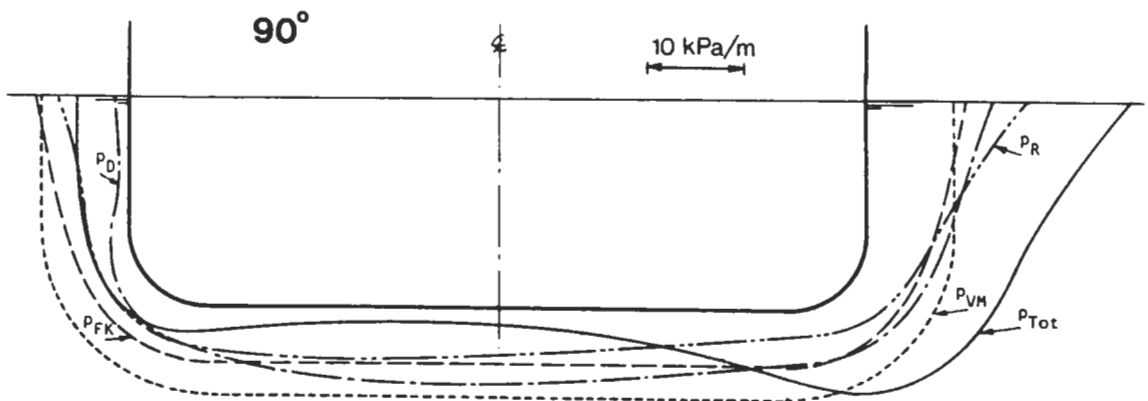


Fig.4.8 Distribution of hydrodynamic pressure amplitudes per wave amplitude at midship section in regular waves. Wave heading 90 deg, wave frequency 0.75 rad/s

4.2 Stress components

The combined stress response functions are determined by the amplitudes and relative phases of the various load components. Different components dominates at different frequency intervals, or at different positions in the structure. In longitudinal members, the hull girder bending moments are of major importance in the midship area, when the stress position is far from the neutral axes of bending. However, at beam seas or at positions close to the ship ends, the local loads usually dominate. In transverse members, the local pressure load is the largest component but the local massforce load is of significant importance since it often reduces the combined stress response due to relative differences in phases.

From the figures in the two appendices it is possible to get a good picture of the relative qualitative and quantitative importance of the various load components.

The stress response functions for regular waves show very large narrow banded peaks at headings ± 45 deg and wave frequency 1.25 rad/s. The encountering frequency at this condition is 0.178 rad/s which is equal to the resonance frequency of roll for the ship, see also fig.4.3. At the resonance frequency, the roll response is very sensitive to the damping which is known to be non-linear, increasing with the amplitude. This has not been taken into account in the presentation of combined non-linear stresses. In irregular seas with mean wave periods over 7s, the spectrum energy at wave frequency 1.25 rad/s is low, and consequently, the narrow peak of roll resonance does only have a major influence on the irregular stress response at low mean periods.

The relative phase between different components varies with the frequency. In some cases this causes very irregular combined response functions for regular waves, see e.g page A1.2. However, when these functions are combined with irregular sea spectra, the significant response becomes a smooth function of the wave mean period.

The importance of phase lag is clearly shown when comparing stress response from vertical and horizontal bending moments in stringer 1 at web 2. At a heading of 135 deg, page A1.24 , the components are in phase and combined stress is about the sum of the two, while at -135 deg, page A1.28, combined stress is less then each individual component.

Stringer 1

The combined normal stress in stringer 1 is primarily determined by the vertical and horizontal bending moments and at the bulkhead, (web 0), also by the local hydrodynamic pressures. Contributions from all five components are however significant.

Hydrodynamic pressure is the most important load component for shear stress in the stringer but there is a significant contribution from mass forces at headings ± 45 deg and 90 deg.

Example of significant stresses in irregular seas for different headings and for different longitudinal positions are shown in figs.4.9-12.

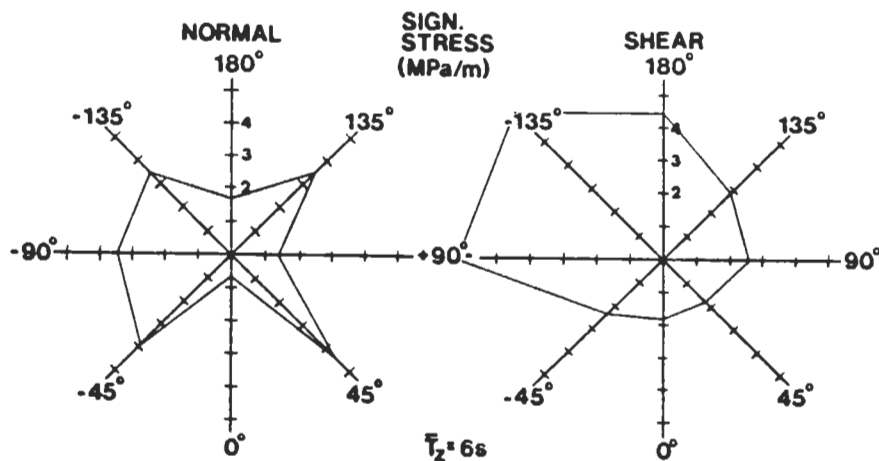


Fig.4.9 Stringer 1 at web 0; linear significant stress response amplitude per significant wave amplitude in irregular sea

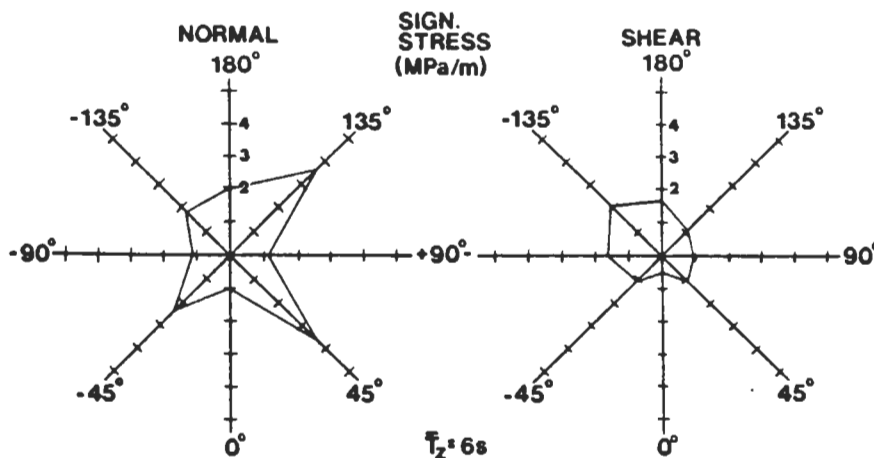


Fig.4.10 Stringer 1 at web 2; linear significant stress response amplitude per significant wave amplitude in irregular sea

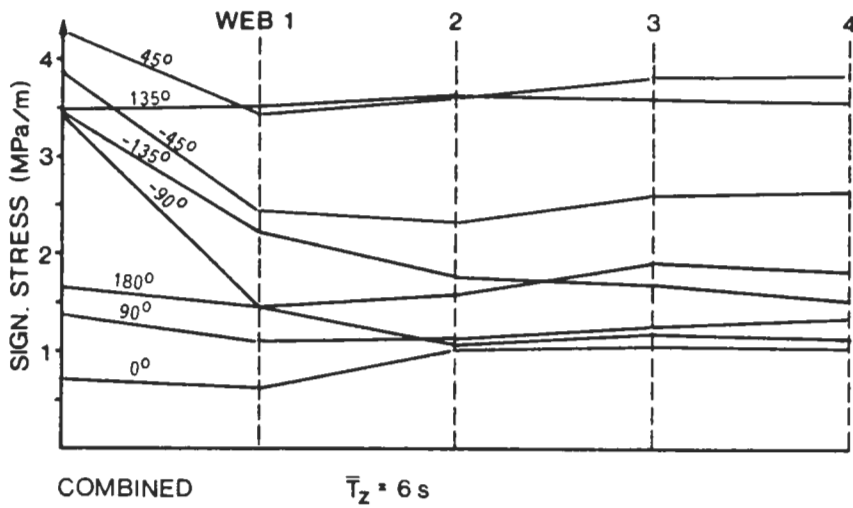
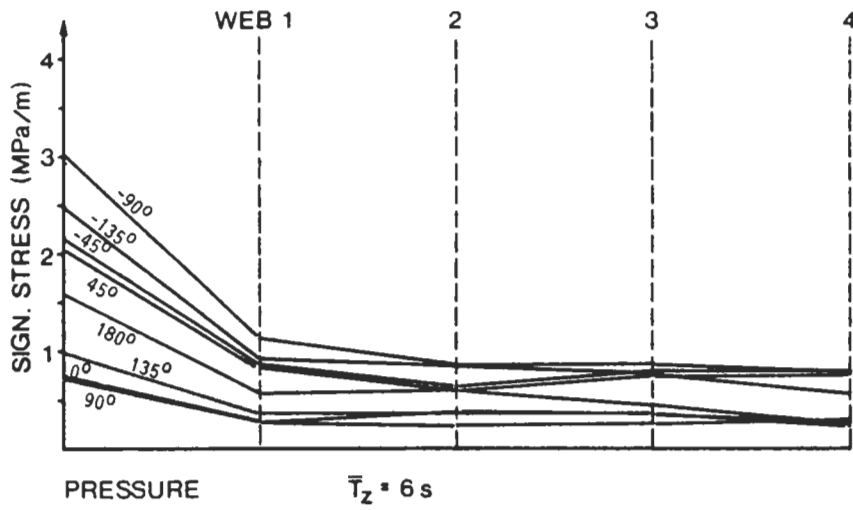


Fig.4.11 Stringer 1; longitudinal distribution of normal stress response in irregular sea

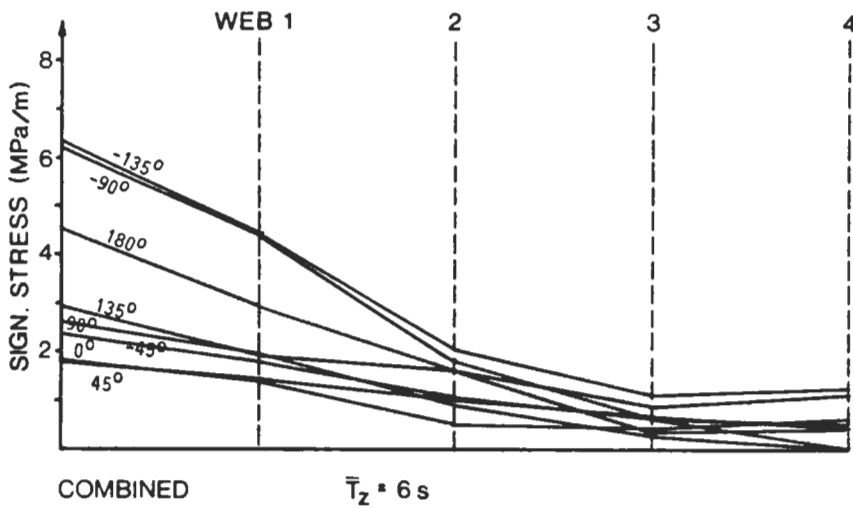


Fig.4.12 Stringer 1; longitudinal distribution of shear stress response in irregular sea

Center girder

Calculated stresses in the center girder are higher than in stringer 1 and web 2. Combined normal stresses are primarily determined by vertical bending moment with significant contribution from local pressure at the bulkhead, (web 0), for headings ± 135 deg and 180 deg. Combined shear stresses are primarily based on local pressure. Shear stress levels at web 2 are about half the values at web 0.

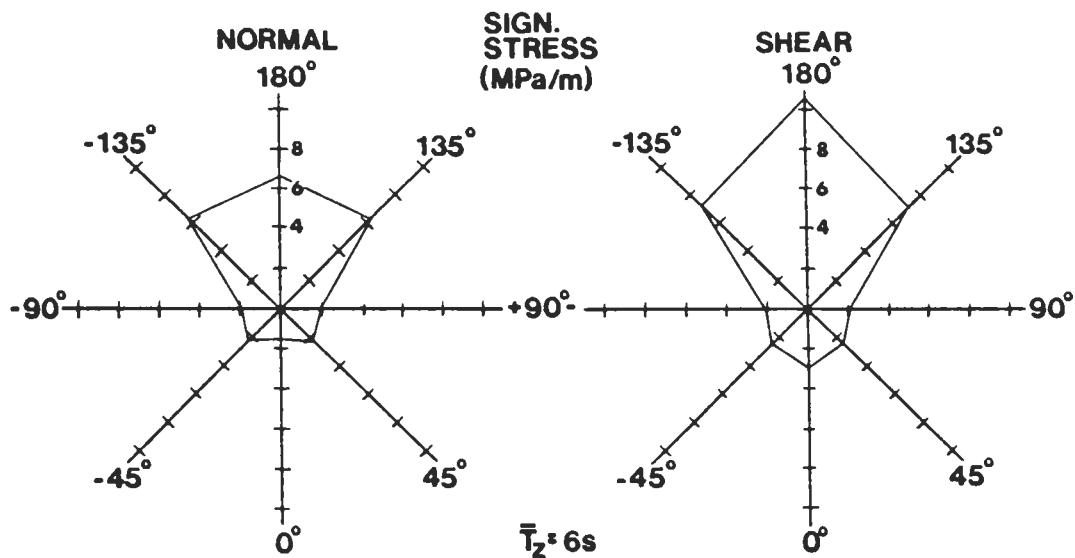


Fig. 4.13 Center girder at web 0; linear significant stress response amplitude per significant wave amplitude in irregular sea

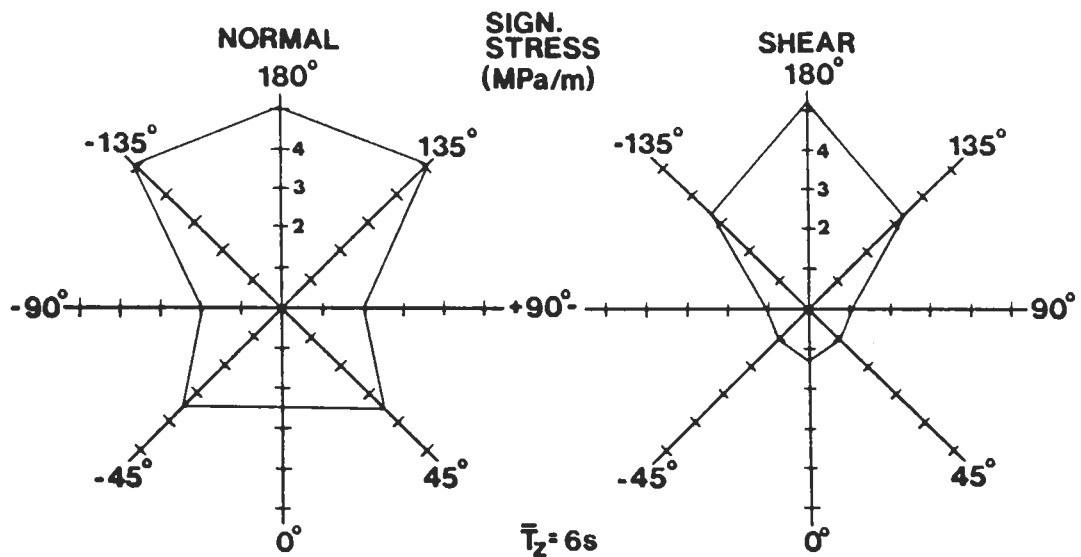


Fig. 4.14 Center girder at web 2; linear significant stress response amplitude per significant wave amplitude in irregular sea

Web 2

For transverse members both normal and shear stresses are determined by local loads only. In web 2 the pressure components are in most cases more than twice as large as the massforce components.

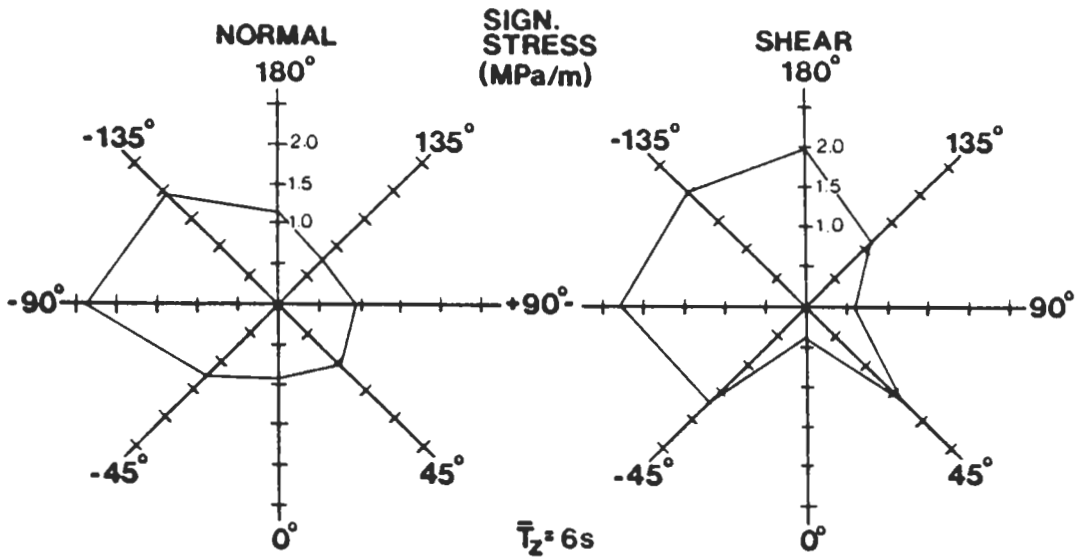


Fig. 4.15 Web 2 at stringer 1; linear significant stress response amplitude per significant wave amplitude in irregular sea

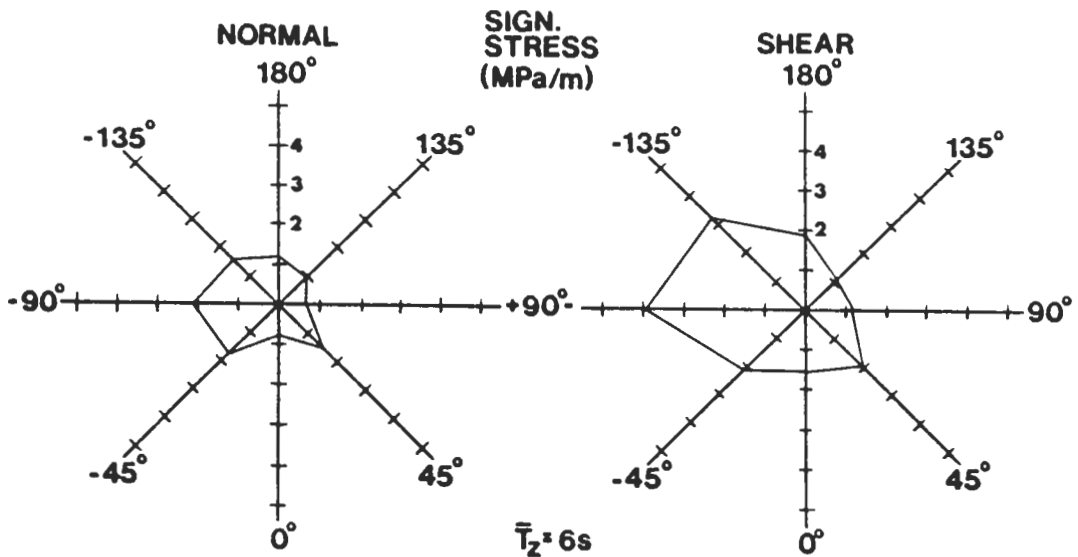


Fig. 4.16 Web 2 at stringer 2; linear significant stress response amplitude per significant wave amplitude in irregular sea

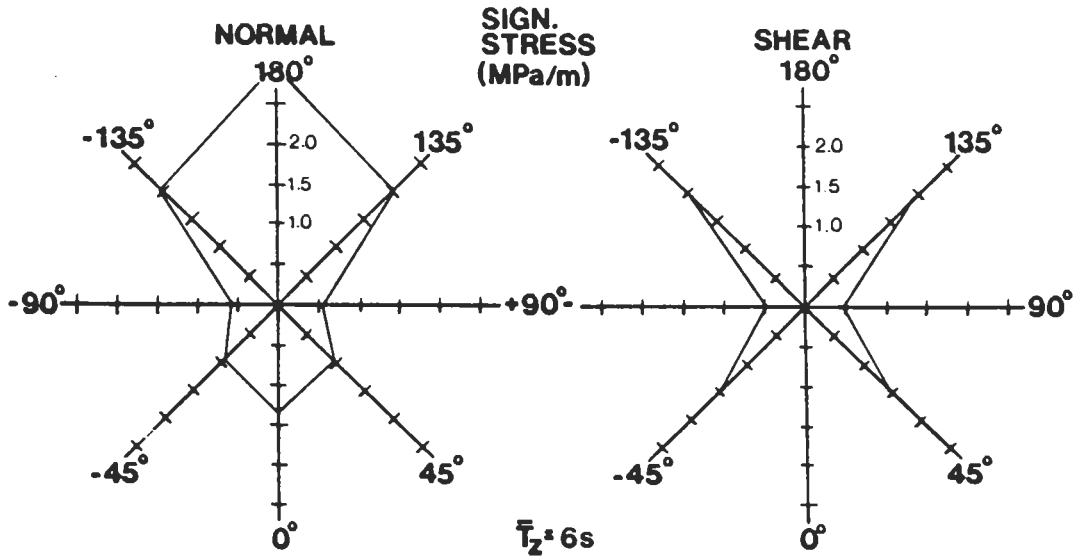


Fig.4.17 Web 2 at center girder; linear significant stress response amplitude per significant wave amplitude in irregular sea

Hatch side coaming

Normal stresses calculated at top of the hatch side coaming are higher than any other calculated nominal stress in the four studied members. The combined stress is determined by the vertical bending moment but with significant contributions from other components at headings ± 45 deg and ± 90 deg.

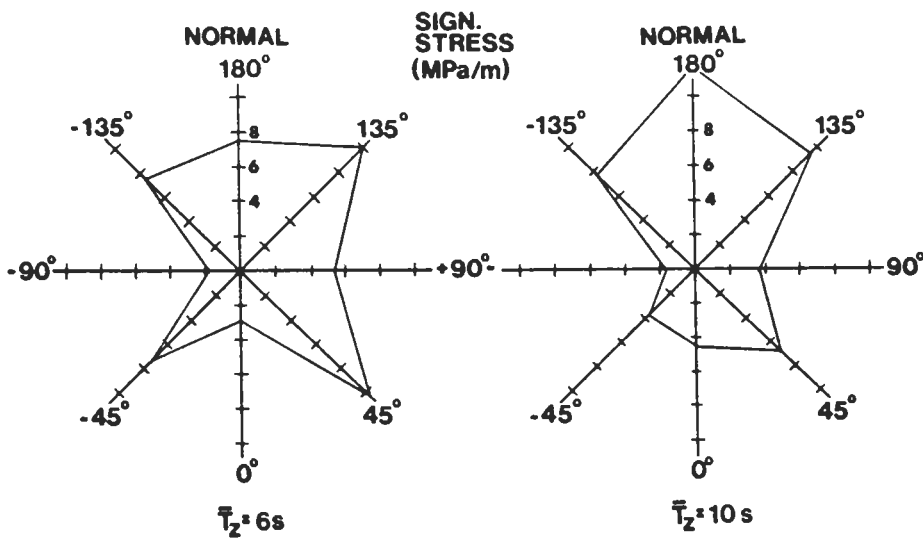


Fig.4.18 Hatch side coaming at web 0; linear significant stress response amplitude per significant wave amplitude in irregular sea

4.3 Non-linear stress response

Non-linear, non-harmonic pressure fluctuations close to the still water line induce non-linearities in the stress responses for members at the side. The influence of this on the combined stresses is shown in App.1 where transfer functions are presented for wave amplitudes h of 0,2,4,6,8 m. 0 m represents here linear superposition.

Both stringer 1 and web 2 at side are significantly affected while in practice the stress response at center girder and hatch side coaming is linear. Generally, non-linearities increase with the wave frequency.

Non-linear stress amplitudes can be evaluated either from peak values as $(\max-\min)/2$ or from *rms*-values calculated from the time step values during one cycle. The first alternative seems appropriate when considering fatigue. However, when several regular stress responses of different frequencies are combined in an irregular sea, the *rms*-value is more relevant for the combined irregular stress response. In App.1 all the non-linear responses are represented by $\text{SQR}(2) \cdot \text{rms}$ which is equivalent to the amplitude of a harmonic variation. There is in most cases no significant difference between the two representations of non-linear amplitude.

A typical example of time step values of non-linear stress response is shown in fig.4.19.

Interaction between different stress components varies with the wave frequency and there seems to be no simple formula by which non-linearities in the combined stress response can be described. To get an overview of the levels, Tables 4.1-2 have been prepared using:

$$T_{\sigma}(h, \omega) = T_{\sigma}(0, \omega) \cdot (1 + qh) \quad (4.4)$$

where T_{σ} is response function σ/h , and q is a first order non-linear factor.

Only pressure induced stress is treated as non-linear and consequently factor q for combined stress is only large at positions and frequencies where the pressure induced stress component is significant for the total combined stress. This can be observed in table 4.1 when comparing normal stress in stringer 1 at web 0 and web 2 respectively. The pressure induced stress component is at web 2 less than half the value at web 0, while stress responses from global hull forces are approximately the same, see App.1.

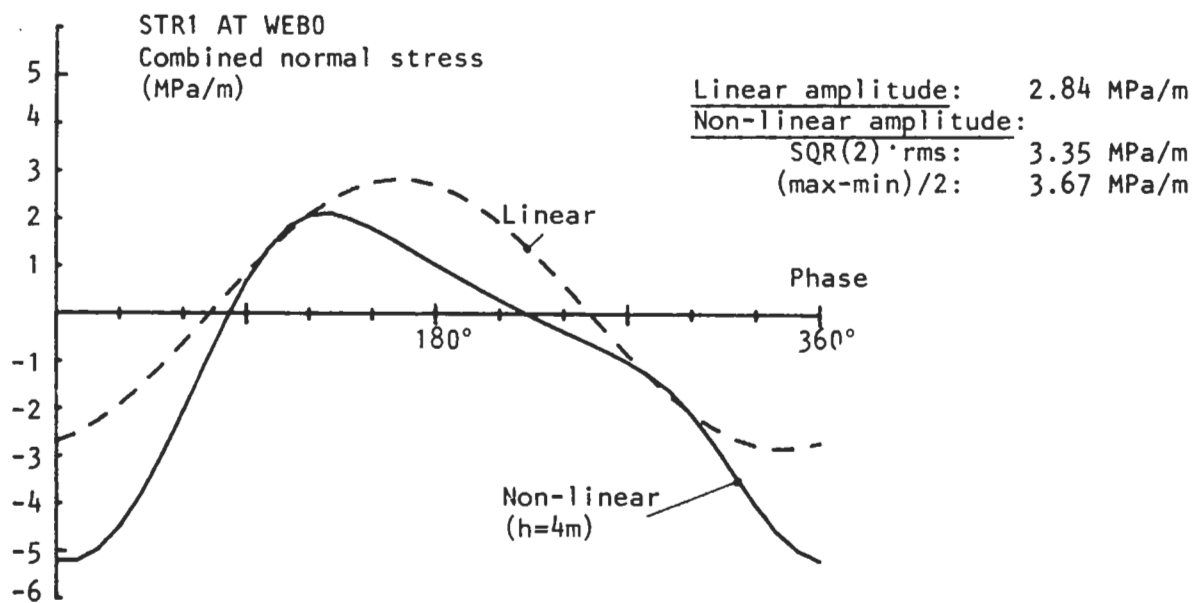
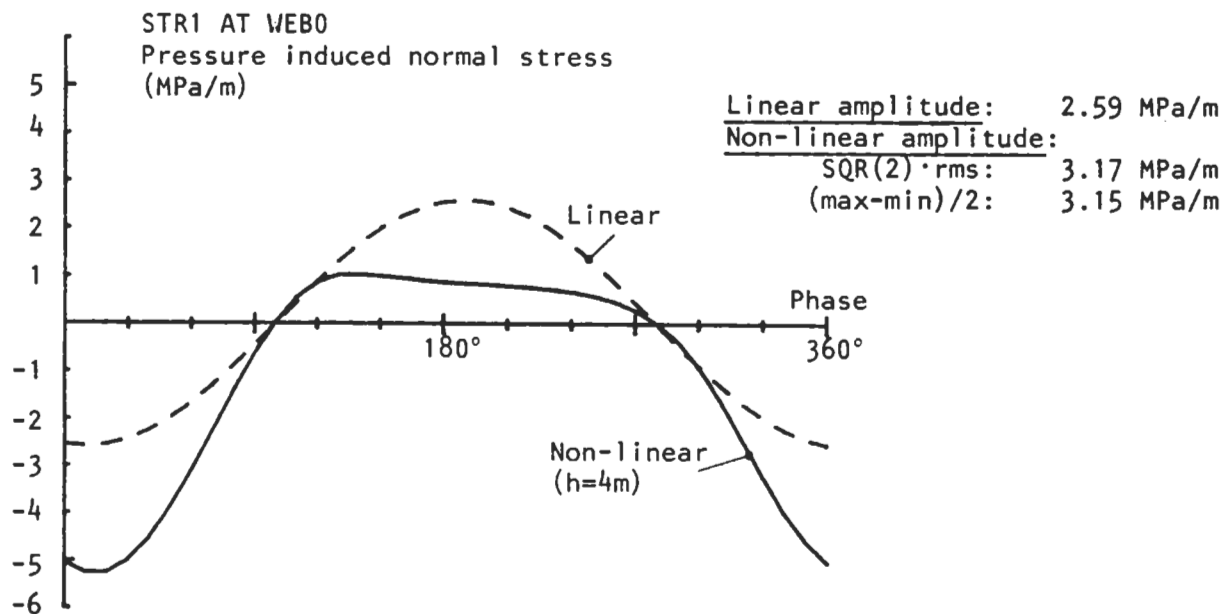


Fig. 4.19 Example of time step values of non-linear stress response
Wave height 4 m, wave heading -135 deg, wave frequency
0.60 rad/s

$$T_{\sigma}(h, \omega) = T_{\sigma}(0, \omega) * (1 + qh)$$

		$\omega=0.45$ $\lambda=1.6L$		$\omega=0.60$ $\lambda=0.9L$		$\omega=0.80$ $\lambda=0.5L$	
position	heading	q	\bar{q}	q	\bar{q}	q	\bar{q}
Stringer 1 at Web 0	0	.001		.002		.022	
	45	.002		.004		.002	
	90	.000		.007		.053	
	135	.000		.004		.003	
	180	.000		-.001		.041	
	-135	.002		.045		.031	
	-90	.002		.018		.075	
	-45	.001	.001	.004	.010	.007	.029
Stringer 1 at Web 0	0	.004		.021		.026	
	45	.082		.086		.016	
	90	.005		.002		-.008	
	135	.001		-.002		.018	
	180	.001		.040		.041	
	-135	.008		.061		.057	
	-90	.012		.042		.110	
	-45	.051	.020	.044	.037	.034	.038
Stringer 1 at Web 2	0	-.002		.000		.015	
	45	.000		.001		.000	
	90	.000		.000		.000	
	135	.000		.000		.001	
	180	.000		.002		.060	
	-135	.001		.011		.013	
	-90	.000		.003		.056	
	-45	.000	.000	.000	.002	-.001	.018
Stringer 1 at Web 2	0	.000		.025		.053	
	45	.052		.433 *)		.024	
	90	.001		-.004		-.022	
	135	.002		-.021		.014	
	180	.000		.031		.038	
	-135	.017		.075		.064	
	-90	.017		.092		.191	
	-45	.024	.014	.087	.090 *)	.062	.053

*) The high value of non-linear factor q is obtained because the linear value of stress response is close to zero at this heading and frequency.

Table 4.1 Stringer 1; Non-linear factor q evaluated at a wave amplitude of 4m.

$$T_{\sigma}(h, \omega) = T_{\sigma}(0, \omega) * (1 + qh)$$

		$\omega=0.45$ $\lambda=1.6L$		$\omega=0.60$ $\lambda=0.9L$		$\omega=0.80$ $\lambda=0.5L$	
position	heading	q	\bar{q}	q	\bar{q}	q	\bar{q}
	0	.001		.008		.012	
	45	.009		.017		.008	
Web 2	90	.001		.002		.004	
at	135	.000		.007		.019	
Stringer 1	180	.000		.028		.046	
	-135	.003		.039		.050	
σ	-90	.004		.020		.066	
	-45	.006	.003	.014	.016	.018	.028
	0	-.007		-.100		-.129	
	45	-.019		-.056		-.037	
Web 2	90	.000		.000		.025	
at	135	.000		.002		-.013	
Stringer 1	180	.000		-.072		-.063	
	-135	-.003		-.098		-.116	
τ	-90	-.006		-.050		-.128	
	-45	-.008	-.005	-.035	-.051	-.100	-.070
	0	-.001		-.009		-.015	
	45	-.005		-.014		-.010	
Web 2	90	.000		.000		.012	
at	135	.000		.005		-.003	
Stringer 2	180	.000		-.017		-.018	
	-135	-.001		-.028		-.031	
σ	-90	-.001		-.012		-.039	
	-45	-.002	-.001	-.010	-.011	-.018	-.015
	0	.000		-.003		-.005	
	45	-.001		-.006		-.002	
Web 2	90	.001		.001		.000	
at	135	.001		.004		.008	
Stringer 2	180	.001		.002		.013	
	-135	.001		.001		.007	
τ	-90	.002		.001		.012	
	-45	.001	.001	-.002	.000	-.004	.004

Table 4.2 Web 2; Non-linear factor q evaluated at a wave amplitude of 4m.

4.4 Correlation of normal and shear stress in irregular sea

Correlation between combined normal and shear stress has been calculated using a correlation coefficient $\rho_{\sigma\tau}$ according to

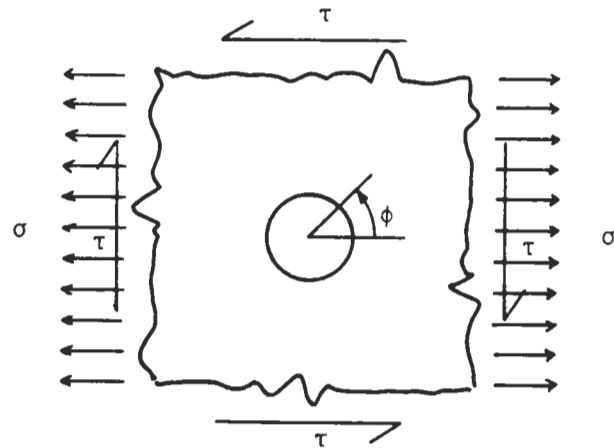
$$\rho_{\sigma\tau} = [(\overline{\sigma+\tau})_{1/3}^2 - \overline{\sigma}_{1/3}^2 - \overline{\tau}_{1/3}^2] / [2\overline{\sigma}_{1/3}\overline{\tau}_{1/3}] \quad (4.5)$$

$\rho_{\sigma\tau}$ is shown together with combined significant stresses as function of mean wave period in App.2.

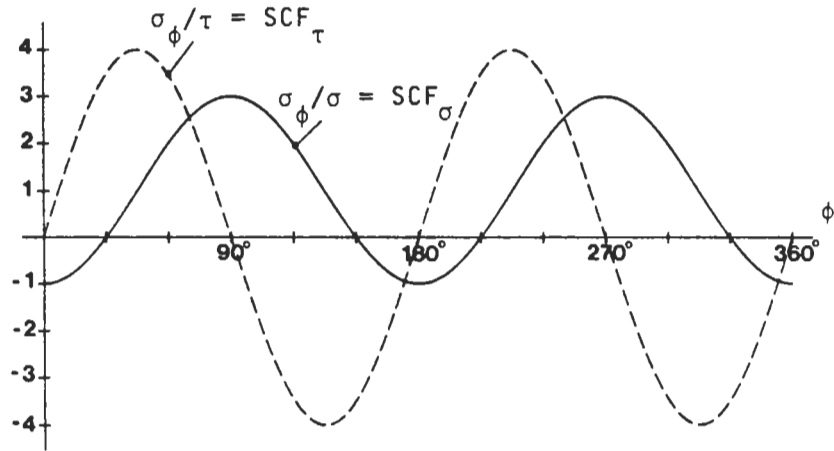
For longitudinal members no general conclusion can be drawn from the results. There is however a significant change of correlation in the interval between mean periods 5 s and 8 s. The transverse web 2 shows a very close correlation between normal and shear stress at side while there is no correlation in the web at center girder.

Correlation coefficients can be used for calculation of hot-spot stress response from nominal stress response with the use of stress concentration factors. If the hot spot stress is coupled to nominal normal stress with stress concentration factor SCF_{σ} , and to nominal shear stress with SCF_{τ} , the significant value in irregular sea becomes:

$$\begin{aligned} \overline{\sigma}_{hs1/3} = & \text{SQRT} [SCF_{\sigma}^2 \overline{\sigma}_{1/3}^2 + SCF_{\tau}^2 \overline{\tau}_{1/3}^2 + \\ & + \rho_{\sigma\tau} 2 SCF_{\sigma} SCF_{\tau} \overline{\sigma}_{1/3} \overline{\tau}_{1/3}] \quad (4.6) \end{aligned}$$



Distribution of stress concentration around hole edge



Distribution of significant stress at hole edge, ($\bar{\sigma}_{1/3}=1, \bar{\tau}_{1/3}=1$)

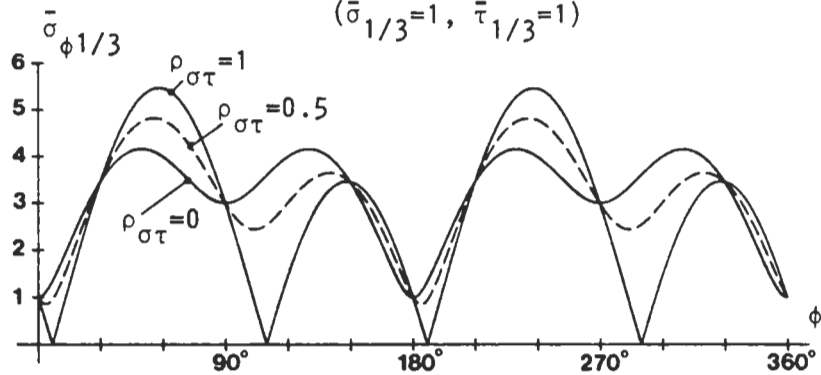


Fig.4.20 Example of stress concentrations around a circular hole in a large plate, subjected to both uniaxial normal stress and shear stress. Influence of correlation coefficient between significant nominal stresses in irregular sea.

4.5 Comments on calculation procedure and results

Results presented in this report are not being claimed to be dramatic in any sense. The studied members have been chosen because they are subjected to different types of combined loadings, rather than to the worst.

Stringer 1 is representative of members where all load components are important. The choice of inner shell interaction as studied stress position is based on this purpose, since the relative proportion of pressure induced stresses and stresses induced by horizontal bending moment is higher here than at the outer shell. The center girder represents a member where one single load component, vertical bending moment, is dominant for normal stress, while web 2 is representative to any transverse member, subjected only to local loads. Finally, the hatch side coaming is the most severely loaded member in the hold.

When judging the nominal stress levels presented here, one must bear in mind that the local stress concentrations can be very different for different strength members, and furthermore, the still water loads must be taken into account.

A complete picture of possible low-frequency wave induced stresses can only be obtained by calculating response at different probable loading conditions and speeds. For the type of vessel investigated here, the draft, trim and mass distribution vary little between different conditions. The speed will however in rough seas be voluntarily reduced, and this should be taken into account when estimating long-term extreme stresses. Two examples of influence of speed reduction on stress response is shown in figs.4.21-22.

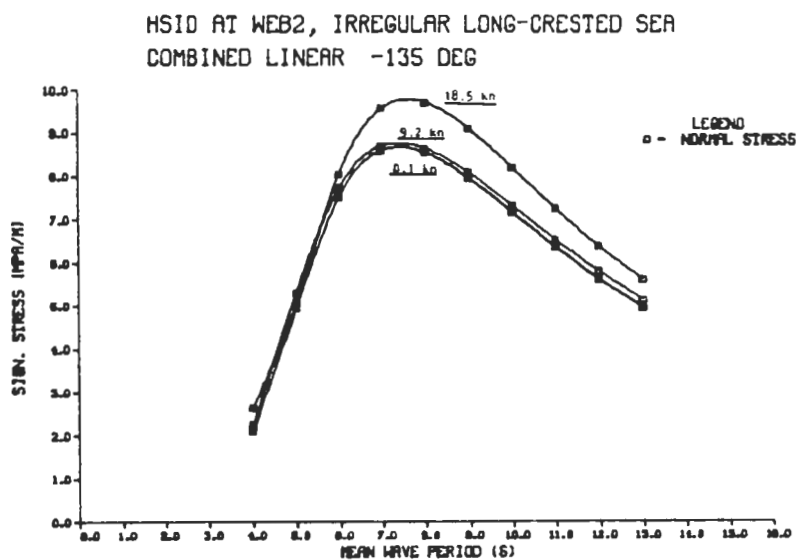


Fig. 4 21 Hatch side coaming at web 2; Stress response in irregular sea. Influence of speed reduction

WEB2 AT STR1, IRREGULAR LONG-CRESTED SEA
COMBINED LINEAR -135 DEG

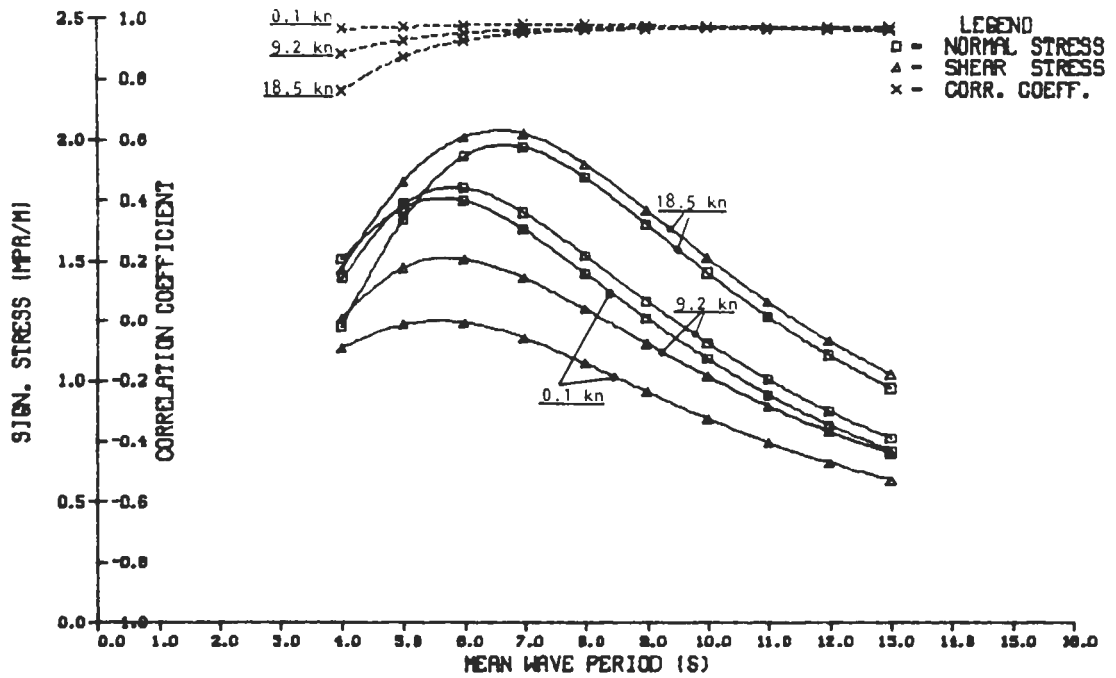


Fig.4.22 Web 2 at stringer 1; Stress response in irregular sea.
Influence of speed reduction

Non-linearities are in this report only correlated to the non-linear pressure distribution close to the still water line. Other non-linearities such as roll damping and non-vertical sides are not taken into account. Nor is the radiated or diffracted wave height included in the calculation of relative motion. In moderate seas these errors are by judgment small compared with other uncertainties involved in the procedure.

Computational costs for the calculations are reasonable. Stress response calculation for one member takes about 12 minutes CPU on a Cyber 180-830 computer. This includes 51 regular wave frequencies, 8 angles of heading and 10 irregular sea spectra. Local stress response is in this example defined by 120 influence coefficients at 4 sections for pressure, and 46 coefficients for massforce for normal and shear stress respectively.

5 CONCLUSIONS AND FURTHER WORK

In this report is shown that it is possible to calculate low-frequency wave induced stress response anywhere in a ship structure, in a direct and rational way. The major advantages of the direct procedure in comparison with an ordinary "design load" procedure are:

- * The relative importance of different load components can be evaluated
- * The actual correlation between load components is taken into account
- * Nominal and hot-spot stresses can be determined at any probability level in the long-term stress history.

As consequence of these advantages the direct procedure can be a valuable tool when designing vessels with new types of structures or vessels for certain specified environmental conditions. Computational and man-time costs can be kept low with the present method and it could even be used for ordinary design purposes, if an optimized structure with respect to fatigue is desired.

Results from calculations of stress response at the midship hold of the container ship show reasonable dynamic stress levels. However, the accuracy of the levels is difficult to judge since no measurements have been performed at the actual ship. Although previous studies show good agreement between calculated and measured stresses from global loads, local load calculations are not yet sufficiently confirmed by experiments or full scale measurements.

The present study also shows the existence of significant non-linearities in the stress response functions at ship sides due to the non-linear variation of hydrodynamic pressure close to the still water line.

In the continuation of this work, stress responses will be calculated for an OBO carrier with a completely different type of hull structure. Results from these two ships will be further analysed with long-term wave statistics to evaluate local stress histories for different structural members.

ACKNOWLEDGEMENT

This research project is to a major part financed with funds from the Swedish Board for Technical Development (STU) and the Swedish Shipyard Association (SVF).

The Johnson Line AB has kindly supported the study by making all structural plans and calculations of the container ship BO JOHNSON available.

The following computer programmes have been used:

- * HP-FE, [44], for FE-calculations of the structure
- * WAIST, [16], for calculation of response to waves
- * DISSPLA, [45], for graphic presentation of results

I wish to acknowledge the valuable assistance of Henrik Hannus in the realization of the computer programme WAIST. In [46], Hannus did present some early preliminary results from stress response calculations of the same ship structure as studied in this report. It is however important to point out for the reader that those results were based on a different approach of non-linear pressure induced stress calculation, and that they furthermore did not include influence from mass forces.

I also wish to thank my colleague Jianbo Hua for stimulating discussions and assistance concerning the hydrodynamic aspects of the calculation procedure.

This work has been performed under the supervision of professor Erik Steneroth. The contribution from his experience is highly appreciated.

REFERENCES

- [1] Third International Ship Structures Congress, Oslo 1967
Report of Committee No 10 on "DESIGN PROCEDURE"
- [2] Lewis E.V., Hoffman D., Maclean W.M., van Hooff R., Zubaly R.B.,
LOAD CRITERIA FOR SHIP STRUCTURAL DESIGN
Ship Structure Committee, Report SSC-240, 1973
- [3] Evans J.H., editor
SHIP STRUCTURAL DESIGN CONCEPTS
Cornell Maritime Press, Maryland, 1975
- [4] Hughes O.,
SHIP STRUCTURAL DESIGN: A RATIONALLY-BASED, COMPUTER-AIDED,
OPTIMIZATION APPROACH
John Wiley & Sons, New York, 1983
- [5] Faulkner D., Sadden J.A.,
TOWARD A UNIFIED APPROACH TO SHIP STRUCTURAL SAFETY
RINA Transactions, 1978
- [6] Stiansen S.G., Mansour A., Jan H.Y., Thayamballi A.,
RELIABILITY METHODS IN SHIP STRUCTURES
RINA Transactions, 1979
- [7] Mansour, A.E, Jan H.Y., Ziegelman C.I., Chen Y.N., Harding S.J.,
IMPLEMENTATION OF RELIABILITY METHODS TO MARINE STRUCTURES
SNAME Transactions, 1984
- [8] Soares C.G.,
PROBABILISTIC MODELS FOR LOAD EFFECTS IN SHIP STRUCTURES
Department of Marine Technology, The Norwegian Institute of
Technology, Report UR-84-38, 1984
- [9] Lewis E.V., Zubaly R.B.,
PREDICTING HULL BENDING MOMENTS FOR DESIGN
SNAME, Paper presented at Extreme Loads Response Symposium, Arlington
1981
- [10] Ivanov L.D.,
STATISTICAL EVALUATION OF THE SHIP'S HULL CROSS SECTION GEOMETRICAL
CHARACTERISTICS AS A FUNCTION OF HER AGE
International Shipbuilding Progress, Vol 33, 1986
- [11] Det Norske Veritas, 1983
MOBILE OFFSHORE UNITS, CLASSIFICATION NOTE, FATIGUE STRENGTH ANALYSIS
- [12] Gurney T.R.,
FATIGUE DESIGN RULES FOR WELDED STEEL JOINTS
The Welding Institute Research Bulletin, Vol 17, 1976

- [13] Munse W.H., Wilbur T.W., Tellalian M.L., Nicoll K., Wilson K.,
FATIGUE CHARACTERIZATION OF FABRICATED SHIP DETAILS FOR DESIGN
Ship Structure Committee, Report SSC-318
- [14] Tomita Y., Fujimoto Y.,
AN ANALYSIS FOR FATIGUE FAILURE OF SHIP STRUCTURAL MEMBERS
JSNA Kansai, No 187, 1982,
- [15] 6th International Ship Structures Congress, Boston 1976
Report of Committee V.1 "DESIGN PROCEDURE"
- [16] Huss M.,
WAIST, PROGRAM FOR CALCULATION OF WAVE INDUCED STRESSES IN SHIPS;
DESCRIPTION AND USERS MANUAL (In Swedish)
RIT, Div of Naval Architecture, Report TRITA-SKP 1058, Stockholm 1986
- [17] Westin H.,
LONG-TERM FORECAST OF DYNAMIC STRESSES IN A TRANSVERSE FRAMEWORK OF A
255 000 TDW TANKER (in Swedish)
RIT, Div of Naval Architecture, Report E-50, Stockholm 1977
- [18] Nagamoto R., Matsuyama M., Taguchi Y., Funaoka K., Sueoka H.,
Yuhara T.,
ON THE TRANSVERSE STRENGTH OF OIL TANKER IN IRREGULAR SEAS
(in Japanese)
Journal of SNAJ, Vol 140, 1976
- [19] Finnigan T.D., Petrauskas C., Bothelo D.L.R.,
TIME-DOMAIN MODEL FOR TLP SURGE RESPONSE IN EXTREME SEA STATES
OTC Proceedings 4657, 1984
- [20] Söding H.,
CALCULATION OF STRESSES ON SHIPS IN A SEAWAY
Schiff und Hafen, Heft 10, 1971
- [21] Abrahamsen E.,
STRUCTURAL DESIGN ANALYSIS OF LARGE SHIPS
SNAME Transactions, 1969
- [22] Little R.S., Lewis E.V.,
A STATISTICAL STUDY OF WAVE-INDUCED BENDING MOMENTS ON LARGE OCEANGOING
TANKERS AND BULK CARRIERS
SNAME Transactions, 1971
- [23] Hoffman D., Williamson J., Lewis E.V.,
CORRELATION OF MODEL AND FULL-SCALE RESULTS IN PREDICTING WAVE BENDING
MOMENT TRENDS
Ship Structure Committee, Report SSC-233, 1972
- [24] Hoffman D., van Hooff R., Lewis E.V.,
EVALUATION OF METHODS FOR EXTRAPOLATION OF SHIP BENDING STRESS DATA
Ship Structure Committee, Report SSC-234, 1972

- [25] Kikuiri H., Mathisen J.,
SOME CORRELATION COEFFICIENTS FOR WAVE INDUCED LOADS IN SERIES 60
SHIPS
Det norske Veritas, Report 73-2-S, 1973
- [26] Westin H.,
WAVE-INDUCED MOTIONS AND LOADS ON CONTAINERSHIPS
RIT, Div of Naval Architecture, 1977
- [27] Nitta A.,
BASIC DESIGN CRITERIA ON THE STRENGTH OF SHIP STRUCTURES
Proceedings from PRADS Symposium Tokyo, 1977
- [28] 6th International Ship Structures Congress, Boston 1976
Report of Committee I.3 "DESIGN LOADS"
- [29] Ulfvarsson A.,
COMBINED LOADS (in Swedish)
The Swedish Ship Research Foundation SSF, Report 5616:4, 1977
- [30] Caretti F.,
A COMPARISON BETWEEN THEORETICAL AND EXPERIMENTAL RESPONSE AMPLITUDE
OPERATORS OF WAVE PRESSURE ON HULLS
Registro Italiano Navale, Technical Bulletin No 73, 1980
- [31] Kim C.H.,
HYDRODYNAMIC LOADS ON THE HULL SURFACE OF A SEAGOING VESSEL
SNAME STAR Symposium Honolulu, 1982
- [32] Jensen J.J., Pedersen P.T.,
WAVE-INDUCED BENDING MOMENTS IN SHIPS - A QUADRATIC THEORY
RINA Transactions 1978
- [33] Jensen J.J., Pedersen P.T.,
BENDING MOMENTS AND SHEAR FORCES IN SHIPS SAILING IN IRREGULAR WAVES
Journal of Ship Research Vol 25 No 4, 1981
- [34] Fujino M., Yoon B.S.,
A STUDY ON WAVE LOADS ACTING ON A SHIP IN LARGE AMPLITUDE WAVES
(in Japanese)
Journal of SNAJ, Vol 158, 1985
- [35] Fujino M., Yoon B.S.,
A PRACTICAL METHOD OF ESTIMATING SHIP MOTIONS AND WAVE LOADS IN LARGE
AMPLITUDE WAVES
International Shipbuilding Progress Vol 33 No 385, 1986
- [36] Fukuda J., Shinkai A.,
STATISTICAL METHODS FOR PREDICTING THE NON-LINEAR STRESS INDUCED ON
THE SHIP HULL IN OCEAN WAVES
Memoirs of the Faculty of Engineering, Kyushu Univ, Vol 42 No 1, 1982

- [37] Hattori K., Sakato T., Iwahashi Y., Mikami K.,
A CONSIDERATION ON THE PHASE DIFFERENCE BETWEEN THE WAVE INDUCED
STRESSES OF LONGITUDINAL AND TRANSVERSE STRENGTH
SNAJ, Selected Papers Vol 23, 1985; from Journal of SNAJ Vol 156, 1984
- [38] Kawamura A., Inoue S., Toki N., Hashimoto K., Kuramoto Y.,
SHIP STRUCTURE DESIGN BASED ON SYNTHETIC EVALUATION OF WAVE LOADS
Journal of SNAJ, Vol 160, 1986
- [39] Prowatke G.,
ZUR ERMITTLERUNG DER ÖRTLICHEN BEANSPRUCHUNGEN IM STEG EINES
BODENWRANGENABSCHNITTES ÜBER EINEN LANGZEITRAUM
Schiffbauforschung Vol 23, 1984
- [40] Kaplan P., Raff A. I.,
EVALUATION AND VERIFICATION OF COMPUTER CALCULATIONS OF WAVE-INDUCED
SHIP STRUCTURAL LOADS
Ship Structure Committee Report SSC-229, 1972
- [41] Salvesen N., Tuck E.O., Faltinsen O.,
SHIP MOTIONS AND SHIP LOADS
SNAME Transactions, 1970
- [42] Tasai F.,
ON THE DAMPING FORCE AND ADDED MASS OF SHIPS HEAVING AND PITCHING
Reports of Research Institute for Applied Mechanics, Kyushu Univ.,
Japan, Vol 7, No 26, 1959
- [43] Tasai F.,
HYDRODYNAMIC FORCE AND MOMENT PRODUCED BY SWAYING AND ROLLING
OSCILLATIONS OF CYLINDERS ON THE FREE SURFACE
Reports of Research Institute for Applied Mechanics, Kyushu Univ.,
Japan, Vol 9, No 35, 1961
- [44] FINITE ELEMENT SYSTEM HP-FE; OPERATING GUIDE
Hewlett-Packard Böblingen, 1984
- [45] DISSPLA; USERS MANUAL. Version 8.2
Integrated Software Systems Corp., 6th printing, 1978
- [46] Hannus H.,
ON THE FATIGUE DESIGN PROCEDURE OF MARINE STRUCTURAL DETAILS
RIT, Div of Naval Architecture, Report TRITA-SKP 1056, 1985

NOTATION

(Only first appearance in equations is given below)

A	Coefficients for added mass, eq. (2.1) Hull girder sectional area, eq. (2.17)
$[B]$	Matrix of damping coefficients, eq. (2.1)
B_{M_y}	Vertical hull girder bending moment, eq. (2.3)
B_{M_z}	Horizontal hull girder bending moment, eq. (2.4)
$[C]$	Matrix of coefficients for restoring forces, eq. (2.1)
C_{M_y}	Stress influence coefficient for vertical bending moment, eq. (2.15)
C_{M_z}	Stress influence coefficient for horizontal bending moment, eq. (2.15)
C_{TM}	Stress influence coefficient for torsional moment eq. (2.15)
C_{T_y}	Stress influence coefficient for horizontal shear force, eq. (2.15)
C_{T_z}	Stress influence coefficient for vertical shear force, eq. (2.15)
$C_{\sigma_{my}}$	Stress influence coefficient for normal stress from transverse mass force, eq. (2.20)
$C_{\sigma_{mz}}$	Stress influence coefficient for normal stress from vertical mass force, eq. (2.20)
$C_{\sigma_{p}}$	Stress influence coefficient for normal stress from hydrodynamic pressure, eq. (2.18)
$C_{\tau_{my}}$	Stress influence coefficient for shear stress from transverse mass force, eq. (2.21)
$C_{\tau_{mz}}$	Stress influence coefficient for shear stress from vertical mass force, eq. (2.21)
$C_{\tau_{p}}$	Stress influence coefficient for shear stress from hydrodynamic pressure, eq. (2.19)
d	Ship draught
F_{I_x}	Longitudinal inertia force, eq. (2.9)
F_{I_y}	Horizontal inertia force, eq. (2.10)

F_{Iz}	Vertical inertia force, eq. (2.11)
F_{mx}	Longitudinal mass force in a ship-fixed system of coordinates, eq. (2.12)
F_{my}	Transverse mass force, eq. (2.13)
F_{mz}	Vertical mass force, eq. (2.14)
$\{F_w\}$	Exciting wave forces, eq. (2.1)
F_y	Horizontal strip force, eq. (2.4)
F_z	Vertical strip force, eq. (2.3)
g	Acceleration of gravity, eq. (2.12)
h	Wave (single) amplitude, eq. (4.4)
$\bar{H}_{1/3}$	Significant wave height (double amplitude), eq. (4.3)
i	Index for stress position, eq. (2.3)
I_y	Sectional moment of inertia around the y-axis, eq. (2.16)
I_z	Sectional moment of inertia around the z-axis, eq. (2.16)
$I_{\sigma\sigma}$	Sectorial moment of inertia, eq. (3.1)
j	Index for pressure position, eq. (2.8)
k	Index for mass force position, eq. (2.9)
L	Ship length
N	Coefficients for mass (mass moment of inertia), eq. (2.1)
N_x	Strip moment around the x-axis, eq. (2.5)
m_x	"Active" mass for longitudinal mass forces, eq. (2.9)
m_y	"Active" mass for transverse mass forces, eq. (2.10)
m_z	"Active" mass for vertical mass forces, eq. (2.11)
M_x	Bimoment, eq. (3.1)
n	Number of cycles
p	Combined hydrodynamic pressure, eq. (2.8)

p_D	Pressure component from diffraction, eq. (2.8)
p_{FK}	Pressure component from wave potential, eq. (2.8)
p_R	Pressure component from radiation, eq. (2.8)
p_{VM}	Pressure component from ship vertical motion, eq. (2.8)
q	Factor of non-linearity, eq. (4.4)
s	Line coordinate along sectional profile, eq. (3.1)
S_w	Spectrum (spectral density function) of wave energy in irregular sea, eq. (4.1)
S_σ	Spectrum (spectral density function) of stress response in irregular sea, eq. (4.1)
SCF_σ	Stress concentration factor for nominal normal stress, eq. (4.6)
SCF_τ	Stress concentration factor for nominal shear stress, eq. (4.6)
SWL	Ship still water line
t	Time, eq. (2.1)
\bar{T}	Mean wave period, eq. (4.3)
T_y	Horizontal shear force, eq. (2.7)
T_z	Vertical shear force, eq. (2.6)
T_σ	Stress response function to regular waves, eq. (4.1)
TN_x	Hull girder torsional moment, eq. (2.5)
V	Ship speed
x	Coordinate, surge motion, fig.2.1
x_b	Longitudinal coordinate of ship bow, eq. (2.3)
y	Coordinate, sway motion, fig.2.1, eq. (2.2)
y_0	Sway (single) amplitude, eq. (2.2)
z	Coordinate, heave motion, fig.2.1, eq. (2.2)
z_0	Heave (single) amplitude, eq. (2.2)
ZNA	Coordinate of ship vertical bending neutral axis, eq. (2.16)

β	Relative direction of waves, fig.2.1
ϵ	Phase lag relative encountering wave elevation, eq. (2.2)
$\{\eta\}$	Vector of ship motions, eq. (2.1)
θ	Pitch motion, fig.2.1, eq. (2.2)
θ_0	Pitch (single) amplitude, eq. (2.2)
λ	Wave length
μ	Coefficient for shear stress sectional distribution, eq. (2.17)
ρ	Correlation coefficient
$\rho_{\sigma\tau}$	Correlation coefficient for nominal normal and shear stress in irregular sea, eq. (4.5)
σ	Stress in general
σ_{σ}	Normal stress response to global hull girder loads, eq. (2.16)
σ_{hs}	"Hot-spot" stress in general, eq. (2.15)
σ_m	Normal stress response to local mass forces, eq. (2.20)
σ_p	Normal stress response to local hydrodynamic pressure, eq. (2.18)
$\bar{\sigma}_{1/3}$	Significant (normal) stress, mean value of the one third largest local maxima in an irregular stress response, eq. (4.2), (4.5)
τ_{σ}	Shear stress response to global hull girder shear forces, eq. (2.17)
τ_m	Shear stress response to local mass forces, eq. (2.21)
τ_p	Shear stress response to local hydrodynamic pressure, eq. (2.19)
$\bar{\tau}_{1/3}$	Significant shear stress, mean value of the one third largest local maxima in an irregular stress response, eq. (4.5)
ϕ	Roll motion, fig.2.1, eq. (2.2)
ϕ_0	Roll (single) amplitude, eq. (2.2)
ψ	Yaw motion, fig.2.1, eq. (2.2)

ψ_0	Yaw (single) amplitude, eq. (2.2)
ω	Wave frequency, eq. (4.1)
ω_w	Wave encountering frequency, eq. (2.2)
Q	Normalized sectorial coordinate (unit warping), eq. (3.1)

APPENDIX 1: STRESS RESPONSE IN REGULAR WAVES

TABLE OF CONTENTS

Stress position	Headings (deg)	Stresses	Pages
STR1 AT WEB0	0, 45, 90, 135, 180, -135, -90, -45	σ , τ	A1.2-17
STR1 AT WEB2	0, 45, 90, 135, 180, -135, -90, -45	σ , τ	A1.18-33
CGIR AT WEB0	0, ± 45 , ± 90 , ± 135 , 180	σ , τ	A1.34-43
CGIR AT WEB2	0, ± 45 , ± 90 , ± 135 , 180	σ , τ	A1.44-53
WEB2 AT STR1	0, 45, 90, 135, 180, -135, -90, -45	σ , τ	A1.54-69
WEB2 AT STR2	0, 45, 90, 135, 180, -135, -90, -45	σ , τ	A1.70-85
WEB2 AT CGIR	0, 180, ± 45 , ± 90 , ± 135	σ , τ	A1.86-93
HSID AT WEB0	0, 45, 90, 135, 180, -135, -90, -45	σ	A1.94-101
HSID AT WEB2	0, 45, 90, 135, 180, -135, -90, -45	σ	A1.102-109

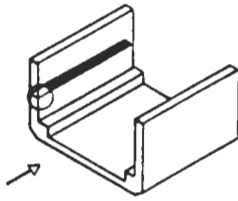
At each position, heading and stress type, components and non-linear combined stresses are presented separately.

Response curves are presented as stress per wave height. This means double amplitude if double amplitude wave height is referred to, or single amplitude if single wave amplitude is referred to.

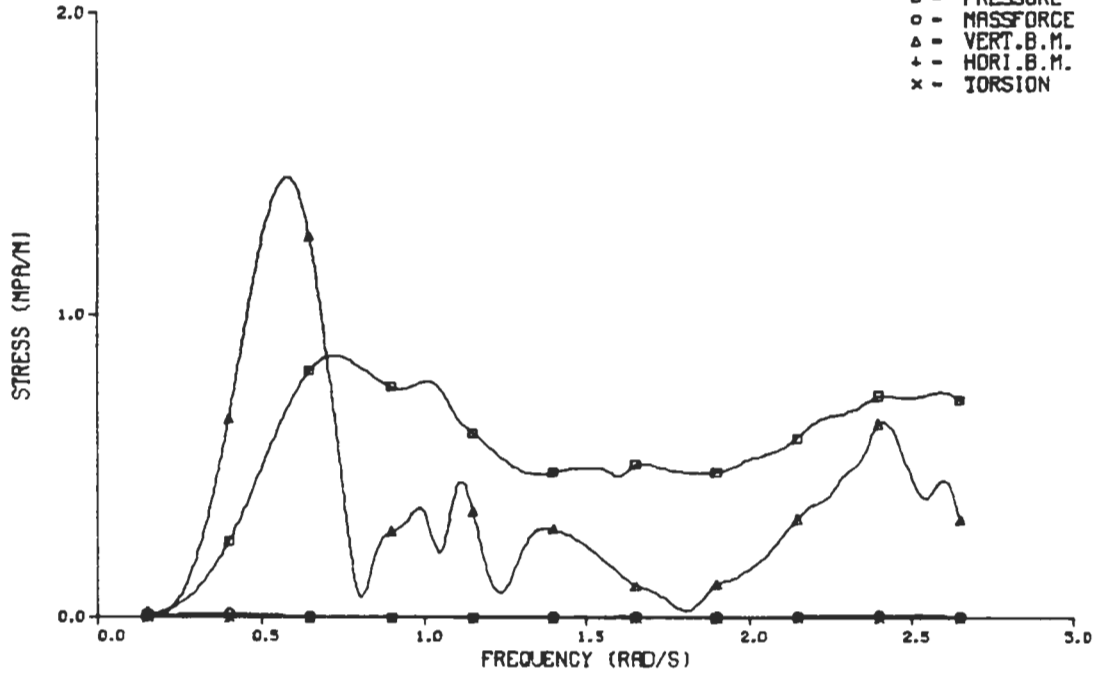
The figures are based on stress calculations at 51 wave frequencies ranging from 0.15 rad/s to 2.65 rad/s with intervals of 0.05 rad/s.

Results have been plotted (not faired) with use of spline functions and the curves are separated from each other by marks at every five calculation point.

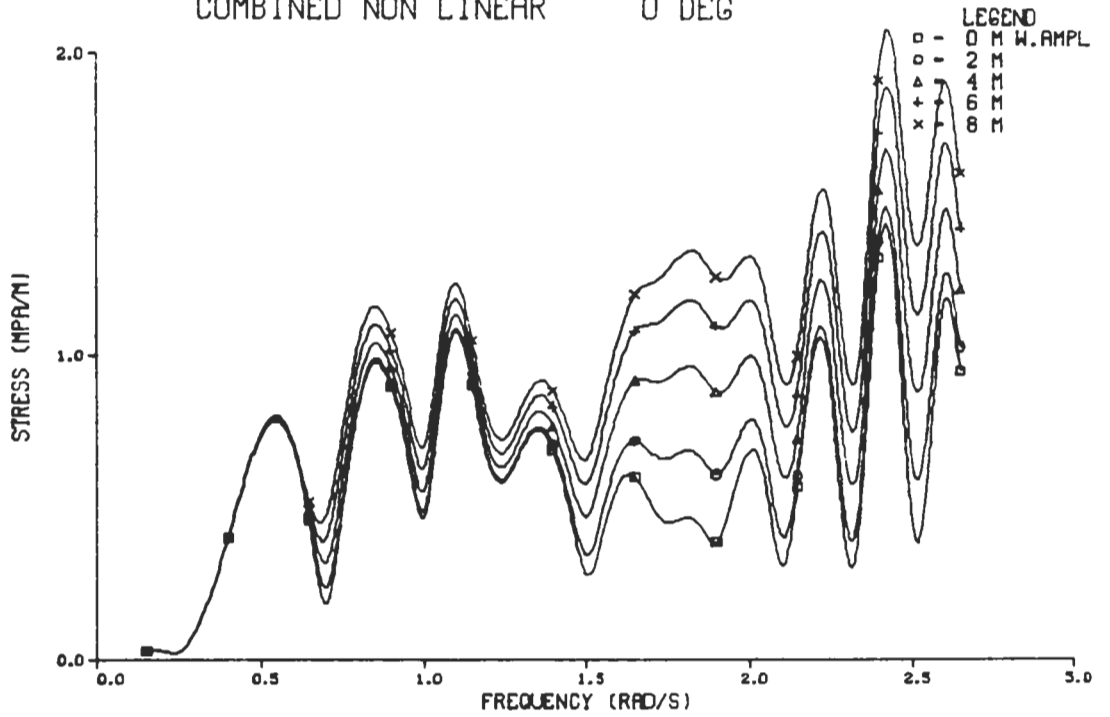
The irregular character of the curves are generally not caused by the spline functions but rather by interference between different components within the calculations.



STR1 AT WEBO, NORMAL STRESS
COMPONENTS LINEAR 0 DEG



STR1 AT WEBO, NORMAL STRESS
COMBINED NON LINEAR 0 DEG



APPENDIX 2: STRESS RESPONSE IN IRREGULAR LONG-CRESTED SEA

TABLE OF CONTENTS

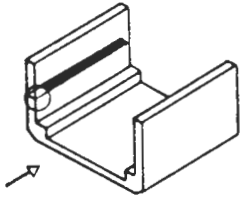
Stress position	Headings (deg)	Stresses	Pages
STR1 AT WEB0	0, 45, 90, 135, 180, -135, -90, -45	σ , τ	A2.2-9
STR1 AT WEB2	0, 45, 90, 135, 180, -135, -90, -45	σ , τ	A2.10-17
CGIR AT WEB0	0, ± 45 , ± 90 , ± 135 , 180	σ , τ	A2.18-22
CGIR AT WEB2	0, ± 45 , ± 90 , ± 135 , 180	σ , τ	A2.23-27
WEB2 AT STR1	0, 45, 90, 135, 180, -135, -90, -45	σ , τ	A2.28-35
WEB2 AT STR2	0, 45, 90, 135, 180, -135, -90, -45	σ , τ	A2.36-43
WEB2 AT CGIR	0, ± 45 , ± 90 , ± 135 , 180	σ , τ	A2.44-48
HSID AT WEB0	0, 45, 90, 135, 180, -135, -90, -45	σ	A2.49-52
HSID AT WEB2	0, 45, 90, 135, 180, -135, -90, -45	σ	A2.53-56

At each position and heading, shear and normal stress components respectively, as well as combined stresses with correlation coefficients, are presented separately.

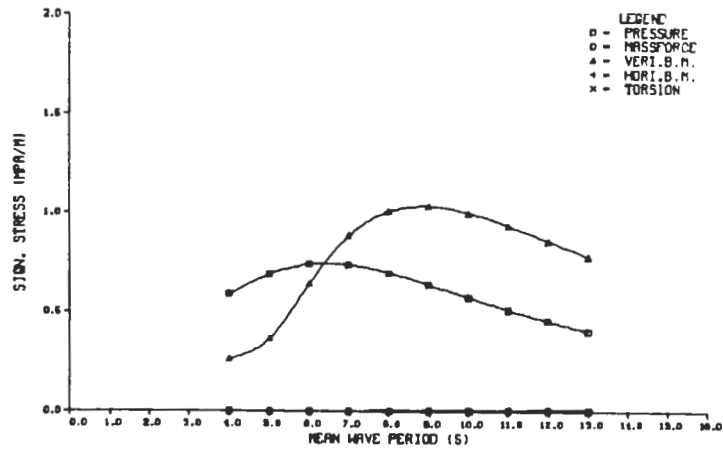
Response curves are presented as significant stress per significant wave height. This means double stress amplitude if the ordinary double amplitude significant wave height $\bar{H}_{1/3}$ is referred to.

Figures are based on results from linear spectrum analysis using ordinary ISSC Pierson-Moskowitz spectra for 10 mean periods \bar{T} . Each result is represented by one mark in the curves which are plotted with use of spline functions.

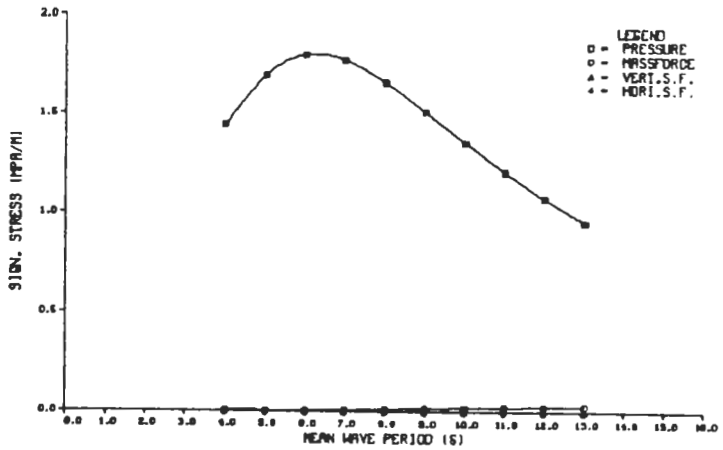
A2.2



STR1 AT WEBO, IRREGULAR LONG-CRESTED SEA
COMPONENTS LINEAR NORMAL STRESS 0 DEG



STR1 AT WEBO, IRREGULAR LONG-CRESTED SEA
COMPONENTS LINEAR SHEAR STRESS 0 DEG



STR1 AT WEBO, IRREGULAR LONG-CRESTED SEA
COMBINED LINEAR 0 DEG

